

LA-UR-17-27500 (Accepted Manuscript)

Rare earth element behavior during groundwater—seawater mixing along the Kona Coast of Hawaii

Telfeyan, Katherine Christina

Provided by the author(s) and the Los Alamos National Laboratory (2018-01-03).

To be published in: Geochimica et Cosmochimica Acta

DOI to publisher's version: 10.1016/j.gca.2016.11.009

Permalink to record: http://permalink.lanl.gov/object/view?what=info:lanl-repo/lareport/LA-UR-17-27500

Disclaimer

Approved for public release. Los Alamos National Laboratory, an affirmative action/equal opportunity employer, is operated by the Los Alamos National Security, LLC for the National Nuclear Security Administration of the U.S. Department of Energy under contract DE-AC52-06NA25396. Los Alamos National Laboratory strongly supports academic freedom and a researcher's right to publish; as an institution, however, the Laboratory does not endorse the viewpoint of a publication or guarantee its technical correctness.



Accepted Manuscript

Rare earth element behavior during groundwater – seawater mixing along the Kona Coast of Hawaii

Karen H. Johannesson, C. Dianne Palmore, Joseph Fackrell, Nancy G. Prouty, Peter W. Swarzenski, Darren A. Chevis, Katherine Telfeyan, Christopher D. White, David J. Burdige

PII: S0016-7037(16)30646-9

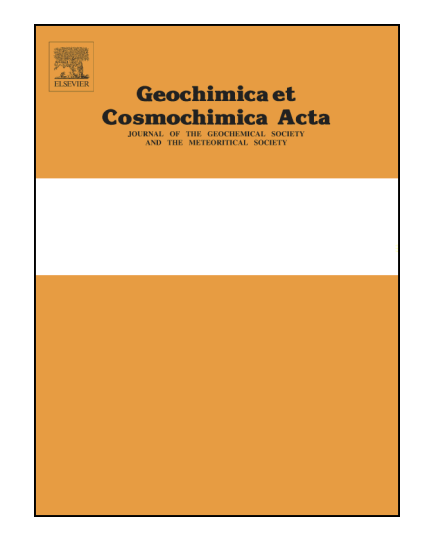
DOI: http://dx.doi.org/10.1016/j.gca.2016.11.009

Reference: GCA 10012

To appear in: Geochimica et Cosmochimica Acta

Received Date: 3 May 2016

Revised Date: 13 September 2016 Accepted Date: 4 November 2016



Please cite this article as: Johannesson, K.H., Dianne Palmore, C., Fackrell, J., Prouty, N.G., Swarzenski, P.W., Chevis, D.A., Telfeyan, K., White, C.D., Burdige, D.J., Rare earth element behavior during groundwater – seawater mixing along the Kona Coast of Hawaii, *Geochimica et Cosmochimica Acta* (2016), doi: http://dx.doi.org/10.1016/j.gca.2016.11.009

This is a PDF file of an unedited manuscript that has been accepted for publication. As a service to our customers we are providing this early version of the manuscript. The manuscript will undergo copyediting, typesetting, and review of the resulting proof before it is published in its final form. Please note that during the production process errors may be discovered which could affect the content, and all legal disclaimers that apply to the journal pertain.

Rare earth element behavior during groundwater - seawater mixing

2	along the Kona Coast of Hawaii
3	
4	Karen H. Johannesson ^a *, C. Dianne Palmore ^a , Joseph Fackrell ^b , Nancy G. Prouty ^c , Peter
5	W. Swarzenski ^{c,d} , Darren A. Chevis ^a , Katherine Telfeyan ^{a,e} , Christopher D. White ^a , and
6 7	David J. Burdige ^f
8	^a Department of Earth and Environmental Sciences, Tulane University, New Orleans, LA
9	70118
10	^b Department of Geology and Geophysics, University of Hawaii at Manoa, Honolulu, HI
11	96822
12	^c United States Geological Survey, Pacific Coastal and Marine Science Center, Santa
13	Cruz, CA 95060
14	^d International Atomic Energy Agency, 98000 Monaco
15	^e Earth and Environmental Sciences Division, Los Alamos National Laboratory, Los
16	Alamos, NM 87545
17	^f Department of Ocean, Earth, and Atmospheric Sciences, Old Dominion University,
18	Norfolk, VA 23529
19	
20	
21	
22	*Corresponding author (kjohanne@tulane.edu)
23	

Abstract

Groundwater and seawater samples were collected from nearshore wells and
offshore along the Kona Coast of the Big Island of Hawaii to investigate rare earth
element (REE) behavior in local subterranean estuaries. Previous investigations showed
that submarine groundwater discharge (SGD) is the predominant flux of terrestrial waters
to the coastal ocean along the arid Kona Coast of Hawaii. Groundwater and seawater
samples were filtered through $0.45~\mu m$ and $0.02~\mu m$ pore-size filters to evaluate the
importance of colloidal and soluble (i.e., truly dissolved ionic species and/or low
molecular weight [LMW] colloids) fractions of the REEs in the local subterranean
estuaries. Mixing experiments using groundwater collected immediately down gradient
from a wastewater treatment facility (WWTF) proximal to the Kaloko-Hanokohau
National Historic Park, and more "pristine" groundwater from a well constructed in a
lava tube at Kiholo Bay, were mixed with local seawater to study the effect of solution
composition (i.e., pH, salinity) on the concentrations and fractionation behavior of the
REEs as groundwater mixes with seawater in Kona Coast subterranean estuaries. The
mixed waters were also filtered through 0.45 or $0.02~\mu m$ filters to ascertain the behavior
of colloidal and soluble fractions of the REEs across the salinity gradient in each mixing
experiment. Concentrations of the REEs were statistically identical (two-tailed Student t-
test, 95% confidence) between the sequentially filtered sample aliquots, indicating that
the REEs occur as dissolved ionic species and/or LMW colloids in Kona Coast
groundwaters. The mixing experiments revealed that the REEs are released to solution
from suspended particles or colloids when Kona Coast groundwater waters mix with
local seawater. The order of release that accompanies increasing pH and salinity follows

light REE (LREE) > middle REE (MREE) > heavy REE (HREE). Release of REEs in the
mixing experiments is driven by decreases in the free metal ion activity in solution and
the concomitant increase in the amount of each REE that occurs in solution as
dicarbonato complexes [i.e., Ln(CO ₃) ₂] as pH increases across the salinity gradient.
Input-normalized REE patterns of Kona Coast groundwater and coastal seawater are
nearly identical and relatively flat compared to North Pacific seawater, indicating that
SGD is the chief source of these trace elements to the ocean along the Kona Coast.
Additionally, REE concentrations of the coastal seawater are between 10 and 50 times
higher than previously reported open-ocean seawater values from the North Pacific,
further demonstrating the importance of SGD fluxes of REEs to these coastal waters.
Taken together, these observations indicate that large-scale removal of REEs, which
characterizes the behavior of REEs in the low salinity reaches of many surface estuaries,
is not a feature of the subterranean estuary along the Kona Coast. A large positive
gadolinium (Gd) anomaly characterizes groundwater from the vicinity of the WWTF.
The positive Gd anomaly can be traced to the coastal ocean, providing further evidence
of the impact of SGD on the coastal waters. Estimates of the SGD fluxes of the REEs to
the coastal ocean along the Kona Coast (i.e., 1.3 – 2.6 mmol Nd day ⁻¹) are similar to
recent estimates of SGD fluxes of REEs along Florida's east coast and to Rhode Island
Sound, all of which points to the importance of SGD as significant flux of REEs to the
coastal ocean.

1. Introduction

71	Submarine groundwater discharge (SGD) is increasingly recognized as an
72	important flux of water, nutrients, and metals to the coastal ocean (Moore, 2010).
73	Although the volume of fresh SGD to the ocean is commonly small compared to river
74	discharge, geochemical reactions in subterranean estuaries (e.g., Moore, 1999) can
75	generate substantial fluxes of nutrients, carbon, and metals to the coastal ocean (Moore,
76	1997; Cai et al., 2003; Charette and Buesseler, 2004; Slomp and van Cappellen, 2004;
77	Charette et al., 2005; Kim et al., 2005; Windom et al., 2006; Roy et al., 2010, 2011;
78	Johannesson et al., 2011; Chevis et al., 2015a, b). Submarine groundwater discharge
79	includes all flow of water from the seafloor into the overlying marine water column
80	within continental margin regions, regardless of chemical composition and physical
81	driving force (Church, 1996; Burnett et al., 2003; Moore, 2010). Thus, SGD includes
82	"fresh submarine groundwater discharge" that originates from meteoric recharge of
83	terrestrial aquifers, as well as "recirculated saline submarine groundwater discharge",
84	which includes water that cycles through coastal aquifers caused by wave set-up, tidal
85	pumping, geothermal or density gradients, and/or bioirrigation (Taniguchi et al., 2002).
86	These components of SGD are commonly referred to as "terrestrial SGD" and "marine
87	SGD", respectively, and their sum represents the total SGD (Martin et al., 2007; Roy et
88	al., 2010).
89	The rare earth elements (REEs, also known as lanthanides) have been utilized to
90	study the petrogenesis of magmatic rocks and for tracing the circulation and mixing of
91	oceanic water masses (Jakeš and Gill, 1970; Hanson, 1980; Piepgras and Wasserburg,
92	1987; McKenzie and O'Nions, 1991). The effectiveness of the REEs as tracers of

geochemical reactions and processes chiefly reflects their uniform trivalent charge (Ce ⁴⁺
and Eu2+ can also occur), and the gradual decrease in their ionic radii with increasing
atomic number (i.e., the lanthanide contraction) that accompanies the progressive filling
of the 4f-electron shell across the REE series. Consequently, the REEs exhibit strong
fractionation as a group due to size and charge, as well as important "within-group"
fractionation that result from the lanthanide contraction (see Johannesson et al. 2005,
2014; and references therein). These distinctive features of the REEs can accordingly
provide insight into complex and subtle geochemical processes that other, single element
tracers cannot readily discriminate (Quinn et al. 2004; Johannesson et al. 2005, 2014).
Investigations of the REEs in surface water estuaries reveal substantial removal of
dissolved REEs (i.e., filtrates that passed through 0.45 μm or 0.22 μm pore size filters;
Sholkovitz, 1992) where river waters first mix with seawater (Martin et al., 1976;
Goldstein and Jacobsen, 1988a; Elderfield et al., 1990; Sholkovitz, 1993, 1995;
Sholkovitz and Szymczak, 2000). Removal of REEs in the low salinity reaches of
estuaries reflects salt-induced coagulation and flocculation of Fe-rich, organic colloids,
which scavenge and fractionate the REEs such that the order of removal is light REE
(LREE) > middle REE (MREE) > heavy REEs (HREE; Sholkovitz, 1995). At higher
salinities the REEs are released back to solution owing to diagenetic reactions within
estuarine sediments and/or displacement from surface sites on suspended particles by
more abundant competing cations (Sholkovitz, 1995; Sholkovitz and Szymczak, 2000).
Here, the order of release also follows LREE > MREE > HREE. Consequently, the
characteristic HREE enriched, shale-normalized REE fractionation pattern that
characterizes seawater (which originates in part during chemical weathering of

continental rocks) is further modified by the competitive effects of aqueous and s	surface
complexation reactions acting on REEs during their transport to the ocean in rive	ers and
estuaries (i.e., Nesbitt, 1979; Hoyle et al., 1984; Goldstein and Jacobsen,	1988b;
Elderfield et al., 1990; Sholkovitz, 1995; Byrne and Liu, 1998).	

116

117

118

119

120

121

122

123

124

125

126

127

128

129

130

131

132

133

134

135

136

137

138

Despite numerous investigations of surface water estuaries, much less is known about the processes that control REE concentrations and fractionation in subterranean estuaries, as well as the importance of SGD fluxes of REEs are for the ocean on a global basis (Duncan and Shaw, 2003; Johannesson and Burdige, 2007; Johannesson et al., 2011; Kim and Kim, 2011; Chevis et al., 2015a, b). Interest in SGD fluxes of REEs to the ocean also stems in part from the possibility that SGD could be an important component of the "missing Nd flux" that would balance the global Nd budget and address the "Nd paradox" (Goldstein and Hemming, 2003; Johannesson and Burdige, 2007). The "Nd paradox" refers to the apparent decoupling of dissolved Nd concentrations, whereby Nd concentrations exhibit nutrient-like profiles in the ocean (indicating vertical cycling and, hence, long residence times, ~10⁴ years), and Nd isotope ratios that exhibit inter- and intra-oceanic variations that preclude vertical cycling and support Nd residence times that are similar to or less than the oceanic mixing time (~500 - 1500 years; Bertram and Elderfield, 1993; Jeandel et al., 1995, 1998; Tachikawa et al., 1997, 1999a, b, 2003; Lacan and Jeandel, 2001; Goldstein and Hemming, 2003; Siddall et al., 2008; Arzouze et al., 2009). Current estimates of riverine and atmospheric fluxes appear to be roughly an order of magnitude too low to balance the global ocean Nd budget and preserve the interand intra-oceanic Nd isotope ratios. The source of the missing Nd flux is thought to reflect "boundary exchange", which is a broadly defined process that involves exchange

of Nd between the continental shelf and the ocean (Lacan and Jeandel, 2005; Jeandel et
al., 2013), and likely includes SGD (Johannesson and Burdige, 2007; Chevis et al.,
2015a, b). Indeed, recent studies demonstrate that SGD associated with small volcanic
islands, including the Hawaiian Islands, have a measureable impact on the REE
concentrations and Nd isotope signatures of coastal waters as well as surface waters in
the open ocean (Kim and Kim, 2011, 2014; Fröllje et al., 2016).

In this contribution we expand on our investigations of REE cycling in subterranean aquifers by presenting REE concentration data for groundwaters and seawater from the arid, Kona Coast of Hawaii where previous investigations have demonstrated the existence of large, nutrient-rich plumes of groundwater, and extensive diffuse seeps of SGD to the coastal ocean (e.g., Johnson et al., 2008; Street et al., 2008; Knee et al., 2010). We employ a modification of the *product* approach for mixing experiments pioneered by Sholkovitz (1976) to study processes that control REE concentrations and fractionation across the salinity gradient of Kona Coast subterranean estuaries.

2. Setting

The study site is located on the arid western coast of the island of Hawaii (Fig. 1), where the overwhelming majority of meteoric water that falls in the region is discharged to the adjacent coastal ocean via SGD (Oki et al., 1999; Duarte et al., 2006; Johnson et al., 2008; Tillman et al., 2014a; Prouty et al., 2016). Precipitation within the immediate study region (e.g., Kaloko – Honokohau National Historic Park) ranges from 500 – 760 mm a⁻¹, whereas annual pan evaporation exceeds 1700 mm (Ekern and Chang, 1985; Oki

162	et al., 1999). Consequently, little recharge, if any, of the local aquifers occurs within the
163	study site. Instead, groundwater recharge is thought to occur further inland to the east at
164	elevations 300-600 m above sea level, where the precipitation exceeds 1500 mm a ⁻¹ (Oki
165	et al., 1999; see also Fig. EA1 in the electronic annex). Groundwater from the study
166	region is unconfined and generally brackish with salinity increasing with depth (Oki et
167	al., 1999). Fresh (i.e., potable) groundwater exists further inland as thin lenses on top of
168	the brackish layer as well as inland at higher elevations where groundwaters are
169	impounded at higher head levels by low permeability structures thought to consist of
170	buried, igneous dike complexes (Zucca et al., 1982; Oki et al., 1999; Tillman et al.,
171	2014a, b).
172	The local geology is characterized by extensive basaltic lava flows that are highly
173	permeable to groundwater flow caused to widespread brecciation of lava flow tops (e.g.,
174	'A'ā lava), cooling fractures, clinker zones, and the presence of lava tubes (Oki et al.,
175	1999; Lau and Mink, 2006). The basaltic rocks exposed at the surface of the study site are
176	alkalic (i.e., chiefly alkali olivine basalt) and were erupted from Hualalai Volcano during
177	the Holocene and late Pleistocene (e.g., Clague and Dalrymple, 1987; Moore et al., 1987;
178	Moore and Clague, 1987; Hanano et al., 2010). Minor amounts of hawaiites are
179	associated with these surficial alkali olivine basalts flows, whereas trachyte erupted from
180	the Puu Waawaa cone (Clague et al., 1980; Moore et al., 1987; Clague and Bohrson,
181	1991; Hanano et al., 2010; Fig. 1). Although not exposed at the surface, the bulk of
182	Hulalai Volcano is thought to be composed of tholeiites erupted during the main shield
183	volcano building stage that is hypothesized to account for the formation of the Hawaiian

184	Islands (Clague and Dalrymple, 1987; Moore and Clague, 1987, 1992; Moore et al.,
185	1987).
186	Previous studies demonstrated that a substantial amount of groundwater
187	discharges to the coastal ocean along the Kona Coast (Adams and Lepley, 1968;
188	Bienfeng, 1980; Oki et al., 1999; Duarte et al., 2006; Peterson et al., 2007; Johnson et al.,
189	2008; Knee et al., 2010). We focus here on SGD in the vicinity of the Honokohau small
190	boat harbor (hereafter, Honokohau Harbor), a portion of the Kaloko-Hanokohau (i.e.,
191	KAHO) National Historic Park located immediately to the north, as well as at Kiholo
192	Bay, roughly 23 km north of Honokohau Harbor (Fig. 1). Honokohau Harbor was
193	constructed by excavating a >5 m deep channel and basin within the local bedrock during
194	the 1970s (Bienfang, 1980). In the process, the excavation intercepted a lava tube that
195	supplies the bulk of the terrestrial SGD to the harbor and adjacent coastal ocean (Johnson
196	et al., 2008).
197	Recent mass balance models using ²²² Rn inventories, salinity, and water fluxes
198	suggest that total SGD from Honokohau Harbor to the coastal ocean is on the order of
199	12,000 m ³ day ⁻¹ , of which approximately 72% (i.e., 8600 m ³ day ⁻¹) is terrestrial sourced
200	SGD, and the remaining 3400 m ³ day ⁻¹ (28%) represents re-circulated marine SGD
201	(Johnson et al., 2008; Peterson et al., 2009). Based on an approximate width of 65 m for
202	the harbor mouth, these values imply along shore SGD fluxes of 182 m ³ day ⁻¹ per meter
203	of shoreline (128 L m ⁻¹ min ⁻¹) for total SGD, and 132 m ³ day ⁻¹ per meter of shoreline (92
204	L m ⁻¹ min ⁻¹) for terrestrial SGD. Other studies have reported higher SGD fluxes, with
205	estimates for fresh and brackish SGD between 274 and 1872 m³ day⁻¹ per meter of
206	shoreline (190 and 1300 L m ⁻¹ min ⁻¹ ; Knee et al., 2010; Gallagher, 1980).

3. Methods

3.1. Sample collection

210	All sampling and laboratory plasticware (HDPE, Teflon®), including filters, were
211	cleaned prior to use by following standard trace element cleaning procedures (e.g.,
212	Johannesson et al., 2004; Fitzsimmons and Boyle, 2012, 2014). Groundwater samples
213	were collected from wells in the vicinity of Honokohau Harbor, the Kaloko-Honokohau
214	National Historic Park (i.e., KAHO wells), and from the Hind "well" located near Kiholo
215	Bay (Fig. 1). The Hind "well" is essentially a fracture in the surface basalt flow that
216	exposes an underlying, partially saturated lava tube. The Honokohau Harbor well is
217	located down hydrologic gradient from the Kealakehe waterwater treatment facility
218	(WWTF), which is thought to cause the high influx of nutrients to the harbor (Oki et al.,
219	1999; Johnson et al., 2008; Prouty et al., 2016). Indeed, between 4900 and 6400 m ³ of
220	effluent from the WWTF is discharged per day into an excavated pit located roughly 1
221	km up gradient from Honokohau Harbor (Parsons et al., 2008). Consequently,
222	groundwater from the Honokohau Harbor well was chosen for study because it has been
223	impacted by anthropogenic-sourced nutrients. In contrast, the Hind "well" was sampled
224	because it is located far from direct anthropogenic sources within a region of the Kona
225	coast that is not highly developed. The KAHO wells sample groundwater from north of
226	Honokohau Harbor, where Johnson et al. (2008) identified large, point source fluxes of
227	SGD to the coastal ocean. Finally, we collected seawater from directly offshore, ~0.62
228	km from the mouth of Honokohau Harbor for REE analysis and for the mixing
229	experiments described below (Fig. 1).

Groundwater was collected from each well using a Fultz pump (Fultz Pumps,
Inc., Lewiston, PA) connected to the surface with LDPE tubing. To be sure that water
samples collected from the wells were representative of groundwaters within the
aquifers/subterranean estuaries and not the well bore, water temperature, specific
conductance, and pH were continuously monitored during well purging, and water
sample collection did not begin until all three parameters had stabilized, which was
typically equivalent to three well volumes (Prouty et al., 2016). Groundwater and
seawater samples were collected into large volume (i.e., 10 L and 40 L, respectively),
pre-cleaned HDPE carboys, and subsequently transported back to the field laboratory for
processing, mixing experiments, and preservation prior to analysis.

At the laboratory, aliquots of groundwaters from each well, as well as the coastal seawater sample, were sequentially filtered first through 0.45 μ m high-capacity (Gelman Sciences, polyether sulfone membrane, Pall Corporation, Port Washington, NY) filter capsules and then through 0.02 μ m pore-size filters (Whatman, Anotop alumina) syringe filters (e.g., Shiller, 2003; Fitzsimmons and Boyle, 2012, 2014), and collected into precleaned HDPE sample bottles. These samples were then acidified to pH < 2 with ultrapure nitric acid (Optima Grade, Thermo Fisher), double bagged in pre-cleaned, Ziplock®-style, polyethylene bags, and stored cold at ~ 4°C in plastic chests until analysis for the REEs. The sequential filtering approach was chosen to separate the dissolved pool of the REEs (i.e., 0.45 μ m passing filtrate) into a colloidal fraction (passed through 0.45 μ m filter but not through 0.02 μ m filter) from the soluble fraction (0.02 μ m passing filtrate; Prouty et al., 2016). The soluble fraction therefore consists of ionic species and low molecular weight (LMW) colloids (Fitzsimmons and Boyle, 2014).

253

254

255

256

257

258

259

260

261

262

263

264

265

266

267

268

269

270

271

272

273

274

275

3.2. Subterranean estuary mixing experiments

Groundwater-seawater mixing experiments were conducted on unfiltered and unacidified water samples on the same day the water samples were collected. Using the seawater sample (i.e., 40 L) collected offshore near the mouth of Honokohau Harbor, two distinct groundwater-seawater mixing experiments were performed, one using groundwater from the Honokohau Harbor well, and the other using groundwater from the more "pristine" Hind well (i.e., Lava tube mixing experiment). Although the coastal seawater sample is appropriate for the Honokohau Harbor mixing experiment, it may not be representative of coastal seawater from Kiholo Bay, and hence, for the Lava tube mixing experiment. For each mixing experiment aliquots of groundwater from the Honokohau Harbor well or the Hind well were mixed in various proportions with the seawater sample to achieve a series of samples with salinities ranging from ≤ 2 to ~ 36.7 ; we refer to this mixing path as endpoint mixing (e.g., Hoyle et al., 1984; Garnier and Guieu, 2003; Schneider et al., 2016). We recognize that serial dilution is an alternative model that could also simulate mixing processes in subterranean estuaries. Both approaches can only approximate the actual mixing path in these settings.

After equilibrating the mixtures for 2 hours (Prouty et al., 2016), aliquots of the mixed water samples were sequentially filtered through 0.45 μ m and then 0.02 μ m poresize filters as described above, and subsequently acidified to pH < 2 with ultrapure nitric acid (Optima Grade, Thermo Fisher). The total time between sample collection and acidification was on the order of 3 hours for the 0.45 μ m filtered aliquots, and 4 hours for the 0.02 μ m filtered aliquots. The mixing and sample processing times were chosen to

276	minimize REE adsorption onto the bottle walls (Fitzsimmons and Boyle, 2012, 2014).
277	The acidified aliquots were then double bagged in pre-cleaned, Zip-lock®-style,
278	polyethylene bags, and stored cold at ~ 4°C in plastic chests until analysis for REEs.
279	
280	3.3 Chemical analysis
281	Major cation and anion concentrations in the groundwaters, the coastal seawater
282	sample, and each mixed water sample from both mixing experiments were determined
283	using high-resolution (magnetic sector) inductively coupled plasma mass spectrometry
284	(HR-ICP-MS Themo Fisher Element 2; Tulane University) and ion chromatography
285	(U.S. Geological Survey, Menlo Park, CA), respectively. Nutrients were analyzed at the
286	Woods Hole Oceanographic Institution by flow injection analysis as described in Prouty
287	et al. (2016). Dissolved organic carbon (DOC) concentrations were quantified by high
288	temperature combustion using a Shimadzu TOC-500 total carbon analyzer as described
289	previously (Burdige and Gardner, 1998). Dissolved Fe and Mn concentrations were
290	measured by HR-ICP-MS following methods described by Roy et al. (2010) and
291	Mohajerin et al. (2016).
292	Groundwater, seawater, and composite waters from the mixing experiments were
293	analyzed for the REEs using similar methods to those described previously (Johannesson
294	et al., 2005, 2011; Willis and Johannesson, 2011; Chevis et al., 2015a, b). Briefly, 30 mL
295	aliquots of the filtered (both 0.45 and 0.02 μm pore-size filters) and acidified samples,
296	$0.45~\mu m$ filtered and acidified laboratory and field blanks, and the National Research
297	Council Canada (Ottawa, Ontario, Canada) Standard Reference Material (SRM) for
298	estuarine waters (SLEW-3) were first loaded onto Poly-Prep columns (Bio-Rad

299	Laboratories) packed with AG 50W-X8 (100 - 200 mesh, hydrogen form, Bio-Rad
300	Laboratories) cation-exchange resin at approximately 1 mL minute ⁻¹ to separate REEs
301	from the major salts (e.g., Elderfield and Greaves, 1983; Greaves et al., 1989;
302	Klinkhammer et al., 1994; Johannesson et al., 2005, 2011). Iron and Ba were then
303	quantitatively eluted from each column using 1.75 M ultra-pure HCl (Optima Grade,
304	Thermo Fisher) and 2 M ultra-pure HNO ₃ (Optima Grade, Thermo Fisher), respectively
305	(Greaves et al., 1989). The REEs were subsequently eluted from the columns using 8 M
306	ultra-pure HNO ₃ (Optima Grade, Thermo Fisher) and collected in Teflon [®] beakers. The
307	eluent was then taken to dryness on a hot plate, and the residue redissolved in 10 mL of a
308	1% v/v ultra-pure HNO ₃ solution. All sample processing was conducted in an ISO 5 rated
309	clean room or ISO 5 rated laminar flow bench (i.e., class 100).
310	Each 10 mL sample was then spiked with 115 In as an internal standard and
311	analyzed for the REEs by HR-ICP-MS (Thermo Fisher Element 2) at Tulane University.
312	We examined ¹³⁹ La, ¹⁴⁰ Ce, ¹⁴¹ Pr, ¹⁴³ Nd, ¹⁴⁵ Nd, ¹⁴⁶ Nd, ¹⁴⁷ Sm, ¹⁴⁹ Sm, ¹⁵¹ Eu, ¹⁵³ Eu, ¹⁵⁵ Gd,
313	¹⁵⁷ Gd, ¹⁵⁸ Gd, ¹⁵⁹ Tb, ¹⁶¹ Dy, ¹⁶³ Dy, ¹⁶⁵ Ho, ¹⁶⁶ Er, ¹⁶⁷ Er, ¹⁶⁹ Tm, ¹⁷² Yb, ¹⁷³ Yb, and ¹⁷⁵ Lu (low-
314	and medium-resolution mode) because most of these isotopes are free of isobaric
315	interferences (Shannon and Wood, 2005; Johannesson et al., 2005; 2011). Furthermore,
316	monitoring more than one isotope of a given element provides an additional check for
317	potential interferences. Europium isotopes (151Eu and 153Eu) as well as the heavy REEs
318	(HREE) were also monitored in high-resolution mode, which allowed us to resolve
319	interferences on ¹⁵¹ Eu and ¹⁵³ Eu from BaO ⁺ species formed in the plasma stream, and
320	LREEO ⁺ and MREEO ⁺ species on the HREEs. The HR-ICP-MS was calibrated and the
321	concentrations of REEs in the samples verified using a series of REE calibration

standards of known concentrations (1 ng kg ⁻¹ , 2 ng kg ⁻¹ , 5 ng kg ⁻¹ , 10 ng kg ⁻¹ , 100 ng kg ⁻¹
¹ , 500 ng kg ⁻¹ , and 1000 ng kg ⁻¹). The calibration standards were prepared from NIST
traceable High Purity Standards (Charleston, SC). In addition, check standards for the
REEs were prepared using Perkin Elmer multi-element solutions. The detection limit for
then REEs ranged between 0.5 and 6 pmol kg ⁻¹ , whereas the field blank exhibited REE
concentrations between 1.4 pmol kg ⁻¹ for Lu and 35 pmol kg ⁻¹ for Ce (Table EA1).
Analytical precision of the REE analyses was always better than 4% relative standard
deviation (RSD), and generally better than 2% RSD, whereas accuracy of the analyses for
SLEW-3 were typically within \pm 5% of the values reported by Lawrence and Kamber
(2006).
3.3 Geochemical modeling

3.3 Geochemical modeling

Solution complexation modeling of the REEs in Kona groundwaters, coastal seawater, and the water samples from the mixing experiments was achieved using the SpecE8 and React programs of the Geochemist's Workbench® (release 9.0; Bethke, 2008; Bethke and Yeakel, 2013). The Lawrence Livermore National Laboratory database (Delaney and Lundeen, 1989) provided with the software (i.e., thermo.dat) was modified by addition of the 14 naturally occurring REEs and their corresponding inorganic, aqueous complexes with carbonate, phosphate, hydroxyl, sulfate, chloride, and fluoride ions. Specifically, infinite dilution stability constants for the LnHCO₃²⁺, LnCO₃⁺, and Ln(CO₃)₂ complexes, where Ln is any of the 14 naturally occurring REEs (i.e., lanthanides), that were added to the database are from Luo and Byrne (2004), those for LnPO₄⁰ and Ln(PO₄)₂³ are from Byrne et al. (1991) and Lee and Byrne (1992), those for

345

346

347

348

349

350

351

352

353

354

355

356

357

358

359

360

361

362

363

364

365

366

367

LnOH ⁺ are from Klungness and Byrne (2000), those for LnSO ₄ ⁺ are from Schijf and
Byrne (2004), those for LnCl ²⁺ are from Luo and Byrne (2001), and those describing the
formation of LnF ²⁺ complexes are from Luo and Byrne (2000). In addition, because a
number of studies have demonstrated that REE phosphate co-precipitate phases limit the
solubility of REEs in natural waters (Jonasson et al., 1985; Byrne and Kim, 1993;
Johannesson et al., 1995), we included the solubility product constants for $LnPO_{4(s)}$
phases estimated by Liu and Byrne (1997) in the thermo.dat database to account for
solubility limitations on the REEs in the geochemical modeling.

The partitioning of the REEs between suspended particles or colloids and the dissolved phase in natural waters can be characterized as a competition between sorption reactions and the formation of aqueous complexes (Byrne and Kim, 1990; Erel and Morgan, 1991; Erel and Stolper, 1993; Quinn et al., 2004). Because we did not measure or characterize the REE content or surface chemistry of suspended particles or colloids from Kona Coast groundwaters, a quantitative evaluation of sorption reactions involving the REEs is currently not possible. Nevertheless, a partitioning model that allows for the evaluation of the relative solution and surface complexation behavior of the REEs in the Kona Coast groundwaters can be formulated using methods described previously (e.g., see Balistrieri et al., 1981; Clegg and Sarmiento, 1989; Byrne and Kim, 1990; Dzombak and Morel, 1990; Erel and Morgan, 1991). The partitioning model, which is described in detail in the electronic annex, computes the distribution of each REE between the aqueous solution and surface sites on suspended particles or colloids as a function of the composition of the aqueous solution. Furthermore, by normalizing the computed distribution coefficients to the same REE, the necessity of knowing the concentration of

the adsorption sites on the suspended particles or colloids is eliminated (Byrne and Kim, 1990; Erel and Morgan, 1991; Erel and Stolper, 1993). Following Byrne and Kim (1990), we chose to normalize the distribution coefficients to Gd, which is located in the middle of the REE series, such that the relative distribution coefficient for each REE is represented by

374
$$D_{Ln}/D_{Gd} = ([Ln]_{T,ads}/[Ln]_{T,soln})/([Gd]_{T,ads}/[Gd]_{T,soln})$$
 (1)

where $[Ln]_{T,ads}$ and $[Gd]_{T,ads}$ are the total concentrations of any given REE and Gd adsorbed on particles and/or colloids, respectively, and $[Ln]_{T,soln}$ and $[Gd]_{T,soln}$ are the corresponding total concentrations in solution. It is critical to point out, however, that distribution coefficients computed in this fashion are independent of the measured REE concentrations, and instead are only a function of the ionic strength corrected equilibrium constants that describe the formation of the various REE solution complexes with different ligands, and the corresponding free ligand concentrations in solution (see equations EA1 – EA8). Therefore, the anomalously high Gd concentrations that characterize groundwaters from the Honokohau Harbor well and the associated mixing experiment (see below) do not affect the calculation of the distribution coefficients.

To determine the solution complexation term (equations EA1-EA4), the formation of bicarbonate, carbonato, dicarbonato, hydroxide, chloride, sulfate, phosphate, and diphosphato complexes of the REEs were considered (see HH_Speciation.xlsx and LT_Speciation.xlsx in electronic annex). Free ligand concentrations were computed for each sample from both mixing experiments using the SPECE8 program of the Geochemist's Workbench® (release 9.0; Bethke, 2008; Bethke and Yeakel, 2013).

Infinite dilution stability constants were then corrected to the appropriate ionic strength (Tables A1, A2) using the approach of Millero and Schreiber (1982) as discussed in Schijf and Byrne (2004) where, for example,

395
$$\log_{CO_3}^{Ln} \beta_1 = \log_{CO_3}^{Ln} \beta_1^0 + \log_{CO_3}^{2n} \gamma_{LnCO_3}^{2n}$$
 (2)

in which $_{\text{CO}_3}^{\text{Ln}}\beta_1^0$ is the stability constant describing the formation of the carbonato complex at I = 0 mol kg⁻¹, and γ_i are the activity coefficients for each species at the given ionic strength of the water sample.

4. Results

4.1. Geochemistry of Kona groundwaters

The major solute compositions of the Kona groundwaters are presented in Table 2 along with nutrient concentrations and other ancillary geochemical parameters. The groundwater are chiefly Na-HCO₃ type waters, although groundwater from the KAHO 2 well is a Na-Cl water with major ion ratios similar to coastal seawater (Fig. 2). The Kona groundwaters are brackish as demonstrated by their measured salinities and electrical conductivities, as well as their computed ionic strengths (Table 2). Groundwater pH ranges between 6.76 and 7.7 and Eh (computed based on the high dissolved oxygen concentrations) ranges from 0.763 to 0.817 volts. Groundwater from the Honokohau Harbor well exhibits elevated nutrient (i.e., NO₃ + NO₂, PO₄; Prouty et al., 2016) and DOC concentrations compared to the other well waters sampled, again reflecting its proximity to the Kealakehe WWTF (Table 2, Fig. 1). The Kona groundwaters also have relatively high dissolved silica concentrations (311 to 432 μmol kg⁻¹; Table 2), which likely reflect chemical weathering of basaltic glass within the aquifer rocks (e.g., Visher

415	and Mink, 1964; Lau and Mink, 2006). High dissolved silica concentrations have been
416	reported for other groundwaters from basalt aquifers (e.g., Stefánsson and Gíslason,
417	2001).
418	Dissolved Fe, Mn, and DOC concentrations (i.e., passed through 0.45 µm filters)
419	of groundwaters from Kona Coast subterranean estuaries are substantially lower than
420	observed in our previous studies of subterranean estuaries beneath the Indian River
421	Lagoon in Florida and the Pettaquamscutt River estuary in Rhode Island (Roy et al.,
422	2010; Johannesson et al., 2011; Chevis et al., 2015a, b). Iron, Mn, and DOC
423	concentrations in the Kona Coast groundwaters range between 11 and 63 nmol kg ⁻¹ , 0.6
424	and 12 nmol kg ⁻¹ , and 36 and 236 µmol kg ⁻¹ , respectively (Table 2). By comparison, Fe,
425	Mn, and DOC concentrations in groundwaters from the Indian River Lagoon
426	subterranean estuary range from 0.009 to 286 μ mol kg ⁻¹ , 0.06 to 2.9 μ mol kg ⁻¹ , and ~80
427	to more than 800 µmol kg ⁻¹ , respectively (Roy et al., 2010; Chevis et al., 2015b), whereas
428	Fe and DOC range between 1 and 6.5 mmol kg ⁻¹ , and 380 and 7300 µmol kg ⁻¹ ,
429	respectively, in groundwaters from the Pettaquamscutt River estuary (Chevis et al.,
430	2015a). Furthermore, the concentrations of Fe, Mn, and DOC in the subterranean estuary
431	beneath the Kona Coast are also generally lower than the concentrations of these species
432	in the majority of surface estuaries where the REEs have also been investigated (Table 3).
433	The exception is groundwater from the Honokohau Harbor well, which exhibits DOC
434	concentrations similar to some surface estuaries.
435	
436	
437	

4.2. REE concentrations and input-normalized fractionation patterns

439	Rare earth element concentrations for coastal seawater and coastal groundwaters
440	from the Kona Coast are presented in Table 4. Rare earth element concentrations of these
441	coastal groundwaters are, on average, lower than in groundwaters from the Indian River
442	Lagoon subterranean estuary in Florida (Johannesson et al., 2011; Chevis et al., 2015b).
443	Specifically, Nd concentrations of Kona Coast groundwaters (i.e., filtered through 0.45
444	μm pore-size filters) range from 158 pmol kg ⁻¹ to 192 pmol kg ⁻¹ , and have a mean (± SD)
445	Nd concentration of 178 \pm 12.9 pmol kg ⁻¹ (Table 4), whereas Nd concentrations
446	measured in SGD from the Indian River Lagoon in Florida that were collected identically
447	(i.e., 0.45 μm pore-size filters) range from 110 pmol kg ⁻¹ to 2409 pmol kg ⁻¹ , and exhibit a
448	mean (\pm SD) Nd concentration of 448 \pm 365 pmol kg ⁻¹ (n = 55; Johannesson et al., 2011;
449	Chevis et al., 2015b). If the sample with the highest Nd concentration from the Indian
450	River Lagoon subterranean estuary (i.e., 2409 pmol kg ⁻¹) is not included, the mean (±SD)
451	Nd concentration of the remaining samples is 412 ± 252 pmol kg ⁻¹ , which is still more
452	than 2-fold higher, on average, than the mean Nd concentration of Kona Coast
453	groundwaters. In contrast, groundwaters discharging to the Pettaquamscutt River estuary
454	in Rhode Island generally exhibit lower REE concentrations than Kona Coast
455	groundwaters. For example, Nd concentrations range from 0.43 pmol kg ⁻¹ to 198 pmol
456	kg^{-1} and exhibit a mean (± SD) of 35.2 ± 79.8 pmol kg^{-1} in Pettaquamscutt groundwaters
457	(n = 6; Chevis et al., 2015a). Recent investigations of coastal groundwaters from Jeju
458	Island in Korea (i.e., Kim and Kim, 2011, 2014) reported substantially higher REE
459	concentrations for identically filtered (0.45 μm pore size filters) samples compared to
460	groundwaters from the Kona Coast, the Indian River Lagoon, and the Pettaquamscutt

461	River estuary. Specifically, the mean (± SD) Nd concentration for coastal groundwaters
462	from Jeju Island is 2672 ± 1357 pmol kg ⁻¹ (n = 16; Kim and Kim, 2011). Although Jeju
463	Island is also largely composed of basaltic rocks in addition to more evolved volcanic
464	rocks such as trachyandesites and trachytes (Tatsumi et al., 2004), the Nd concentrations
465	of the coastal groundwaters are 15-fold higher, on average, than the Nd concentrations of
466	Kona Coast groundwater.
467	An outstanding feature of the Kona Coast groundwater data is that the REE
468	concentrations of water filtered through $0.02\ \mu m$ pore-size filters are statistically
469	indistinguishable (Student's <i>t</i> -test; $p > 0.05$) from those filtered through 0.45 μ m pore-
470	size filters (Table 4, Fig. 3). The REE concentrations of the groundwaters are also similar
471	to those of the coastal seawater sample (Table 2; Fig. 4). Specifically, the Nd
472	concentration of the coastal seawater sample (filtered through 0.45 μm pore-size filters) is
473	169 pmol kg ⁻¹ compared to 158-192 pmol kg ⁻¹ for the groundwaters (Table 4). Moreover,
474	the REE concentrations of the Kona Coast seawater samples are substantially higher than
475	open-ocean seawater from the North Pacific (Fig. 4). For example, Alibo and Nozaki
476	(1999) report Nd concentrations that range between 6.64 and 24.5 pmol kg ⁻¹ (mean ± SD
477	= 15.6 ± 6.5 pmol kg ⁻¹) for seawater from the Northwest Pacific Ocean, and Piepgras and
478	Jacobsen (1992) present Nd data for the North Pacific that range between 5 and 63 pmol
479	kg^{-1} (mean \pm SD = 29 \pm 14.3 pmol kg^{-1}). It is important to note that the REE data
480	presented by Alibo and Nozaki (1999) were filtered through 0.04 µm pore-size filters,
481	whereas those from Piepgras and Jacobsen (1992) are for unfiltered water samples.
482	Consequently, the data from Alibo and Nozaki (1999) would include colloids larger than
483	those sampled by the 0.02 µm pore-size filters used here for Kona seawater, whereas the

484	REE concentrations for North Pacific seawater presented by Piepgras and Jacobsen
485	(1992) represent the maximum concentrations of the REEs in the analyzed seawater
486	samples (i.e., dissolved, colloidal, and particulate). For either case, REE concentrations
487	for Kona Coast seawater exceed those for North Pacific seawater by at least a factor of 7,
488	and as much as a factor of 29 for the LREEs. Thus, the enrichment of REEs in Kona
489	Coast seawater compared to North Pacific seawater can not be explained by particulate or
490	colloidal association of REEs in Kona Coast seawaters because the 0.02 μm filtered
491	coastal seawater is enriched in REEs over the $0.04~\mu m$ filtered North Pacific seawater
492	samples of Alibo and Nozaki (1999).
493	Shale-normalized REE fractionation patterns of Kona Coast groundwaters and
494	coastal seawater are all enriched in the HREEs relative to the LREEs (Figs. 4). The shale-
495	normalized Yb/Nd ratios [i.e., $(Yb/Nd)_{SN}$, where $SN = shale$ -normalized], which provides
496	a measure of fractionation across the REE series, are all greater than unity for Kona Coast
497	waters (Table 4). Specifically, the $(Yb/Nd)_{SN}$ ratios of the 0.45 μm filtered water samples
498	range from 1.25 to 1.74 (mean \pm SD = 1.57 \pm 0.17), and for the 0.02 μm filtered samples,
499	this ratio varies between 1.41 and 1.87 (mean \pm SD = 1.58 \pm 0.18). The REE patterns of
500	the Kona Coast groundwaters and coastal seawater are also less fractionated than North
501	Pacific seawater (Fig. 4). By comparison, the (Yb/Nd) _{SN} ratios for the North Pacific
502	seawater samples analyzed by Alibo and Nozaki (1999) range from 3.49 to 5.29 (i.e.,
503	0.04 μ m filtered), and exhibit a mean (± SD) of 4.49 ± 0.52.
504	Another important feature of the shale-normalized fractionation patterns for Kona
505	Coast water is the substantial positive Gd anomaly of groundwater from the Honokohau
506	Harbor well (Fig. 4). Specifically, the Gd anomaly for the 0.45 μm and 0.02 μm filtered

Honokohau Harbor well waters are 5.05 ar	and 6.84, respectively (Table 4). These values
exceed the commonly observed positive Gd	anomalies of open ocean seawater (e.g., Kim
et al., 1991), which ranges, for example, fro	om 1.04 to 1.23 (mean \pm SD = 1.15 \pm 0.06) in
the North Pacific seawater samples analy	zed by Alibo and Nozaki (1999). Coastal
seawater from Kona also exhibits a positive	e Gd anomaly that exceeds the reported mean
value for North Pacific seawater by between	en 18 to 28%, based again on the data from
Alibo and Nozaki (1999). Positive, shale-	normalized Gd anomalies larger than those
reported for open ocean seawater are no	t a characteristic of the other Kona Coast
groundwaters.	

Normalization of the REE concentrations of Kona Coast waters to shale composites is instructive for comparisons to other natural waters. However, because the local bedrock consists of basalts and their weathering products, a more appropriate normalizing standard is the local basaltic bedrock. Figure 5 presents REE fractionation patterns of Kona Coast groundwaters and coastal seawater normalized to a composite of local basalts. The basalt composite represents the average REE content of alkali, Hualalai basalts (n = 12) presented in Hanano et al. (2010). A key feature of Fig. 5 is the generally flat fractionation pattern between La and Dy, and the marked enrichment in REEs heavier than Dy in these groundwaters and the coastal seawater sample compared to the basalts. Positive, basalt-normalized Gd anomalies are apparent for both Honokohau Harbor well water as well as coastal seawater. In addition, all of the Kona Coast waters exhibit negative Eu and small, positive Ce anomalies when normalized to the local basalt composite (Fig. 5).

1 2	17	• .
43	Mixino	experiments
1.5.	minis	experiments

The results of the Honokohau Harbor and Lava Tube mixing experiments for Nd, Gd, and Yb are presented in Figs. 6 and 7, respectively. Because the REE concentrations of Kona Coast waters filtered through 0.45 μ m and 0.02 μ m pore-size filters were not statistically different (Student's *t*-test; p > 0.05), only data for waters filtered through 0.45 μ m filters are shown. Nonetheless, the full datasets for these mixing experiments are included in the Appendix (Tables A1, A2).

The REE concentrations in the coastal groundwater endmembers are only slightly enriched (between 1.1 to 2 times) over their concentrations in coastal seawater. The only exception is Gd in the Honokohau Harbor mixing experiment, which is 4.5-fold higher in Honokohau Harbor well water compared to the coastal seawater sample. In general, positive deviations from the conservative mixing line connecting the groundwater endmembers with the coastal seawater sample characterize the majority of the REE data for both mixing experiments. Again, the chief exception is Gd in the Honokohau Harbor mixing experiment, which exhibits a nearly linear dilution trend, indicating conservative behavior (Fig. 6). Gadolinium did not, however, exhibit conservative behavior in the Lava Tube mixing experiment (Fig. 7).

The majority of the REE concentrations for both mixing experiments plot above the conservative mixing line indicating that REEs were released from suspended particles or colloids upon mixing. For the Honohohau Harbor mixing experiment, the greatest REE release occurred at salinities between 7 and 15 where between 22 and 38 pmol kg⁻¹ of Nd was mobilized (Fig. 6). The greatest release occurred at slightly lower salinities (i.e., 5 to 8) in the Lava Tube mixing experiment where 25 to 35 pmol kg⁻¹ of Nd was released

(Fig. 7). Two exceptions occurred for both mixing experiments where the measured REE
concentrations plotted below the conservative dilution lines suggesting removal of the
REEs. These include the 5.3 and 31.9 salinity samples from the Honokohau Harbor
mixing experiments, and the 4.4 and 20.1 salinity samples from the Lava Tube mixing
experiment (Tables A1, A2). The relative amount of release generally followed that
sequence LREE > MREE > HREE in both mixing experiments, and the overall amounts
of REE release were greater in the Honokohau Harbor mixing experiment than for the
Lava Tube mixing experiment (Figs. 6, 7).

4.4. Geochemical modeling

The results of the solution complexation modeling for REEs in Kona Coast groundwaters and the coastal seawater sample are presented in Fig. 8. The Geochemist's Workbench® software package employs the "B-dot" model to estimate activity coefficients of solutes in solution (Helgeson, 1969). The B-dot model is described in the electronic annex along with a comparison of its performance against a combined specific ion interaction and ion-pairing model.

The speciation model predicts that REEs chiefly occur in Kona Coast groundwaters and coastal seawater as complexes with carbonate ions. Specifically, the dicarbonato complex, Ln(CO₃)₂, is predicted to predominate for all of the REEs in the Kona Coast groundwaters and coastal seawater. The only exceptions are La and Ce in the Honokohau Harbor well water, where the carbonato complex, LnCO₃⁺, is predicted to account for more (i.e., La) and approximately equal amounts (i.e., Ce) than the dicarbonato complex (Fig. 8). More specifically, the model predicts that between 77%

(i.e., La in Honokohau Harbor well water) and ~100% of each REE occurs as carbonate complexes [i.e., $LnCO_3^+ + Ln(CO_3)_2^-$] in Kona Coast waters.

576

577

578

579

580

581

582

583

584

585

586

587

588

589

590

591

592

593

594

595

596

597

598

Results of the solution complexation modeling for the two mixing experiments are summarized in Figs. 9 and 10. The activity of the free metal ion, [Ln³⁺]_F, decreases dramatically with increasing salinity in each mixing experiment as progressively more of each REE is complexed with dissolved carbonate ions. The negatively charged dicarbonato complex, [i.e., Ln(CO₃)₂] is again the chief form of each REE in solution, and the percentage of each REE that occurs as discarbonato complexes increases with increasing salinity, increasing pH, and increasing atomic number (Figs. 9, 10; Tables A1, A2). The results of the solution complexation modeling for the Honokohau Harbor mixing experiment exhibit greater variation than the Lava Tube mixing experiment chiefly because of the greater pH change across the salinity gradient for the Honokohau Harbor experiment (Tables A1, A2). Specifically, pH changes from 6.9 to 8.03 for the Honokohau Harbor mixing experiment compared a pH change from 7.7 to 8.03 for the Lava Tube mixing experiment. Hence, greater amounts of each REE are predicted to occur as carbonato complexes [i.e., $NdCO_3^+ \sim 30 - 35\%$; YbCO₃⁺ ~ 12 - 13%;] and free metal ions [Nd³⁺ $\sim 1.5\%$; Yb³⁺ $\sim 0.2\%$] in the lower salinity portions of the Honokohau Harbor mixing experiment compared to the Lava Tube mixing experiment. By comparison, NdCO₃⁺ and Nd³⁺ are predicted to account for ~11% and 0.1% of total aqueous Nd, and YbCO₃⁺, and Yb³⁺ for less than 3% and 0.005%, respectively, of total dissolved Yb in the low salinity waters of the Lava Tube mixing experiment (Fig. 10).

The results of the solution – surface partitioning model for the REEs in the Honokohau Harbor mixing experiments are presented in Fig. 11. Here the inverse of

equation 1, [i.e., $(D_{Ln}/D_{Gd})^{-1}$], is plotted as a function of salinity. Hence, values that
exceed unity indicate that the particular REE has a greater proclivity for the solution
phase compared to Gd at any given salinity (e.g., Byrne and Kim, 1990). Values less than
one indicate that the REE has a greater preference for O-donor surface sites on suspended
particles or colloids relative to Gd. Again, the partition coefficients are not computed
using the REE concentrations measured in the waters, and hence are not influenced by,
for example, the anomalously high Gd concentrations of Honokohau Harbor well waters
and the mixing experiments performed with this well water. For the Honokohau Harbor
mixing experiment, the model indicates that REEs lighter than Gd, such as La and Nd,
exhibit a greater affinity for the solution phase than for surface sites of particles or
colloids compared to Gd, but that the preference of the LREEs for the solution phase
decreases with increasing salinity and increasing pH across the mixing gradient. In
contrast, REEs heavier than Gd (i.e., Dy, Yb, Lu) prefer to be adsorbed on suspended
particles or colloids at lower salinities and lower pH (Fig. 11). Nevertheless, as salinity
and pH increases, HREEs exhibit an increasing affinity for the solution phase such that
they are expected to preferentially partition to the solution phase when salinity exceeds ~
15 and pH exceeds ~ 7.5. Prouty et al. (2016) noted that peak release of colloidal bound
phosphate also occurred at a salinity of 15. For the Lava Tube mixing experiment, the
model indicates that all of the REEs exhibit a preference for the solution phase relative to
Gd, such that the solution - surface partitioning behavior of the REEs varies little with
changing salinity.

5. Discussion

5.1. REEs in Kona Coast groundwaters

The nearly identical shale-normalized REE fractionation patterns of Kona Coast
groundwaters and the local seawater provides strong evidence that SGD is the chief
source of REEs to the coastal ocean (Fig. 4). Furthermore, the positive Eu anomalies that
are apparent in REE patterns when Kona Coast groundwaters are normalized to the
coastal seawater values (Fig. 12) likely reflect a weathering signature of the local basalts
(e.g., Tanaka et al., 2008; Ren et al., 2009; Fröllje et al., 2016). The importance of SGD
as the principal source of REEs to the coastal ocean is underscored by the substantially
higher REE concentrations of Kona Coast seawater, especially the LREEs, when
compared to North Pacific seawater (Fig. 4). Moreover, because the 0.45 μm and 0.02 μm
filtered water samples returned REE concentrations that are statistically indistinguishable
from each other based on a two-tailed Student's t -test, the data demonstrate that the REEs
are either in solution as truly dissolved ionic species or are associated with LMW colloids
(i.e.,< 0.02 μm in diameter). The identical (Yb/Nd) $_{SN}$ ratios of the 0.45 μm and 0.02 μm
filtered Kona Coast waters further support this observation.
The relatively large positive Gd anomaly that characterizes the shale-normalized
REE pattern of the Kona Coast seawater sample indicates that treated wastewater from
the Kealakehe WWTF influences these coastal waters offshore of Honokohau Harbor.
Specifically, large positive Gd anomalies commonly reflect anthropogenic Gd that
originates from highly stable Gd containing contrast agents, such as Gd-(DPTA)2-, that
are used in magnetic resonance imaging (Bau and Dulski, 1996). The dissolved Gd-
(DPTA) ²⁻ complex is subsequently transferred to environmental waters via waste water

treatment facilities with little apparent breakdown during the treatment process (e.g., Bau
and Dulski, 1996; Kümmerer and Helmers, 2000; Verplanck et al., 2005). Because the
WWTF discharges effluent to an excavated pit located approximately 1 km up gradient
from the Honokohau Harbor well (Parsons et al., 2008), and because groundwater from
this well exhibits an even larger positive Gd anomaly, the smaller, albeit significant,
positive Gd anomaly observed in Kona seawater can be explained by mixing of local
wastewater-impacted SGD with North Pacific seawater. The results of the Honokohau
Harbor mixing experiment where Gd behaves conservatively when Honokohau Harbor
well waters are mixed with local seawater supports this hypothesis (Fig. 6). Indeed, the
Honokohau Harbor mixing experiment confirms that anthropogenic Gd behaves
conservatively during mixing in subterranean estuaries, as previously suggested in field
studies of surface estuaries (e.g., Kulaksız and Bau, 2007; Hatje et al., 2016). Therefore,
anthropogenic Gd may be a potential tracer of sewage discharge to natural waters,
including the coastal ocean.
The Hualalai basalt-normalized REE patterns of Kona Coast groundwaters are
relatively flat between La and Dy (Fig. 5). These flat patterns support the notion that
chemical weathering of the local basalt is the chief source of REEs to the groundwaters,
and hence, to the coastal ocean. Furthermore, the flat basalt-normalized REE patterns of
the groundwaters indicate that little fractionation of the LREEs and the MREEs occurs
during chemical weathering and dissolution of the Hualalai basalts, and subsequent
transport of REEs through the subterranean estuary. In contrast, REEs heavier than Dy
(i.e., Ho through Lu) are enriched in Kona Coast groundwaters when normalized to the

Hualalai basalts compared to the LREEs and MREEs, indicating that the HREEs are

668	more mobile during chemical weathering of the local Kona Coast basalts. These
669	observations are consistent with many previous studies of REE behavior during chemical
670	weathering (Nesbitt, 1979; Duddy, 1980; Braun et al., 1990, 1993; Nelson et al., 2004).
671	The origin of the REE fractionation patterns of Kona Coast groundwaters can be
672	understood by considering the following conceptual model. When local rainwater (pH ~
673	4.8; Eriksson, 1957; Berner and Berner, 2012) infiltrates the Hualalai basalts, its acidity
674	is sufficient to corrode the volcanic glass that dominates these basalts as well as any
675	phenocryst minerals (e.g., olivine), releasing REEs into solution. The relative distribution
676	(i.e., fractionation pattern) of the REEs in the initial weathering solution/groundwater will
677	likely resemble the fractionation pattern of the bulk rock, or more specifically, the
678	dominant basaltic glass component of these basalt flows (e.g., Price et al., 1991).
679	Secondary minerals formed during low-temperature chemical weathering of basaltic glass
680	(e.g., clay minerals, Fe/Mn oxides/oxyhydroxides, and especially rhabdophane)
681	preferentially capture the LREEs, and to a lesser extent, the MREEs, that are mobilized
682	during weathering compared to the HREEs, which are more stable in solution as
683	carbonate complexes (Humphris, 1984; Eggleton et al., 1987; Price et al., 1991; Fodor et
684	al., 1992a, b, 1994; Gillis et al., 1992; Nesbitt and Wilson, 1992; Daux et al., 2004;
685	Cotton et al., 1995; Stefánsson and Gíslason, 2001; Ziegler et al., 2003). As chemical
686	weathering proceeds, bicarbonate ions are produced and pH rises, as does the
687	concentrations of dissolved carbonate ions. Together, these processes act to
688	preferentially sequester LREEs and MREEs by adsorption onto, or uptake within,
689	secondary minerals, whereas the HREEs are preferentially mobilized from sites of active
690	weathering by strong complexing ligands like carbonate ions and subsequently

691	transported, as dissolved complexes, with flowing groundwater (Ronov et al., 1967;
692	Aagaard, 1974; Nesbitt, 1979; Duddy, 1980; Braun et al., 1990, 1993; Johannesson et al.,
693	1999; 2005; Tang and Johannesson, 2010a). Comparable arguments have been advanced
694	to explain the similar input-normalized REE fractionation patterns of groundwaters from
695	the Wanapum Basalt aquifer in northern Idaho and eastern Washington (Nelson et al.,
696	2004).
697	The enrichment of the HREEs in the Kona Coast groundwaters compared to the
698	basaltic aquifer rocks is consistent with the conceptual model as well as the results of the
699	solution complexation modeling, which predicts that HREEs chiefly occur in these
700	groundwater as highly stable, negatively charged dicarbonato complexes, Ln(CO ₃) ₂ (Fig.
701	8). In contrast, substantial amounts of the LREEs (e.g., more than 40% and 8% of La in
702	Honokohau Harbor Well waters) are predicted to occur in solution as positively charged
703	carbonato complexes, LnCO ₃ ⁺ , and free metal ions, Ln ³⁺ , respectively (Fig. 8). Because
704	the stability constants describing the formation of dissolved REE carbonato and
705	dicarbonato complexes increase by more than 10- and 117-fold, respectively, with
706	increasing atomic number across the REE series (Luo and Byrne, 2004), the HREEs form
707	stronger aqueous carbonate complexes than either the LREEs or MREEs. The formation
708	of strong aqueous complexes lowers the activity of the free metal ion, which inhibits
709	surface complexation of the HREEs onto - or uptake within - secondary minerals like
710	metal oxides/oxyhydroxides, compared to the LREEs, and to a lesser degree, the MREEs,
711	during weathering and subsequent transport of the REEs through the coastal basalt
712	aquifers (Byrne and Kim, 1990; Koeppenkastrop and De Carlo, 1992, 1993; Quinn et al.,
713	2004, 2006; Tang and Johannesson, 2005). We note that estimates of the point of zero net

proton charge for Hawaiian basalts are less than 6.2 and 5.8 for 0.001 and 0.01 molar solutions, respectively (Chorover et al., 2004), suggesting that in addition to free metal ions, REE carbonato complexes, but not dicarbonato complexes, will also adsorb onto surfaces of the local basalt aquifer. Consequently, the HREEs are predicted to be more mobile in the Kona Coast groundwater system compared to the MREEs, and especially the LREEs.

5.2. Mixing experiments

The results of the Kona Coast mixing experiments differ dramatically from similar experiments involving river waters. Specifically, substantial removal of REEs from solution is commonly reported in laboratory experiments in which river water is mixed with seawater, with the majority of the REEs being removed at low salinity (i.e., 0 to 10; Hoyle et al., 1984; Sholkovitz, 1995). In contrast, the REEs were released into solution when Kona Coast groundwaters were mixed with local seawater (Figs. 6, 7). It should be noted that in the mixing experiments conducted by Sholkovitz (1995) the water samples were filtered through 0.22 µm filters prior to mixing, whereas in our experiments, the water samples were mixed prior to filtration. Consequently, our experiments are more akin to those of Hoyle et al. (1984) in which river water filtered through 18 µm pore-size filters were mixed with seawater that had been filtered through 5 µm pore-size filters. Consequently, because we mixed Kona Coast groundwaters with seawater prior to filtration, suspended particulate matter, as well as colloids, were available to coagulate, flocculate, and remove REEs from solution. Nevertheless, the

Kona Coast	mixing	experiments	induced	mobilization	of	REEs	to	the	dissolved	phase
instead of rea	moval (F	Figs. 6, 7).								

The loss of REEs from solution observed in earlier laboratory investigations that
employed river waters was ascribed to salt-induced coagulation and flocculation of Fe-
rich, organic colloids at low salinity, which scavenged the REEs and other trace metals
from solution, and then settled out of suspension (Sholkovitz, 1976, 1993, 1995; Boyle et
al., 1977, 1982; Sholkovitz and Copland, 1981; Hoyle et al., 1984). Transects through a
number of surface estuaries also reveal substantial removal of REEs from solution in the
low salinity regions where river water initially encounters seawater, in agreement with
the bottle mixing experiments discussed above (e.g., Martin et al., 1976; Goldstein and
Jacobsen, 1988a; Sholkovitz and Elderfield, 1988; Elderfield et al., 1990; Sholkovitz,
1993, 1995; Sholkovitz and Szymczak, 2000; Lawrence and Kamber, 2006; Censi et al.,
2007; Åström et al., 2012; Rousseau et al., 2015). Again, the same mechanism of salt-
induced coagulation and flocculation of Fe-rich, organic colloids, can explain REE
removal from the water column in the low salinity region of these surface water estuaries.
It should be noted that a number of field-based estuarine studies have also reported
release of REEs back to the water column at mid to high salinities (i.e., salinity > 20),
although the fraction of REEs released back to solution is generally small compared to
the amount removed in the low salinity region of the estuary (e.g., Sholkovitz, 1995;
Sholkovitz and Szymczak, 2000; Lawrence and Kamber, 2006). The release of REEs in
the mid to high salinity region of estuaries likely reflects diagenetic processes occurring
in estuary sediments and associated porewaters such as reductive dissolution of
Fe(III)/Mn(IV) oxides/oxyhydroxides and subsequent release of sorbed or co-precipitated

759	REEs, remineralization of organic matter containing sorbed/complexed REEs, and/or
760	displacement of REEs from mineral surfaces by marine salts (Elderfield and Sholkovitz,
761	1987; Sholkovitz et al., 1989, 1992; Haley et al., 2004). Release of REE in the Kona
762	Coast subterranean estuary mixing experiments occurs as substantially lower salinities (7
763	- 8) compared to the mid to high salinities where REE release is reported to occur in
764	surface estuaries (> 20; Sholkovitz and Szymczak, 2000).
765	A possible explanation of the REE behavior in the Kona Coast mixing experiment
766	may be related to the fact that these coastal groundwaters are brackish and not fresh
767	(Table 2), and consequently REEs were previously removed from solution further up
768	gradient in the subterranean estuary where fresh groundwater first encounters
769	recirculating seawater. In this case, fresh Kona Coast groundwater (i.e., salinity ~ 0)
770	would be expected to exhibit higher REE concentrations than the nearshore, brackish
771	groundwaters analyzed here. However, a number of features of the Kona Coast
772	subterranean estuary argue against this possibility. First, other than Gd in the Honokohau
773	Harbor well, there is relatively little difference in the REE concentrations of the Kona
774	Coast groundwater samples despite their range in salinity. For example, notwithstanding
775	the fact that groundwater from the KAHO 3 well is 6-fold more saline, exhibits a Cl
776	concentration that is 6 times higher, and an ionic strength that is a factor of 3.6 greater
777	than groundwater from the Hind (i.e., Lava tube) well, the Nd concentration of the fresher
778	Hind well groundwater is only 1.2 times higher than in the more saline KAHO 3 well
779	groundwater (Tables 2, 4). Moreover, the Nd concentration of the fresher groundwater
780	from the Hind well is less than a factor of 1.1 higher than Nd in the Honokohau Harbor

well groundwater, regardless of the fact that the latter groundwater is 2.4 times more

782	saline. Furthermore, Tillman et al. (2014a) recently reported concentrations for some
783	REEs in groundwaters from the Kona Coast, including fresh (salinity ~ 0), groundwaters
784	from wells that are up gradient from the brackish nearshore groundwaters we sampled.
785	Although Tillman et al. (2014a) do not report data for the majority of the REEs, they do
786	present concentrations for La (mean \pm standard deviation = 8.8 \pm 5.5 pmol kg ⁻¹ , n = 3),
787	Ce (mean = 21 pmol kg $^{-1}$, n = 2), and Pr (mean = 27.6 pmol kg $^{-1}$, n = 2) for fresh Kona
788	Coast groundwaters. The La and Ce concentrations of these fresh groundwaters are, on
789	average, 16-fold lower than in the nearshore, brackish Kona Coast groundwaters, and Pr
790	is nearly 1.5 times lower in the fresh groundwaters (Table 4). Taken together, these
791	observations, and the fact that the nearshore Kona Coast groundwaters exhibit similar
792	REE concentrations to the coastal seawater (Fig. 4), indicate that large-scale removal of
793	REEs, which characterizes the behavior of the REEs in the low salinity region of many
794	surface estuaries, is not a feature of the subterranean estuary along the Kona Coast.
795	The lack of removal of REEs from solution in the Kona Coast mixing
796	experiments, and by inference, the Kona Coast subterranean estuary, instead likely
797	reflects the much lower dissolved organic carbon concentrations, as well as the lower
798	dissolved Fe and Mn concentrations, of these groundwaters compared to previously
799	studied rivers and associated surface estuaries that exhibit REE removal (Table 3). For
800	example, DOC concentrations are between 4 and 21 times greater in these rivers and their
801	associated estuaries than in Kona Coast groundwaters, excluding groundwater from the
802	Honokohau Harbor well, which again receives effluent from the WWTF (e.g., Parsons et
803	al., 2008; Hunt, 2014; Prouty et al., 2016; Table 3). Dissolved Fe concentrations in these
804	rivers and surface estuaries are also commonly between 2- and 5-fold higher than in Kona

Coast groundwaters (Tables 2, 3). In fact, the Kona Coast groundwaters have Fe
concentrations that are either identical to the coastal seawater sample (i.e., 11.6 nmol kg
1) or below detection (i.e., < 3 nmol kg $^{-1}$; Table 2). The one exception is groundwater
from the KAHO 2 well, which has a Fe concentration of 62.5 nmol kg ⁻¹ . The low DOC
and Fe concentrations that characterize Kona Coast groundwaters likely inhibit salt-
induced flocculation and coagulation, and hence REE removal, when the groundwater
mixes with seawater in local subterranean estuaries. The low DOC concentrations of
Kona Coast groundwaters reflect the arid climate and sparse surface vegetation of this
leeward desert, whereas the low Fe and Mn concentrations are explained by the oxic
nature of these groundwaters (83.4 μ mol kg ⁻¹ \leq DO \leq 252 μ mol kg ⁻¹ ; Table 2), and their
relatively short groundwater residence times in the aquifer (~ 30 years; Kelly and Glenn,
2015). We note that Hoyle et al. (1984) also reported no detectable REE loss across the
salinity gradient in the organic matter-poor Wharfe River estuary in the United Kingdom.
The release of REEs to solution in the mixing experiments reflects a combination
of processes that are related to changes in REE solution complexation across the salinity
gradients in each experiment (Figs. 9, 10). These changes are chiefly driven by increasing
pH, which leads to increases in the concentrations of carbonate ions, [CO ₃ ² -], and to a
lesser extent by the salinity increase that accompanies mixing of the terrestrial
groundwaters with coastal seawater. The effect of increasing pH and changing solution
composition is to increase the amount of each REE in solution that is complexed to
strong dissolved ligands, namely carbonate ions [i.e., LnCO ₃ +, Ln(CO ₃) ₂ -], which
concomitantly decreases the amount of each REE in solution that occurs as free metal
ions, Ln ³⁺ (Figs. 9, 10). The decrease in free metal ion activity across the mixing gradient

helps drive REE desorption from suspended particles or colloids during mixing (Figs. 9,
10; Comans and van Dijk, 1988). Hence, the lower pH of Honokohau Harbor well water
(pH 6.9) compared to groundwater from the Hind well (pH 7.7) explains, in part, the
greater release of REEs in general, and the LREEs in particular, in the lower salinity
samples from the Honokohau Harbor mixing experiment compared to the Lava Tube
mixing experiment. The predicted predominance of aqueous REE dicarbonato complexes
across the salinity gradient of both mixing experiments (Figs. 9, 10) further inhibits REE
adsorption, and instead promotes desorption of REEs from suspended particles or
colloids in these mixed solution (e.g., Tang and Johannesson, 2005).

Increasing salinity also likely plays a role in the release of REEs from suspended particles or colloids during mixing. More specifically, increases in the concentrations of competing cations, namely Mg²⁺ and Ca²⁺, that accompanies increasing salinity can promote desorption of REEs (Tang and Johannesson, 2005, 2010b). Moreover, competitive sorption reactions are commonly more important at low pH where these reactions affect the LREEs to a greater extent than either the MREEs or HREEs (Tang and Johannesson, 2005, 2010b).

The results of the solution – surface partition model for the REEs are also generally in agreement with the observations of the mixing experiments. For example, the partition model suggests that the LREEs exhibit a greater affinity for the solution phase at lower salinities in the Honokohau Harbor mixing experiment compared to the MREEs and HREEs, which is also observed in the mixing experiment. The greater affinity of the LREEs for the solution phase predicted for the Honokohau Harbor mixing experiment compared to the Lava Tube mixing experiment can again be explained by the lower pH

of the endmember groundwater (Honokohau Harbor well water, pH 6.9) compared to the
Hind well (pH 7.7). The partition model results are consistent with the notion that
relatively more of the REEs in general, and the LREEs in particular, are released from
suspended particles or colloids in the Honokohau Harbor mixing experiment as pH
increases and the formation of strong aqueous, dicarbonato complexes become
progressively more abundant. In contrast, because groundwater from the Hind well is
nearly a whole pH unit higher than Honokohau Harbor well water, the majority of surface
bound REEs have already been stripped from suspended particles or colloids by
formation of aqueous REE dicarbonato complexes. As a consequence the partition model
predicts only small variations in the partitioning behavior of the REEs across the salinity
gradient for the Lava Tube mixing experiment.

5.3. Submarine groundwater discharge fluxes

The groundwater flux of REEs to the ocean along the Kona Coast is estimated using the volumetric SGD fluxes determined by Peterson et al. (2009), and assuming that the behavior of the REEs in the mixing experiments is representative of their behavior in Kona Coast subterranean estuaries. The SGD fluxes from Peterson et al. (2009) are employed because these researchers investigated SGD at both Honokohau Harbor, as well as at Kiholo Bay, which corresponds with our Lava Tube mixing experiments, hence, providing a consistent set of SGD estimates for our two study sites.

To model REE release across the salinity gradient at the Honokohau Harbor and Kiholo Bay sites, we employ the method developed by Li and Chan (1979) for trace elements that behave nonconservatively in estuarine systems. The approach follows from

874	the work of Boyle et al. (1977), Hanor and Chan (1977), and Officer (1979), whereby	y the
875	release rate of a particular nonconservative trace element is estimated by constructi	ng a
876	chord or a tangent line from the ocean endmember through the highest salinity point(s	s) on
877	the nonconservative trace element concentration versus salinity distribution curve fo	r the
878	estuary, or in our case, the salinity gradient of the mixing experiment (Li and Chan, 1	979;
879	Maeda and Windom, 1982; Swarzenski et al., 1995). Commonly, the tangent lin	ne is
880	approximated by linear regression from the ocean endmember through the more sa	aline
881	water samples and back to 0 salinity (Li and Chan, 1979; Swarzenski et al., 1995; No	zaki
882	et al., 2001). The resulting y-intercept of the tangent line, or computed linear regres	ssion
883	line, is an estimate of the effective terrestrial water endmember concentration of	f the
884	nonconservative trace element (Li and Chan, 1979; Head, 1985, and references there	ein).
885	For the Kona Coast subterranean estuaries, the resulting y-intercept is the effect	ctive
886	freshwater endmember concentration of the particular REE.	
887	The model assumes steady state conditions, which implies mass balance equat	tions
888	for water, salts, and the nonconservative species of interest (Li and Chan, 1979). Fo	r the
889	water balance, we have	
890	$Q_{TotSGD} = Q_{TSGD} + Q_{MarineSGD}, ($	3)
891	in which Q _{TSGD} and Q _{MarineSGD} are the terrestrial and marine SGD (m ³ day ⁻¹), which w	vhen
892	combined, gives the total SGD flux, Q _{TotSGD} (e.g., Martin et al., 2007; Johannesson e	t al.,
893	2011). The salt mass balance, written in terms of the salinity, S , is	
894	$Q_{\text{TotSGD}}S_{\text{TotSGD}} = Q_{\text{TSGD}}S_{\text{TSGD}} + Q_{\text{MarineSGD}}S_{\text{MarineSGD}}, \tag{4}$	4)

- where S_{TotSGD} , S_{TSGD} , and $S_{\text{MarineSGD}}$ represent the salinity of the total SGD, the terrestrial sourced SGD, and the marine sourced SGD fluxes. The mass balance for each REE is then given by
- $Q_{\text{TotSGD}}[\text{Ln}]_{\text{TotSGD}} = Q_{\text{TSGD}}[\text{Ln}]_{\text{TSGD}} + Q_{\text{MarineSGD}}[\text{Ln}]_{\text{MarineSGD}} + J_{\text{desorb}}^{[\text{Ln}]}$ (5)
- where [Ln]_{TotSGD}, [Ln]_{TSGD}, and [Ln]_{MarineSGD} are the individual REE concentrations in the
- 900 total, terrestrial sourced, and marine sourced SGD, and $J_{\rm desorb}^{\rm [Ln]}$ is the desorption (i.e.,
- 901 release rate) flux of each individual REE from suspended particles or colloids to solution
- 902 (e.g., Li and Chan, 1979; Swarzenski et al., 1995). Combining equations 3 through 5,
- and rearranging yields

904
$$[Ln]_{TSGD} + \frac{J_{desorb}^{[Ln]}}{Q_{TSGD}} = [Ln]_{TotSGD} - (S_{TotSGD} - S_{TSGD}) \frac{[Ln]_{TotSGD} - [Ln]_{MarineSGD}}{S_{TotSGD} - S_{MarineSGD}},$$

or, more simply

906
$$[Ln]_{TSGD} + \frac{J_{desorb}^{[Ln]}}{Q_{TSGD}} = [Ln]_{TotSGD} - (S_{TotSGD} - S_{TSGD}) \frac{\Delta[Ln]}{\Delta S},$$
 (6)

- where the left hand side of equation 6 is the effective terrestrial SGD concentration for any given REE, which again represents the *y*-intercept of the tangent line described above
- 909 (Li and Chan, 1979; Head, 1985; Swarzenski et al., 1995).
- Our mixing experiments is difficult because the data commonly exhibit multiple peaks and troughs (Figs. 6, 7). Moreover, models for desorbing, nonconservative trace elements (e.g., Hanor and Chan, 1977) imply that plots of trace element concentrations versus salinity may be persistently concave-down that is, there may be no straight-line region of the trend from which to construct the dilution line as is commonly recommended (Boyle et al., 1974). However, these issues can be approached statistically, whereby the

917

918

919

920

921

922

923

924

925

926

927

928

929

930

931

932

933

934

935

936

937

938

trace element concentration variations across the salinity gradient can be modeled using a bootstrap (see electronic annex and Fig. EA3 for details), which approximates plausible sampling distributions by drawing with replacement (Efron and Tibshirani, 1986). The nonlinear character of the REE concentration versus salinity curves (e.g., Figs. 6 and 7) can be modeled using local regressions or *loess* fits to each of the bootstrap samples (see electronic annex; Cleveland et al., 1992). The loess fit can then be scanned to find the point $(S, [Ln]_{aq})$ for which $\frac{[Ln]_{aq}^{Marine} - [Ln]_{aq}}{S^{Marine} - S}$ is maximized. This point represents the point of maximum desorption/release of the REE in the mixing experiment, which can occur anywhere between the two endmembers. Here, [Ln]_{aq}^{Marine} is the concentration of the particular REE in the ocean endmember sample and S^{Marine} is the salinity of the ocean endmember, whereas $[Ln]_{aq}$ and S are the REE concentration and salinity value for any sample between the terrestrial and ocean endmembers. The statistical analysis of the mixing experiment data was implemented in statistical software (R Core Team, 2015). The bootstrap procedure was modified so that the endmembers of the mixing experiments are always included in the sample, and the loess fit is forced through the endmembers (Fig. EA3 in the electronic annex). For each bootstrap sample, estimated errors at each measured sample point (including endmembers) were added to the measurements. A large bootstrap sample (10⁴) yielded stable estimates of the effective terrestrial groundwater endmember (i.e., salinity of zero) REE concentration (y-intercept = $[Ln]_{TSGD} + \frac{J_{desorb}^{[Ln]}}{Q_{TSGD}}$), along with its nonparametric distributions (Figs. 13 and EA3). Distributions can also be computed for the desorptiondilution line and the measurements per se (see Fig. 13).

Application of the model to Nd is shown in Fig. 13 for both the Honokohau
Harbor and Lava Tube mixing experiments. Results for the other 13 REEs for both the
Honokohau Harbor and Lava Tube mixing experiments are presented in the Figs. EA4
through EA17 in the electronic annex. The orange-brown curved line shows the median
loess fit to the measured Nd concentrations, and the orange-brown field represents the
95% confidence interval for the loess fit to the data. Likewise, the dark blue straight line
constructed from the ocean endmember to salinity of zero, the corresponding y-intercept,
is the median of the bootstrap sample for the tangent line of these data, whereas the light
blue triangular field is the 95% confidence interval. That is, the effective terrestrial
groundwater Nd concentrations for the mixing experiment data should fall within the
range of potential y-intercepts shown on Fig. 13 with 95% confidence, with the median
effective terrestrial groundwater Nd concentration of the bootstrap depicted as the blue
circle. The inferred distributions of the effective terrestrial groundwater REE
concentrations are commonly skewed (Figs. EA18 – EA31), which motivated the use of
nonsymmetric confidence intervals along with the median as a point estimate.

Combining the terrestrial groundwater discharge fluxes for Honokohau Harbor (8600 m³ day⁻¹) and Kiholo Bay (6300 m³ day⁻¹) from Peterson et al. (2009), with our computed estimates of the effective terrestrial groundwater REE concentrations determined as shown above for Nd, and the other 13 REEs in Figs. EA4 – EA17 in the electronic annex, provides estimates of the total SGD fluxes of REEs to the coastal ocean at Honokohau Harbor and Kiholo Bay (Tables 5 and 6). For example, in the case of Nd, we estimate that the total SGD flux of Nd to the coastal ocean ranges between 1909 µmol day⁻¹ and ca. 2590 µmol day⁻¹ (median ca. 2200 µmol day⁻¹) in the vicinity of Honokohau

Harbor, and between 1290 μmol day ⁻¹ and 1700 μmol day ⁻¹ (median ca. 1450 μmol day ⁻¹)
at Kiholo Bay (Tables 5 and 6). The desorption flux, or release rate, of Nd during mixing
in the subterranean estuary is estimated to range from 370 μ mol day ⁻¹ to 1050 μ mol day ⁻¹
(median ca. 660 μmol day ⁻¹) at Honokohau Harbor, and from 82 μmol day ⁻¹ to 490 μmol
day ⁻¹ (median ca. 239 μmol day ⁻¹) at Kiholo Bay. Hence, the Nd desorption flux
represents between 19% and 41% (median ca. 30%) of the total SGD flux of Nd to the
coastal ocean near Honokohau Harbor, and between 6.3% and 29% (median = 16.5%) of
the total SGD flux of Nd at Kiholo Bay. Consequently, our estimates suggest that REE
release from suspended particles or colloids in subterranean estuaries along the Kona
Coast represents a significant fraction of the total groundwater flux of REEs to the coastal
ocean. Field-testing by sampling groundwaters from wells/piezometers constructed along
a salinity gradient will be necessary to verify whether REE release from suspended
particles or colloids upon mixing of groundwater and seawater is characteristic of Kona
Coast subterranean estuaries.
The SGD fluxes of the REEs estimated for the Kona Coast are of the same order
of magnitude as our recent estimates for SGD fluxes of REEs to the coastal ocean in
Rhode Island and Florida (Chevis et al., 2015a, b). Specifically, Chevis et al. (2015b)
estimated a SGD flux of Nd of 26 ± 11 mmol day ⁻¹ in the vicinity of the Pettaquamscutt
River estuary in Rhode Island, and Chevis et al. (2015b) computed a SGD flux for Nd to
the Indian River Lagoon in Florida of 9.4 ± 1 mmol day ⁻¹ . Again, our best estimate of the
SGD flux of Nd to the coastal ocean near Honokohau Harbor is 2.2 mmol day ⁻¹ , whereas
at Kiholo Bay, our best estimate is 1.4 mmol day ⁻¹ of Nd delivered to the coastal ocean
via SGD (Tables 5.6). The SGD fluxes of the RFFs to the coastal ocean in the vicinity of

the Pettaquamscutt River estuary in Rhode Island and the Indian River Lagoon in Florida are also of similar magnitude to the estimated surface water influxes to both systems (36 mmol day⁻¹ and 7.7 ± 1 mmol day⁻¹, respectively; Chevis et al., 2015a, b). Although no streams discharge to the ocean along the studied portion of the Kona Coast, the slightly lower SGD fluxes of the REEs to these coastal waters (e.g., when compared to the Pettaquamscutt River estuary and Indian River Lagoon) are sufficient to overwhelm background seawater REE concentrations, which results in REE concentrations that are ca. 10-fold higher, and as much as 50-fold higher than REE concentrations measured in North Pacific surface waters. These observations suggest that even arid regions of oceanic islands can generate SGD fluxes of the REEs that represent the major source of these trace elements to the proximal ocean (see also Fröllje et al., 2016). Our results support previous investigations at Jeju Island, South Korea, where SGD fluxes of REEs also appear to comprise the primary material flux of these trace elements to coastal waters (Kim and Kim, 2011, 2014).

6. Conclusions

The similarity in the REE fractionation patterns between the Kona Coast groundwater and coastal seawater, the 10- to 50-fold enrichment in REEs concentrations of Kona Coast seawater over open-ocean, North Pacific seawater, and the lack of surface streams along the Kona Coast, all point to SGD being the chief source of REEs to the coastal ocean along the Kona Coast of the Big Island of Hawaii. This notion is further supported by the nearly identical shale-normalized REE pattern of local groundwaters and seawater, which are markedly flatter than the shale-normalized REE patterns of

North Pacific seawater. Treated wastewaters from a local wastewater treatment facility
(WWTF) can also be traced from nearshore well waters into the coastal ocean by means
of large positive Gd anomalies, which further supports SGD as the chief source of REEs
to these coastal waters. Normalization of the groundwater REE concentrations to the REE
content of local Hualali basalt flows indicate that chemical weathering of these basalts is
the primary source of REEs to the groundwater, and hence, coastal ocean, and that
dissolved HREE concentrations are enhanced relative to the basalts by formation of
strong solution complexes with dissolved carbonate ions. Sequential filtration of the
groundwaters through $0.45~\mu m$ and then $0.02~\mu m$ filters returns statistically
indistinguishable REE concentrations indicating that dissolved REEs are transported in
Kona groundwaters to the ocean as "truly dissolved" ionic species or low molecular
weight colloids.

Laboratory mixing experiments reveal that the REEs are released from suspended particles or colloids to solution when Kona Coast groundwaters are mixed with local seawater. The lack of REE removal from solution in the mixing experiments, and hence, by inference, Kona Coast subterranean estuaries, is attributed to the low DOC and Fe concentrations of the local groundwater. This finding differs from observations of the behavior of REEs in many surface estuaries where REEs are removed to a large degree from solution where river waters first mix with seawater. Geochemical modeling indicates that REE release to solution in the mixing experiments is driven by increases in pH, decreasing free metal ion activity, and the concomitant formation of strong, aqueous REE dicarbonato complexes [i.e., Ln(CO₃)₂]. Formation of REE dicarbonato complexes accounts for progressively more of each REE as pH and salinity increases. These strong

aqueous complexes outcompete adsorption for the REEs, and hence facilitate release of REEs to the solution phase. Rare earth element release is also likely enabled by competition from more abundant cations (e.g., Mg²⁺, Ca²⁺) for solid phase surface sites as salinity increases, which can displace sorbed REEs from suspended particles or colloids.

Estimates of REE fluxes to the coastal ocean via SGD (i.e., 1.3 – 2.6 mmol Nd day⁻¹) are of similar magnitude to our recent estimates for SGD fluxes of REEs to the Indian River Lagoon in Florida, and to Rhode Island Sound in the vicinity of the Pettaquamscutt River estuary. Our investigation of the Kona Coast, in conjunction with our previous studies of subterranean estuaries beneath the Indian River Lagoon and the Pettaquamscutt River estuary, all indicate that SGD is an important source of REEs to the coastal ocean. Moreover, our research, along with recent studies in Korean (Kim and Kim, 2011, 2014), are consistent with SGD being an important, albeit, previously unrecognized component of the global oceanic REE budget.

Acknowledgements

This project was supported by NSF grants OCE-0825920 to Johannesson and OCE-0825895 to Burdige, as well as USGS Natural Resources Preservation Program (NRPP) and Park Oriented Biological Support (POBS) Award to Prouty. The authors wish to thank C. H. Conaway at the U.S. Geological Survey in Menlo Park, California, for the ion chromatography analyses of the anion concentrations, and D. Gross and S. Beavers (NPS) for logistical support. The lead author is indebted to Michael and Mathilda Cochran for endowing the Cochran Family Professorship in Earth and Environmental Sciences at Tulane University. We thank two anonymous reviewers and

1054	the associate editor Jerôme Gaillardet whose comments greatly improved this paper.
1055	This paper is dedicated to the memory of Lutetium Johannesson.
1056	
1057	References
1058	Aagaard P. (1974) Rare earth element adsorption on clay minerals. Bull. Group. Franc.
1059	Argiles 26 , 193-199.
1060	Adams W. M. and Lepley L. K. (1968) Infrared images of the Kau and Puna coastlines
1061	on Hawaii. Water Resources Research Center, University of Hawaii at Manoa,
1062	Tech. Rept. No. 26, HIG Series, HIG-WRRC-2, Honolulu, 15 p.
1063	Alibo D. S. and Nozaki Y. (1999) Rare earth elements in seawater: Particle association,
1064	shale-normalization, and Ce oxidation. Geochim. Cosmochim. Acta 63, 363-372.
1065	Arsouze T., Dutay JC., Lacan F. and Jeandel C. (2009) Reconstructing the Nd oceanic
1066	cycle using a coupled dynamical-biogeochemical model. Biogeosci. Discuss. 6,
1067	5549-5588.
1068	Åström M. E., Österholm P., Gustaffson J. P., Nystrand M., Peltola P., Normmyr L., and
1069	Boman A. (2012) Attenuation of rare earth elements in a boreal estuary. Geochim.
1070	Cosmochim. Acta 96 , 105-119.
1071	Balistrieri L., Brewer P. G., and Murray J. W. (1981) Scavenging residence times of trace
1072	metals and surface chemistry of sinking particles in the deep ocean. Deep-Sea
1073	Res. 28A, 101-121.
1074	Bau M. and Dulski P. (1996) Anthropogenic origin of positive gadolinium anomalies in
1075	river waters. Earth. Planet. Sci. Lett. 143, 245-255.
1076	Berner E. K. and Berner R. A. (2012) Global Environment: Water, Air, and Geochemical

Cycles. 2nd ed. Princeton University Press, Princeton, NJ, 444 p. 1077 1078 Bertram C. J. and Elderfield H. (1993) The geochemical balance of the rare earth 1079 elements and neodymium isotopes in the oceans. Geochim. Cosmochim. Acta 57, 1080 1957-1986. Bethke C. M. (2008) Geochemical and Biogeochemical Reaction Modeling, 2nd 1081 1082 Cambridge University Press, Cambridge, UK (543 pp.) Bethke C. M. and Yeakel S. (2013) The Geochemist's Workbench®, Release 9.0. GWB 1083 1084 Essentials Guide. Aqueous Solutions, LLC., Champaign, IL (130 pp.) 1085 Bienfang P. (1980) Water quality characteristics of Honokohau Harbor: A subtropical 1086 embayment affected by groundwater intrusion. Pac. Sci. 34, 279-291. 1087 Boyle E. A., Collier R., Dengler A. T., Edmond J. M., Ng A. C., and Stallard R. F. (1974) On the chemical mass-balance in estuaries. Geochim. Cosmochim. Acta 38, 1719-1088 1089 1728. Boyle E. A., Edmond J. M., and Sholkovitz E. R. (1977) The mechanism of iron removal 1090 in estuaries. Geochim. Cosmochim. Acta 41, 1313-1324. 1091 1092 Boyle E. A., Huested S. S., and Grant B. (1982) The chemical mass balance of the 1093 Amazon Plume – II. Copper, nickel, and cadmium. Deep-Sea Res. 11A, 1355-1364. 1094 1095 Braun J. J., Pagel M., Muller J. P., Bilong P., Michard A., and Guillet B. (1990) Cerium 1096 anomalies in lateritic profiles. Geochim. Cosmochim. Acta 54, 597-605. Braun J. J., Pagel M., Herbillon A. and Rosen C. (1993) Mobilization and redistribution 1097 1098 of REEs and thorium in a syenitic lateritic profile: A mass balance study. 1099 Geochim. Cosmochim. Acta 57, 4419-4434.

1100	Burdige D. J. and Gardner K. G. (1998) Molecular weight distribution of dissolved
1101	organic carbon in marine sediment pore waters. Mar. Chem. 62, 45-64.
1102	Burnett W. C., Bokuniewicz H., Huettel M., Moore W. S. and Taniguchi M. (2003)
1103	Groundwater and pore water inputs to the coastal zone. Biogeochemistry 66, 3-
1104	33.
1105	Byrne R. H. and Kim KH. (1990) Rare earth element scavenging in seawater. <i>Geochim</i> .
1106	Cosmochim. Acta 54 , 2645-2656.
1107	Byrne R. H. and Kim KH. (1993) Rare earth precipitation and coprecipitation behavior:
1108	The limiting role of PO ₄ ³⁻ on dissolved rare earth concentrations in seawater.
1109	Geochim. Cosmochim. Acta 57, 519-526.
1110	Byrne R. H., Lee J. H., and Bingler L. S. (1991) Rare earth element complexation by
1111	PO ₄ ³⁻ ions in aqueous solution. <i>Geochim. Cosmochim. Acta</i> 55 , 2729-2735.
1112	Byrne, R.H., Liu, X., 1998. A coupled riverine-marine fractionation model for dissolved
1113	rare earths and yttrium. Aquatic Geochem. 4, 103-121.
1114	Cai WJ., Wang Y., Krest J. and Moore W. S. (2003) The geochemistry of dissolved
1115	inorganic carbon in a surficial groundwater aquifer in North Inlet, South Carolina,
1116	and the carbon fluxes to the coastal ocean. Geochim. Cosmochim. Acta 67, 631-
1117	637.
1118	Censi P., Sprovieri M., Saiano F., Di Geronimo S. I., Larocca D., and Placenti F. (2007)
1119	The behaviour of REEs in Thailand's Mae Klong estuary: Suggestions from the
1120	Y/Ho ratios and lanthanide tetrad effects. Estuar. Coast. Shelf Sci. 71, 569-579.
1121	Charette M. A. and Buesseler K. O. (2004) Submarine groundwater discharge of nutrients
1122	and copper to an urban subestuary of Chesapeake Bay (Elizabeth River). Limnol.

1123	Oceanogr. 49 , 376-385.
1124	Charette M. A., Sholkovitz E. R. and Hansel C. M. (2005) Trace element cycling in a
1125	subterranean estuary: Part 1. Geochemistry of the permeable sediments. Geochim.
1126	Cosmochim. Acta 69 , 2095-2109.
1127	Chevis D. A., Johannesson K. H., Burdige D. J., Tang J., Moran S. B., and Kelly R. P.
1128	(2015a) Submarine groundwater discharge of rare earth elements to a tidally-
1129	mixed estuary in Southern Rhode Island. Chem. Geol. 397, 128-142.
1130	Chevis D. A., Johannesson K. H., Burdige D. J., Cable J. E., Martin J. B., and Roy M.
1131	(2015b) Rare earth element cycling in a sandy subterranean estuary in Florida,
1132	USA. Mar. Chem. 176 , 34-50.
1133	Chorover J., Amistadi M. K., and Chadwick O. A. (2004). Surface charge evolution of
1134	mineral-organic complexes during pedogenesis in Hawaiian basalt. Geochim.
1135	Cosmochim. Acta 23 , 4859-4876.
1136	Church T. M. (1996) An underground route for the water cycle. <i>Nature</i> 380 , 579–580.
1137	Clague D. A. and Bohrson W. A. (1991) Origin of xenoliths in the trachyte of Puu
1138	Waawaa, Hualalai Volcano, Hawaii. Contrib. Mineral. Petrol. 108, 439-452.
1139	Clague D. A. and Dalrymple G. B. (1987) The Hawaiian-Emperor volcanic chain. Part 1:
1140	Geologic evolution. In: R. W. Decker, T. L. Wright, and P. H. Stauffer (Eds),
1141	Volcanism in Hawaii, U. S. Geol. Surv. Prof. Pap. 1350, 5-55.
1142	Clague D. A., Jackon E. D., and Wright T. L. (1980) Petrology of Hualalai Volcano,
1143	Hawaii: Implications for mantle composition. <i>Bull. Volcanol.</i> 43-3 , 641-656.
1144	Clegg S. L. and Sarmiento J. L. (1989) The hydrolytic scavenging of metal ions by
1145	marine particulate matter. <i>Prog. Oceanog.</i> 23 , 1-21.

1146	Cleveland W. S., Grosse E., and Shyu W. M. (1992) Chapter 8. Local regression models.
1147	In: J. M. Chambers, T. J. Hastie (eds.) Statistical Models in S, Chapman &
1148	Hall/CRC Press, Boca Raton, FL, pp. 309-374.
1149	Comans R. N. J. and van Dijk C. P. J. (1988) Role of complexation processes in cadmium
1150	mobilization during estuarine mixing. <i>Nature</i> 336 , 151-154.
1151	Cotton J., Le Dez A., Bau M., Caroff M., Maury R. C., Dulski P., Fourcade S., Bohn M.,
1152	and Brousse R. (1995) Origin of anomalous rare-earth element and yttrium
1153	enrichments in subaerially exposed basalts: Evidence from French Polynesia.
1154	Chem. Geol. 119, 115-138.
1155	Daux V., Crovisier J. L., Hemond C., and Petit J. C. (1994) Geochemical evolution of
1156	basaltic rocks subjected to weathering: Fate of the major elements, rare earth
1157	elements, and thorium. Geochim. Cosmochim. Acta 58, 4941-4954.
1158	Delaney J. M. and Lundeen S. R. (1989) The LNLL thermochemical database. Lawrence
1159	Livermore National Laboratory, Report UCRL-21658.
1160	Duarte T. K., Hemond H. F., Frankel D., and Frankel S. (2006) Assessment of submarine
1161	groundwater discharge by handheld aerial infrared imagery: Case study of Kaloko
1162	fishpond and bay, Hawai'i. Limnol. Oceanogr. Methods 4, 227-236.
1163	Duddy I. R. (1980) Redistribution and fractionation of the rare-earth and other elements
1164	in weathering profiles. Chem. Geol. 30, 363-381.
1165	Duncan T. and Shaw T. J. (2003) The mobility of the rare earth elements and redox
1166	sensitive elements in the groundwater/seawater mixing zone of a shallow coastal
1167	aquifer. Aquatic Geochem. 9, 233-255.
1168	Dupré B., Gaillardet J., and Allègre C. J. (1996) Major and trace elements of river-borne

1169	material: the Congo Basin. Geochim. Cosmochim. Acta 60, 1301-1321.
1170	Dzombak D. A. and Morel F. M. M. (1990) Surface Complexation Modeling. John Wiley
1171	and Sons, New York.
1172	Efron B. and Tibshirani R. (1986) Bootstrap methods for standard errors, confidence
1173	intervals, and other measures of statistical accuracy. Stat. Sci. 1, 54-77.
1174	Ekern P. C. and Chang JH. (1985) Pan evaporation: State of Hawai'i, 1894-1983. State
1175	of Hawaii, Department of Land and Natural Resources, Report 74R, 172 p.
1176	Eggleton R. A., Foudoulis C., and Varkevisser D. (1987) Weathering of basalt: Changes
1177	in rock chemistry and mineralogy. Clays Clay Minerals 35, 161-169
1178	Elderfield H., Greaves M. J. (1982) The rare earth elements in seawater. <i>Nature</i> 296 , 214-
1179	219.
1180	Elderfield H. and Sholkovitz E. R. (1987) Rare earth elements in the pore waters of
1181	reducing nearshore sediments. Earth Planet. Sci. Lett. 82, 280-288.
1182	Elderfield H., Upstill-Goddard R., Sholkovitz E. R. (1990) The rare earth elements in
1183	rivers, estuaries, and coastal seas and their significance to the composition of
1184	ocean waters. Geochim. Cosmochim. Acta 54, 971-991.
1185	Erel Y. and Morgan J. J. (1991) The effect of surface reactions on the relative abundances
1186	of trace metals in deep-ocean water. Geochim. Cosmochim. Acta 55, 1807-1813.
1187	Erel Y. and Stolper E. M. (1993) Modeling of rare-earth element partitioning between
1188	particles and solution in aquatic environments. Geochim. Cosmochim. Acta 57,
1189	513-518.
1190	Ericksson E. (1957) The chemical composition of Hawaiian rainfall. <i>Tellus</i> 9 , 509-520.

1191 Fitzsimmons J. N	and Boyle E. A. (2012) An intercalibration between the GEOTRACES
1192 GO-FLO	and the MITESS/Vanes sampling systems for dissolved iron
concentrat	tion analyses (and a closer look at adsorption effects). Limnol. Oceanographic
1194 Methods 1	10 , 437-450.
1195 Fitzsimmons J. N	I. and Boyle E. A. (2014) Assessment and comparison of Anopore and
1196 cross flow	w filtration methods for the determination of dissolved iron size
1197 fractionati	on into soluble and colloidal phases in seawater. Limnol. Oceanogr.
1198 Methods 1	12 , 246-263.
1199 Fodor R. V., Frey	F. A., Bauer G. R., and Clague D. A. (1992a) Ages, rare-earth element
1200 enrichmen	nt, and petrogenesis of theoleiitic and alkaline basalts from Kahoolawe
1201 Island, Ha	waii. Contrib. Mineral. Petrol. 110, 442-462.
1202 Fodor R. V., Dob	oosi G., and Bauer G. R. (1992b) Anomalously high rare-earth element
1203 abundance	es in Hawaiian lavas. Anal. Chem. 64, 639-643.
1204 Fodor R. V., Jac	obs R. S., and Bauer G. R. (1994) Hollandite in Hawaiian basalt: a
relocation	site for weathering-mobilized elements. <i>Mineral. Mag.</i> 58 , 589-596.
1206 Fox L. E. (1990)	Geochemistry of dissolved phosphate in the Sepik River and estuary,
1207 Papua, Ne	w Guinea. Geochim. Cosmochim. Acta 54 , 1019-1024.
1208 Fröllje H., Pahnk	te K., Schnetger B., Brumsack HJ., Dulai H., and Fitzsimmons J. N.
1209 (2016) Ha	waiian imprint on dissolved Nd and Ra isotopes and rare earth elements
in the cer	ntral North Pacific: Local survey and seasonal variability. Geochim.
1211 Cosmochi	m. Acta 189 , 110-131.
1212 Gaillardet J., Vier	J., and Dupré B. (2005) Trace elements in river waters. In: J. I. Drever
1213 (ed.) Sur	face and Ground Water, Weathering, and Soils. Treatises on

1214	Geochemistry, Vol. 5. Elservier, Amsterdam, pp. 225-272.
1215	Gallagher B. (1980) Physical structure and circulation in Honokohau, a small Hawaiian
1216	harbor affected by groundwater. Pac. Sci. 34, 301-311.
1217	Garnier JM. and Guieu C. (2003) Release of cadmium in the Danube estuary:
1218	contribution of physical and chemical processes as determined by an experimental
1219	approach. Mar. Environ. Res. 55, 5-15.
1220	Gillis K. M., Ludden J. N., and Smith A. D. (1992) Mobilization of REE during crustal
1221	aging in the Troodos Ophiolite, Cyprus. Chem. Geol. 98, 71-86.
1222	Goldstein S. L. and Hemming S. R. (2003) Long-lived isotopic tracers in oceanography,
1223	paleoceanography, and ice-sheet dynamics. Treatise on Geochem. 6, 453-489.
1224	Goldstein S. J. and Jacobsen S. B. (1988a) REE in the Great Whale River estuary,
1225	northwest Quebec. Earth Planet. Sci. Lett. 88, 241-252.
1226	Goldstein S. J. and Jacobsen S. B. (1988b) Rare earth elements in river waters. Earth
1227	Planet. Sci. Lett. 89 , 35-47.
1228	Greaves M. J., Elderfield H., and Klinkhammer G. P. (1989) Determination of the rare
1229	earth elements in natural waters by isotope-dilution mass spectrometry. Anal.
1230	Chim. Acta 218, 265-280.
1231	Haley B. A., Klinkhammer G. P., and McManus J. (2004) Rare earth elements in pore
1232	waters of marine sediments. Geochim. Cosmochim. Acta 68, 1265-1279.
1233	Hanano D., Weis D., Scoates J. S., Aciego S., and DePaolo D. J. (2010) Horizontal and
1234	vertical zoning heterogeneities in the Hawaiian mantle plume from the
1235	geochemistry of consecutive postshield volcano pairs: Kohala - Mahukona and
1236	Mauna Kea – Hualalai. Geochem. Geophys. Geosyst. 11(1), Q01004, doi:

1237	10.1029/2009GC002782.
1238	Hanor J. S. and Chan LH. (1977) Non-conservative behavior of barium during mixing
1239	of Mississippi River and Gulf of Mexico waters. Earth Planet. Sci. Lett. 37, 242-
1240	250.
1241	Hanson G. N. (1980) Rare earth elements in petrogenetic studies of igneous systems.
1242	Ann. Rev. Earth Planet. Sci. 8, 371-406.
1243	Hatje V., Bruland K. W., and Flegal A. R. (2016) Increases in anthropogenic gadolinium
1244	anomalies and rare earth element concentrations in San Francisco Bay over a 20
1245	year record. Environ. Sci. Technol. Doi:10.1021/acs.est5b04322.
1246	Head P. C. (1985) Data presentation and interpretation. In P. C. Head (ed.) Practical
1247	Estuarine Chemistry: A Handbook. Cambridge University Press, Cambridge, UK,
1248	pp. 278-330.
1249	Helgeson H. C. (1969) Thermodynamics of hydrothermal systems at elevated
1250	temperatures and pressures. Am. J. Sci. 267, 729-804.
1251	Hoyle J., Elderfield H., Gledhill A., and Greaves M. (1984) The behaviour of the rare
1252	earth elements during the mixing of river and sea waters. Geochim. Cosmochim.
1253	Acta 48, 143-149.
1254	Humphris S. E. (1984) The mobility of the rare earth elements in the crust. In: P.
1255	Henderson (Ed.) Rare Earth Element Geochemistry. Elsevier, Amsterdam, pp.
1256	317-342.
1257	Hunt C. D., Jr. (2014) Baseline water-quality sampling to infer nutrient and contaminant
1258	sources at Kaloko-Honokohau National Historic Park, Island of Hawaii, 2009.
1259	U.S. Geol. Surv. Scientific Invest. Rept. 2014-5158, 52 p.

1260	Jakeš P., Gill J. (1970) Rare earth elements and the island arc tholeitic series. <i>Earth</i>
1261	Planet. Sci. Lett. 9, 17-28.
1262	Jeandel C., Bishop J. K. and Zindler A. (1995) Exchange of neodymium and its isotopes
1263	between seawater and small and large particles in the Sargasso Sea. Geochim.
1264	Cosmochim. Acta 59 , 535-547.
1265	Jeandel C., Thouron D. and Fiuex M. (1998) Concentrations and isotopic compositions of
1266	neodymium in the eastern Indian Ocean and Indonesian straits. Geochim.
1267	Cosmochim. Acta 62 , 2597-2607.
1268	Jeandel C., Delattre H., Grenier M., Pradoux C., and Lacan F. (2013) Rare earth element
1269	concentrations and Nd isotopes in the Southeast Pacific Ocean. Geochem.
1270	Geophys. Geosyst. 14, 328-341, doi:10.1029/2012GC003409.
1271	Johannesson K. H., Burdige D. J. (2007) Balancing the global oceanic neodymium
1272	budget: evaluating the role of groundwater. Earth Planet. Sci. Lett. 253, 129-142.
1273	Johannesson K. H., Lyons W. B., Stetzenbach K. J., and Byrne R. H. (1995) The
1274	solubility control of rare earth elements in natural terrestrial waters and the
1275	significance of PO ₄ ³⁻ and CO ₃ ²⁻ in limiting dissolved rare earth concentrations: A
1276	review of recent information. Aquatic Geochem. 1, 157-173.
1277	Johannesson K. H., Farnham I. M., Gou C., and Stetzenbach K. J. (1999) Rare earth
1278	element fractionation and concentration variations along a groundwater flow path
1279	within a shallow, basin-fill aquifer, southern Nevada, USA. Geochim.
1280	Cosmochim. Acta 63 , 2697-2708.

1281	Johannesson, K.H., Tang, J., Daniels, J.M., Bounds, W.J., and Burdige, D.J. (2004) Rare
1282	earth element concentrations and speciation in organic-rich blackwaters of the
1283	Great Dismal Swamp, Virginia, USA. Chem. Geol. 209, 271-294.
1284	Johannesson K. H., Cortés A., Ramos Leal J. A., Ramírez A. G., Durazo J. (2005)
1285	Geochemistry of rare earth elements in groundwaters from a rhyolite aquifer,
1286	central México. In: Johannesson K. H. (ed) Rare earth elements in groundwater
1287	flow systems. Springer, Dordrecht, pp. 187-222.
1288	Johannesson K.H., Chevis D. A., Burdige D. J., Cable J. E., Martin J. B., Roy M. (2011)
1289	Submarine groundwater discharge is an important net source of light and middle
1290	REEs to coastal waters of the Indian River Lagoon, Florida, USA. Geochim.
1291	Cosmochim. Acta 75 , 825-843.
1292	Johannesson K. H., Telfeyan K., Chevis D. A., Rosenheim B. E., Leybourne M. I. (2014)
1293	Rare earth elements in stromatolites - 1. Evidence that modern terrestrial
1294	stromatolites fractionate rare earth elements during incorporation from ambient
1295	waters. In: Y. Dilek, H. Furnes (eds.), Evolution of Archean Crust and Early Life,
1296	Modern Approaches in Solid Earth 1 Sciences 7, Springer, Dordrecht, 385-411.
1297	Johnson A. G., Glenn C. R., Burnett W. C., Peterson R. N., and Lucey P. G. (2008)
1298	Aerial infrared imaging reveals large nutrient-rich groundwater inputs to the
1299	ocean. Geophys. Res. Lett. 35, L15606, doi:10.1029/2008/GL034574.
1300	Jonasson R. G., Bancroft G. M., and Nesbitt H. W. (1985) Solubilites of some hydrous
1301	REE phosphates with implications for diagenesis and seawater concentrations.
1302	Geochim. Cosmochim. Acta 49, 2133-2139.
1303	Kelly J. L. and Glenn C. R. (2015) Chlorofluorocarbon apparent ages of groundwaters

1304	from west Hawaii, USA. J. Hydrol. 527 , 355-366.
1305	Kim KH., Byrne R. H., and Lee J. H. (1991) Gadolinium behavior in seawater: a
1306	molecular basis for gadolinium anomalies. Mar. Chem. 36, 107-120.
1307	Kim I. and Kim G. (2011) Large fluxes of rare earth elements through submarine
1308	groundwater discharge from a volcanic island, Jeju, Korea. Mar. Chem. 127, 12-
1309	19.
1310	Kim I. and Kim G. (2014) Submarine groundwater discharge as a main source of rare
1311	earth elements in coastal water. Mar. Chem. 160, 11-17.
1312	Kim G., Ryu JW., Yang HS. and Yun ST. (2005) Submarine groundwater discharge
1313	(SGD) into the Yellow Sea revealed by ²²⁸ Ra and ²²⁶ Ra isotopes: implications for
1314	global silicate fluxes. Earth Planet. Sci. Lett. 237, 156-166.
1315	Klinkhammer G., German C. R., Elderfield H., Greaves M. J., and Mitra A. (1994) Rare
1316	earth elements in hydrothermal fluids and plume particulates by inductively
1317	coupled plasma mass spectrometry. Mar. Chem. 45, 170-186.
1318	Klungness G. D. and Byrne R. H. (2000) Comparative hydrolysis behavior of the rare
1319	earths and yttrium: the influence of temperature and ionic strength. Polyhedron
1320	19 , 99-107.
1321	Knee K. L., Street J. H., Grossman E. E., Boehm A. B., and Paytan A. (2010) Nutrient
1322	inputs to the coastal ocean from submarine groundwater discharge in a
1323	groundwater-dominated system: Relation to land use (Kona Coast, Hawaii, U. S.
1324	A.). Limnol. Oceanogr. 53 , 1105-1122.
1325	Koeppenkastrop D. and De Carlo E. H. (1992) Sorption of rare-earth elements from
1326	seawater onto synthetic mineral particles: An experimental approach. Chem. Geol.

1327 **95**, 251-263. 1328 Koeppenkastrop D. and De Carlo E. H. (1993) Uptake of rare earth elements from 1329 solution by metal oxides. Environ. Sci. Technol. 27, 1796-1802. Kraepiel A. M. L., Chiffoleau J.-F., Martin J.-M., and Morel F. M. M. (1997) 1330 1331 Geochemistry of trace metals in the Gironde estuary. Geochim. Cosmochim. Acta 1332 **61**, 1421-1436. 1333 Kulaksız S. and Bau M. (2007) Contrasting behaviour of anthropogenic gadolinium and 1334 natural rare earth elements in estuaries and the gadolinium input to the North Sea. 1335 Earth Planet. Sci. Lett. 260, 361-371. Kümmerer K. and Helmers E. (2000) Hospital effluents as a source of gadolinium in the 1336 1337 aquatic environment. Environ. Sci. Technol. 34, 573-577. Lacan F. and Jeandel C. (2001) Tracing Papua New Guinea imprint on the Equatorial 1338 Pacific Ocean using neodymium isotopic compositions and rare earth element 1339 patterns. Earth Planet. Sci. Lett. 186, 497-512. 1340 Lacan F. and Jeandel C. (2005) Neodymium isotopes as a new tool for quantifying 1341 1342 exchange fluxes at the continent-ocean interface. Earth Planet. Sci. Lett. 232, 245-257. 1343 Lau L. S. and Mink J. F. (2006) Hydrology of the Hawaiian Islands. University of 1344 Hawai'i Press, Honolulu. 1345 1346 Lawrence M. G. and Kamber B. S. (2006) The behaviour of the rare earth elements 1347 during estuarine mixing – revisted. *Mar. Chem.* **100**, 147-161. 1348 Lee J. H. and Byrne R. H. (1992) Examination of comparative rare earth element 1349 complexation behavior using linear free-energy relationships. Geochim.

1350 Cosmochim. Acta 56, 1127-1137. Li Y.-H and Chan L.-H. (1979) Desorption of Ba and ²²⁶Ra from river-borne sediments in 1351 1352 the Hudson estuary. Earth Planet. Sci. Lett. 43, 343-350. 1353 Liu X. and Byrne R. H. (1997) Rare earth and yttrium phosphate solubilities in aqueous 1354 solution. Geochim. Cosmochim. Acta 61, 1625-1633. 1355 Luo Y.-R. and Byrne R. H. (2000) The ionic strength dependence of rare earth and 1356 yttrium fluoride complexes at 25°C. J. Sol. Chem. 30, 837-845. Luo Y.-R. and Byrne R. H. (2001) Yttrium and rare earth element complexation by 1357 chloride ions at 25°C. J. Sol. Chem. 30, 837-845, 1358 Luo Y.-R. and Byrne R. H. (2004) Carbonate complexation of yttrium and the rare earth 1359 1360 elements in natural waters. Geochim. Cosmochim. Acta 68, 691-699. 1361 Maeda M. and Windom H. L. (1982) Behavior of uranium in two estuaries of the south-1362 eastern United States. Mar. Chem. 11, 427-436. Martin J. B., Cable J. E., Smith C., Roy M. and Cherrier J. (2007) Magnitudes of 1363 1364 submarine groundwater discharge from marine and terrestrial sources: Indian 1365 River 43, Lagoon, Florida. W05440. Water Resour. Res., doi:10.1029/2006WR005266. 1366 Martin J.-M., Høgdahl O., and Philippot J. C. (1976) Rare earth supply to the ocean. J. 1367 Geophys. Res. 81, 3119-3124. 1368 1369 McKenzie D., O'Nions R. K. (1991) Partial melt distributions from inversion of rare earth element concentrations. J. Petrol. 32, 1021-1091. 1370 1371 Millero F. J. and Schreiber D. R. (1982) Use of the ion pairing model to estimate activity 1372 coefficients of the ionic components of natural waters. Am. J. Sci. 282, 1508-

1373 1540. 1374 Milliman J. D. and Farnsworth K. L. (2011) River Discharge to the Coastal Ocean: A 1375 Global Synthesis. Cambridge University Press, Cambridge, UK, 384 p. 1376 Mohajerin T. J., Helz G. R., and Johannesson K. H (2016) Tungsten – molybdenum 1377 fractionation in estuarine environments. Geochim. Cosmochim. Acta 177, 105-1378 119. 1379 Moore J. G. and Clague D. (1987) Coastal lava flows from Mauna Loa and Hualalai volcanoes, Kona, Hawaii. Bull. Volcanol. 49, 752-764. 1380 Moore J. G. and Clague D. A. (1992) Volcano growth and evolution of the island of 1381 1382 Hawaii. Geol Soc. Am. Bull. 104, 1471-1484. 1383 Moore J. G., Clague D. A., Rubin M., and Bohrson W. A. (1987) Hualalai Volcano: A 1384 preliminary summary of geologic, petrologic, and geophysical data. In: R. W. 1385 Decker, T. L. Wright, and P. H. Stauffer (Eds), Volcanism in Hawaii, U. S. Geol. Surv. Prof. Pap 1350, 571-585. 1386 1387 Moore W. S. (1997) High fluxes of radium and barium from the mouth of the Ganges-1388 Brahmaputra River during low river discharge suggest a large groundwater 1389 source. Earth Planet. Sci. Lett. 150, 141-150. Moore W. S. (1999) The subterranean estuary: A reaction zone of groundwater and 1390 seawater. Mar. Chem. 65, 111-125. 1391 1392 Moore W. S. (2010) The effect of submarine groundwater discharge on the ocean. Annu. 1393 Rev. Mar. Sci. 2, 59-88. 1394 Nance W. B. and Taylor S. R. (1976) Rare earth element patterns and crustal evolution – 1395 I. Australian post-Archean rocks. *Geochim. Cosmochim. Acta* 40, 1539-1551.

1396 Nelson B. J., Wood S. A., and Osiensky J. L. (2004) Rare earth element geochemistry in 1397 the Palouse Basin, northern Idaho - eastern Washington. Geochem. Explor. 1398 Environ. Anal. 4, 227-241. 1399 Nesbitt H. W. (1979) Mobility and fractionation of the rare earth elements during 1400 weathering of a granodiorite. *Nature* **279**, 206-210. 1401 Nesbitt H. W. and Wilson R. E. (1992) Recent chemical weathering of basalts. Am. J. Sci. 1402 **292**, 740-777. Nozaki Y., Yamamoto Y., Manaka T., Amakawa H., and Snidvongs A. (2001) Dissolved 1403 1404 barium and radium isotopes in the Chao Phraya River estuarine mixing zone in 1405 Thailand. Continent. Shelf Res. 21, 1435-1448. 1406 Officer C. B. (1979) Discussion of the behaviour of nonconservative dissolved constituents in estuaries. Estuar. Coast. Mar. Sci. 9, 91-94. 1407 Oki D. S., Tribble G. W., Souza W. R., and Bolke E. L. (1999) Groundwater resources in 1408 1409 Kaloko-Honokohua National Historic Park, Island of Hawaii, and numerical 1410 simulation of the effects of groundwater withdrawals. U. S. Geol. Surv. Water 1411 Resour. Invest. Rep., 99-4070, 49 pp. 1412 Parsons M. L., Walsh W. J., Settlemeir C. J., White D. J., Ballauer J. M., Ayotte P. M., 1413 Osada K. M., and Carman B. (2008) A multivariate assessment of the coral ecosystem health of two embayments on the less of the island of Hawai'i. Mar. 1414 1415 Pollut. Bull. 56, 1138-1149. 1416 Peterson R. N., Burnett W. C., Glenn C. R., and Johnson A. G. (2007) A box model to 1417 quantify groundwater discharge along the Kona coast of Hawaii using natural 1418 tracers. In: W. Sanford et al. (Eds) A New Foocus on Groundwater-Seawater

1419	Interactions, IAHS Publ. 312, 142-149.
1420	Peterson R. N., Burnett W. C., Glenn C. R., and Johnson A. G. (2009) Quantification of
1421	point-source groundwater discharges to the ocean from the shoreline of the Big
1422	Island, Hawaii. Limnol. Oceanogr. 54, 890-904.
1423	Piepgras D. J. and Jacobsen S. B. (1992) The behavior of rare earth elements in seawater:
1424	Precise determination of variations in the North Pacific water column. Geochim.
1425	Cosmochim. Acta 56 , 1851-1862.
1426	Piepgras D. J. and Wasserburg G. J. (1987) Rare earth element transport in the western
1427	North Atlantic inferred from Nd isotopic observations. Geochim. Cosmochim.
1428	Acta 51 ,1257-1271.
1429	Price R. C., Gray C. M., Wilson R. E., Frey F. A., and Taylor S. R. (1991) The effects of
1430	weathering on rare-earth element, Y and Ba abundances in Tertiary basalts from
1431	southeastern Australia. Chem. Geol. 93, 245-265.
1432	Prouty N. G., Swarzenski P. W., Fackrell J. K., Johannesson K., and Palmore D. (2016)
1433	Groundwater-derived nutrients and trace element transport to a nearshore Kona
1434	coral ecosystem: Experimental mixing model results. J. Hydrol.: Reg. Stud.,
1435	http://dx.doi.org/10.1016/j.ejrh.2015.12.058.
1436	Quinn K. A., Byrne R. H. and Schijf J. (2004) Comparative scavenging of yttrium and
1437	the rare earth elements in seawater: Competitive influences of solution and
1438	surface chemistry. Aquatic Geochem. 10, 59-80.
1439	Quinn K. A., Byrne R. H. and Schijf J. (2006) Sorption of yttrium and rare earth elements
1440	by amorphous ferric hydroxide: Influence of solution complexation with
1441	carbonate. Geochim. Cosmochim. Acta 70, 4151-4165.

1442	R Core Team (2015) R: A Language and Environment for Statistical Computing. R
1443	Foundation for Statistical Computing, Vienna, Austria.
1444	Ren ZY., Hanyu T., Miyazaki T., Chang Q., Kawabata H., Takahashi T., Hirahara Y.
1445	Nichols A. R. L., and Tatsumi Y. (2009) Geochemical differences of the
1446	Hawaiian shield labes: Implications for melting process in the heterogeneous
1447	Hawaiian plume. J. Petrol. 50 , 1553-1573.
1448	Ronov A. B., Balashov Y. A., and Migdisov A. A. (1967) Geochemistry of the rare earth
1449	elements in the sedimentary cycle. Geochem. Internat. 4, 1-17.
1450	Rousseau T. C. C., Sonke J. E., Chmeleff J., van Beek P., Souhaut M., Boaventura G.,
1451	Seyler P., and Jeandel C. (2015) Rapid neodymium rlease to marine waters from
1452	lithogenic sediments in the Amazon estuary. Nature Commun. 6:7592
1453	doi:10.1038/ncomms8592.
1454	Roy M., Martin J. B., Cherrier J., Cable J. E. and Smith C. G. (2010) Influence of sea
1455	level rise on iron diagenesis in an east Florida subterranean estuary. Geochim.
1456	Cosmochim. Acta 74 , 5560–5573.
1457	Roy M., Martin J. B., Smith C. G., and Cable J. E. (2011) Reactive-transport modeling of
1458	iron diagenesis and associated organic carbon mineralization in a Florida (USA)
1459	subterranean estuary. Earth Planet. Sci. Lett. 304, 191-201.
1460	Schijf J. and Byrne R. H. (2004) Determination of $SO_4\beta_1$ for yttrium and the rare earth
1461	elements at $I = 0.66 m$ and $t = 25^{\circ}\text{C}$ – Implications for YREE solution speciation
1462	in sulfate-rich waters. Geochim. Cosmochim. Acta 68, 2825-2837.
1463	Schneider A. B., Kochinsky A., Kiprotich J., Poehle S., and do Nascimento P. C. (2016)
1464	An experimental study on the mixing behavior of Ti, Zr, V and Mo in the Elbe,

1465	Rhine and Weser estuaries. Estuar. Coast. Shelf Sci. 170, 34-44.
1466	Shannon W. M. and Wood S. A. (2005) The analysis of pictogram quantities of rare earth
1467	elements in natural waters. In: K. H. Johannesson (ed.) Rare Earth Elements in
1468	Groundwater Flow Systems. Springer, Dordrecht, 1-37.
1469	Shiller A. M. (2003) Syringe filtration method for examining dissolved and colloidal
1470	trace element distributions in remote field locations. Environ. Sci. Technol. 37,
1471	3953-3957.
1472	Sholkovitz E. R. (1976) Flocculation of dissolved organic and inorganic matter during the
1473	mixing of river water and seawater. Geochim. Cosmochim. Acta 40, 831-845.
1474	Sholkovitz E. R. (1992) Chemical evolution of rare earth elements: fractionation between
1475	colloidal and solution phases of filtered river water. Earth Planet Sci. Lett. 114,
L476	77-84.
1477	Sholkovitz E. R. (1993) The geochemistry of rare earth elements in the Amazon River
1478	estuary. Geochim. Cosmochim. Acta 57, 2181-2190.
L479	Sholkovitz E. R. (1995) The aquatic chemistry of rare earth elements in rivers and
1480	estuaries. Aquatic Geochem. 1, 1–34.
1481	Sholkovitz E. R. and Copland D. (1981) The coagulation, solubility and adsorption
1482	properties of Fe, Mn, Cu, Ni, Cd, Co and humic acids in river water. Geochim.
1483	Cosmochim. Acta 45 , 181-198.
1484	Sholkovitz E. R. and Elderfield H. (1988) Cycling of dissolved rare earth elements in
1485	Chesapeake Bay. Global Biogeochem. Cycles 2, 157-176.
1486	Sholkovitz E. R. and Szymczak R. (2000) The estuarine chemistry of rare earth elements:
1487	comparison of the Amazon, Fly, Sepik and the Gulf of Papua systems. Earth

1488	Planet. Sci. Lett. 179 , 299-309.
1489	Sholkovitz E. R., Piepgras D. J., and Jacobsen S. B. (1989) The pore water chemistry of
1490	rare earth elements in Buzzards Bay sediments. Geochim. Cosmochim. Acta 53,
1491	2847-2856.
1492	Sholkovitz E. R., Shaw T. J., and Schneider D. L. (1992) The geochemistry of rare earth
1493	elements in the seasonally anoxic water column and porewaters of Chesapeake
1494	Bay. Geochim. Cosmochim. Acta 56 , 3389-3402.
1495	Siddall M., Khatiwala S., van de Flierdt T., Jones K., Goldstein S. L., Hemming S. and
1496	Anderson R. F. (2008) Towards explaining the Nd paradox using reversible
1497	scavenging in an ocean general circulation model. Earth Planet. Sci. Lett. 274,
1498	448-461.
1499	Slomp C. P. and Van Cappellen P. (2004) Nutrient inputs to the coastal ocean through
1500	submarine groundwater discharge: controls and potential impact. J. Hydrol. 295,
1501	64–86.
1502	Stefánsson A. and Gíslason S. R. (2001) Chemical weathering of basalts, Southwestern
1503	Iceland: Effect of rock crystallinity and secondary minerals on chemical fluxes to
1504	the ocean. Am. J. Sci. 301, 513-556.
1505	Street J. H., Knee K. L., Grossman E. E., Paytan A. (2008) Submarine groundwater
1506	discharge and nutrient addition to the coastal zone and coral reefs of leeward
1507	Hawai'i. Mar. Chem. 109, 355-376.
1508	Swarzenski P. W., McKee B. A., and Booth J. G. (1995) Uranium geochemistry on the
1509	Amazon shelf: Chemical phase partitioning and cycling across as a salinity
1510	gradient. Geochim. Cosmochim. Acta 59, 7-18.

1511	Tachikawa K., Jeandel C. and Dupre B. (1997) Distribution of rare earth elements and
1512	neodymium isotopes in settling particulate material of the tropical Atlantic Ocean
1513	(EUMELI site). Deep-Sea Res. I 44, 1769-1792.
1514	Tachikawa K., Jeandel C. and Roy-Barman M. (1999a) A new approach to Nd residence
1515	time: The role of atmospheric inputs. Earth Planet. Sci. Lett. 170, 433-446.
1516	Tachikawa K., Jeandel C., Vangriesheim A. and Dupre B. (1999b) Distribution of rare
1517	earth elements and neodymium isotopes in suspended particles of the tropical
1518	Atlantic Ocean (EUMELI site). Deep-Sea Res. I 46, 733-756.
1519	Tachikawa K., Athias V. and Jeandel C. (2003) Neodymium budget in the modern ocean
1520	and paleo-oceanographic implications. J. Geophys. Res. 108, 3254.
1521	doi:10.1029/1999JC000285.
1522	Tanaka R., Makishima A., and Nakamura E. (2008) Hawaiian double volcanic chain
1523	triggered by an episodic involvement of recycled material: Constraints from
1524	temporal Sr-Nd-Hf-Pb isotopic trend of the Loa-type volcanoes. Earth Planet. Sci.
1525	Lett. 265 , 450-465.
1526	Tang J. and Johannesson K. H. (2005) Adsorption of rare earth elements onto Carrizo
1527	sand: Experimental investigations and modeling with surface complexation.
1528	Geochim. Cosmochim. Acta 69 , 5247-5261.
1529	Tang J. and Johannesson K. H. (2010a) Ligand extraction of rare earth elements from
1530	aquifer sediments: Implications for rare earth element complexation with organic
1531	matter in natural waters. <i>Geochim. Cosmochim. Acta</i> 74 , 6690-6705.
1532	Tang J. and Johannesson K. H. (2010b) Rare earth adsorption onto Carrizo sand:
1533	Influences of strong solution complexation. Chem. Geol. 279, 120-133.

1534 Taniguchi M., Burnett W. C., Cable J. E. and Turner J. V. (2002) Investigation of 1535 submarine groundwater discharge. *Hydrol. Process.* **16**, 2115–2129. 1536 Tatsumi T., Shukuno H., Yoshikawa M., Chang Q., Sato K., and Lee M. W. (2004) The 1537 petrology and geochemistry of volcanic rocks on Jeju Island: Plume magmatism 1538 along the Asian continental margin. J. Petrol. 46, 523-553. 1539 Taylor S. R. and McLennan S. M. (1985) The Continental Crust: Its Composition and 1540 Evolution. Blackwell Scientific Publications, Oxford, UK. Tillman F. D., Oki D. S., Johnson A. G., Barber L. B., and Beisner K. R. (2014a) 1541 1542 Investigation of geochemical indicators to evaluate the connection between inland 1543 and coastal groundwater systems near Kaloko-Honokōhau National Historical 1544 Park, Hawai'i. Applied Geochem. 51, 278-292. 1545 Tillman F. D., Oki D. S., and Johnson A. G. (2014b) Water-chemistry data collected in 1546 and near Kaloko-Honokōhau National Historical Park, Hawai'I, 2012-2014. U. S. Geol. Surv. Open-File Rept. 2014-1173. 1547 1548 Verplanck P. L., Taylor H. E., Nordstrom D. K., and Barber L. B. (2005) Aqueous 1549 stability of gadolinium in surface waters receiving sewage treatment plant effluent, Boulder Creek, Colorado. Environ. Sci. Technol. 39, 6923-6929. 1550 1551 Visher F. N. and Mink J. F. (1964) Ground-water resources in southern Oahu, Hawaii. U. S. Geol. Surv. Water Supply Pap. 1778, 133 p. 1552 1553 Willis S. S., Johannesson K. H. (2011) Controls on the geochemistry of rare earth 1554 elements in sediments and groundwaters of the Aquia aquifer, Maryland, USA. 1555 Chem. Geol. 285, 32-49. 1556 Windom H. L., Moore W. S., Niencheski L. F. H. and Jahnke R. A. (2006) Submarine

1557	groundwater discharge: A large, previously unrecognized source of dissolved iron
1558	to the South Atlantic Ocean. Mar. Chem. 102, 252–266.
1559	Ziegler K., Hsieh J. C. C., Chadwick O. A., Kelly E. F., Hendricks D. M., and Savin S.
1560	M. (2003) Halloysite as a kinetically controlled end product of arid-zone basalt
1561	weathering. Chem. Geol. 202, 461-478.
1562	Zucca J. J., Hill D. P., and Kovach R. L. (1982) Crustal structure of Mauna Loa Volcano,
1563	Hawaii, from seismic refraction and gravity data. Bull. Seismol. Soc. Am. 72,
1564	1535-1550.
1565	
1566	Figure Captions
1567	
1568	Figure 1. Map of the study site on the Big Island of Hawaii is shown in panel (a). Panel
1569	(b) depicts the general setting of the portion of the Kona Coast investigated and includes
1570	the location of the Hind well on Kiholo Bay and the groundwater wells in the Kaloko-
1571	Honokohau National Historic Park. Panel (c) is a detailed map of the vicinity of the
1572	Kaloko-Honokohau National Historic Park showing the locations of the Honokohau
1573	Harbor well, the three KAHO wells within the Park, and the location of where the coastal
1574	seawater sample was collected.
1575	
1576	Figure 2. Piper diagram for Kona Coast groundwaters and coastal seawater.
1577	Groundwaters are largely Na-HCO ₃ to Na-Cl waters.
1578	

1579	Figure 3. Shale-normalized REE patterns for groundwaters and the coastal seawater
1580	sample collectd from the Kona Coast. Shown are the results for waters filtered through
1581	$0.45~\mu m$ (filled symbols) and through $0.02~\mu m$ (open symbols) filters, except for panel
1582	(b), which shows duplicate samples from the KAHO 1 well. For each case, the symbol
1583	and error bars represent the mean and relative standard deviation (RSD) for five replicate
1584	analyses, and hence, show the instrument precision. The KAHO 1 analyses represent the
1585	sampling and laboratory precision. Rare earth element concentrations measured in each
1586	water sample are normalized to the Post Archean Australian Shale (PAAS) composite
1587	(Nance and Taylor, 1976).
1588	
1589	Figure 4. Shale-normalized REE patterns for Kono Coast groundwaters and coastal
1590	seawaters compared to open-ocean North Pacific seawater. Panel (a) demonstrates the
1591	nearly identical shale-normalized REE patterns of Kona groundwaters and seawater
1592	samples. The chief exception is that the majority of groundwaters do not exhibit a large
1593	positive Gd anomaly that evident in groundwater from the Honokohau Harbor well as
1594	well as the coastal seawater sample. Panel (b) compares Kona Coast seawater with a
1595	number of open-ocean seawater samples from various depths taken from Alibo and
1596	Nozaki (1999). Although the North Pacific seawater samples were filtered through 0.04
1597	μm pore-size filters, Kona Coast seawater filtered through 0.02 μm has substantially
1598	higher REE concentrations. See text for details.
1599	
1600	Figure 5. Kona Coast groundwaters and coastal seawater normalized to the mean REE
1601	content of twelve, alkali Hualali basalts from Hanano et al. (2010). Panels (a) and (b)

1602	present the basalt-normalized REE patterns of waters filtered through 0.45 μm and 0.02
1603	μm pore-size filters, respectively.
1604	
1605	Figure 6. Results of the Honokohau Harbor mixing experiment for (a) Nd, (b) Gd, and (c)
1606	Yb, plotted as a function of salinity. Each symbol shows the mean and the RSD for each
1607	analysis. The dashed line depicts the hypothetic conservative mixing/dilution line
1608	between Honokohau Harbor well groundwater and coastal seawater.
1609	
1610	Figure 7. Results of the lava tube mixing experiment for (a) Nd, (b) Gd, and (c) Yb,
1611	plotted as a function of salinity. Each symbol shows the mean and the RSD for each
1612	analysis. The dashed line depicts the hypothetic conservative mixing/dilution line
1613	between Hind well groundwater and coastal seawater.
1614	
1615	Figure 8. Solution complexation model results for Kona Coast groundwaters and coastal
1616	seawater, where Ln represents each of the individual REEs (i.e., lanthanides). Major ion
1617	chemistry used for the modeling is presented in Table 2.
1618	
1619	Figure 9. Results of solution complexation modeling for the Honokohau Harbor mixing
1620	experiment (see electronic annex). Panel (a) presents the activity of the free metal ions.
1621	[Ln ³⁺] _F , for La, Nd, Gd, Dy, and Yb as a function of salinity, whereas panels (b) and (c)
1622	present the predicted speciation of Nd (a LREE) and Yb (a HREE) as a function of
1623	salinity, respectively. Panels (b) and (c) only show aqueous species that are predicted to
1624	account for 1% and greater of any of the REEs.

1625	
1626	Figure 10. Results of solution complexation modeling for the lava tube mixing
1627	experiment (see electronic annex). Panel (a) presents the activity of the free metal ions.
1628	[Ln ³⁺] _F , for La, Nd, Gd, Dy, and Yb as a function of salinity, whereas panels (b) and (c)
1629	present the predicted speciation of Nd (a LREE) and Yb (a HREE) as a function of
1630	salinity, respectively. Panels (b) and (c) only show aqueous species that are predicted to
1631	account for at 0.1% and greater of any of the REEs.
1632	
1633	Figure 11. Calculated Gd-normalized solution-surface partition coefficient $(D_{Ln}/D_{Gd})^{-1}$ as
1634	a function of salinity for the Honokohau Harbor mixing experiment.
1635	
1636	Figure 12. Kona Coast groundwaters normalized to the Kona seawater sample. The
1637	generally flat patterns with normalized ratios around unity emphasize the similarity of
1638	these groundwaters and the coast seawater.
1639	
1640	Figure 13. Analysis of the (a) Honokohau Harbor and (b) lava tube mixing experiments
1641	for Nd as a function of salinity. Measured concentration data are show as open circles and
1642	the hypothetical conservative mixing/dilution line is represented by the dashed line
1643	(compare with Figs. 6a and 7a). Solid orange-brown curved line is the median loess fit to
1644	the measured Nd concentration data and the orange-brown field represents the 95%
1645	confidence interval for the loess fit. The solid blue straight line is the median tangent line
1646	constructed from the seawater endmember back to the freshwater endmember (salinity of
1647	zero) and the blue, triangle shaped field is the corresponding 95% confidence interval.

1648	The resulting median y-intercept shown by the blue dot on the ordinate at zero salinity,
1649	which is mathematically equal to $[Ln]_{TSGD} + \frac{J_{desorb}^{[Ln]}}{Q_{TSGD}}$, and reflects the effective,
1650	freshwater (terrestrial) SGD concentration of Nd. See text for details.
1651	
1652	
1653	

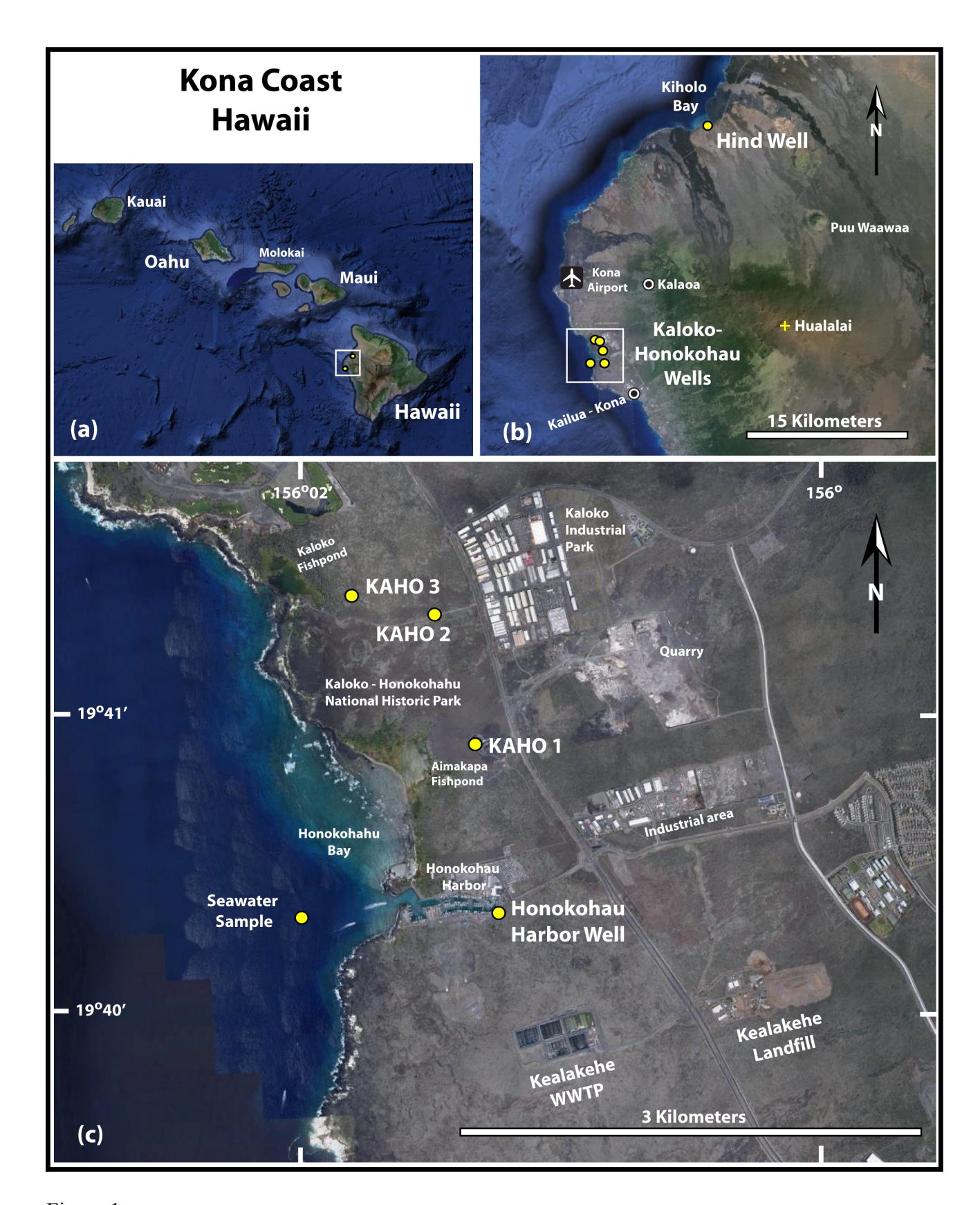


Figure 1

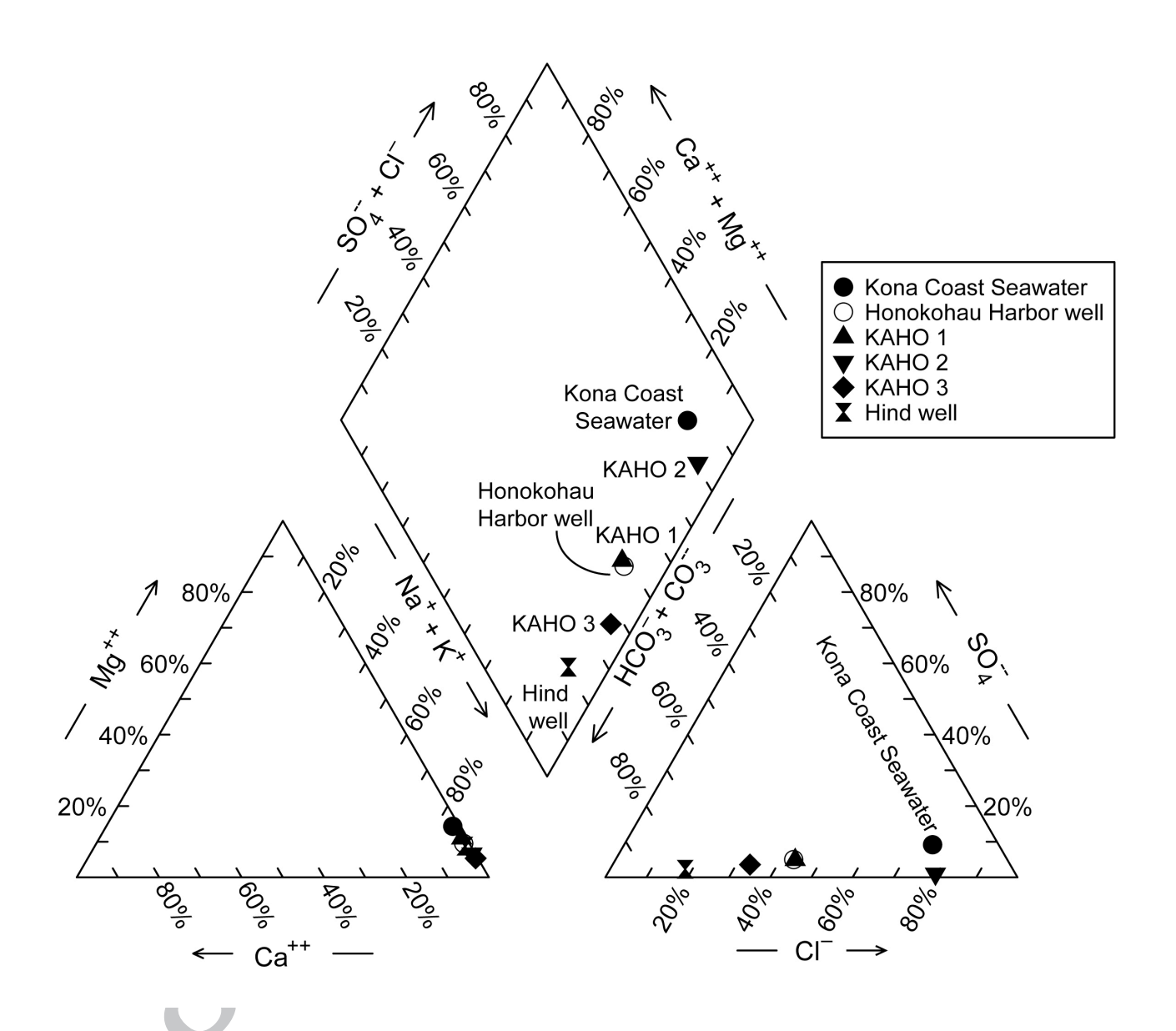


Figure 2

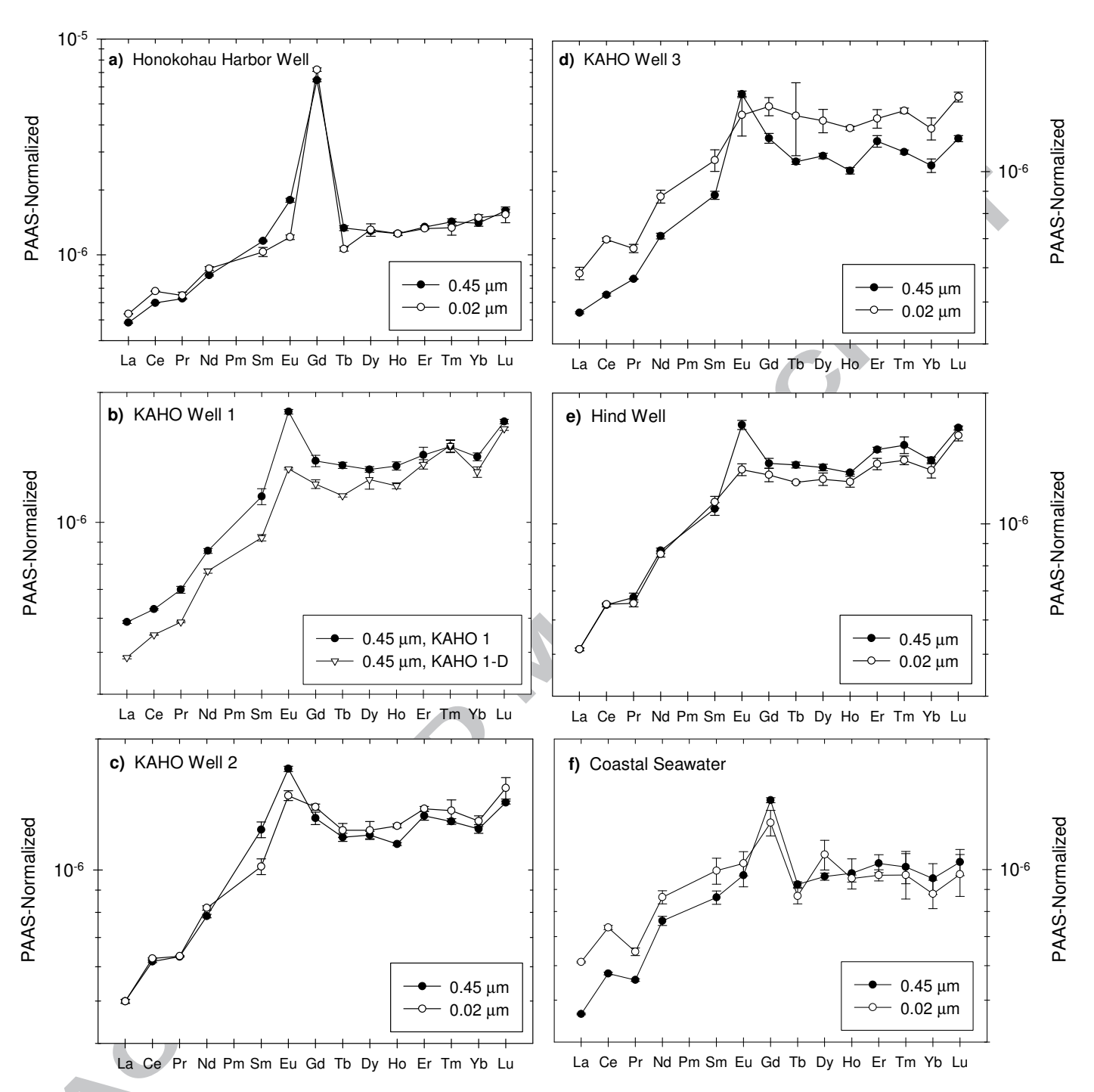


Figure 3

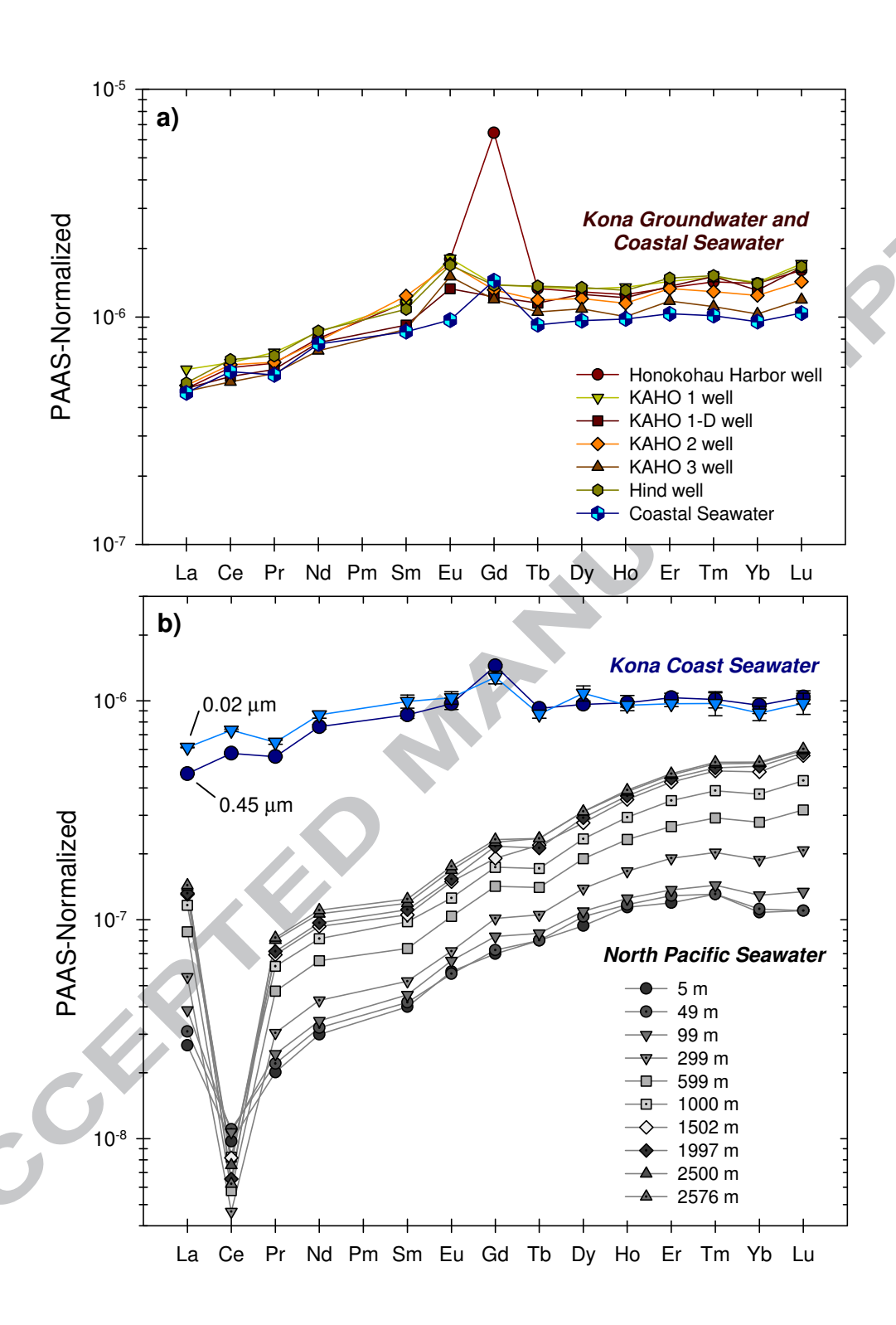


Figure 4

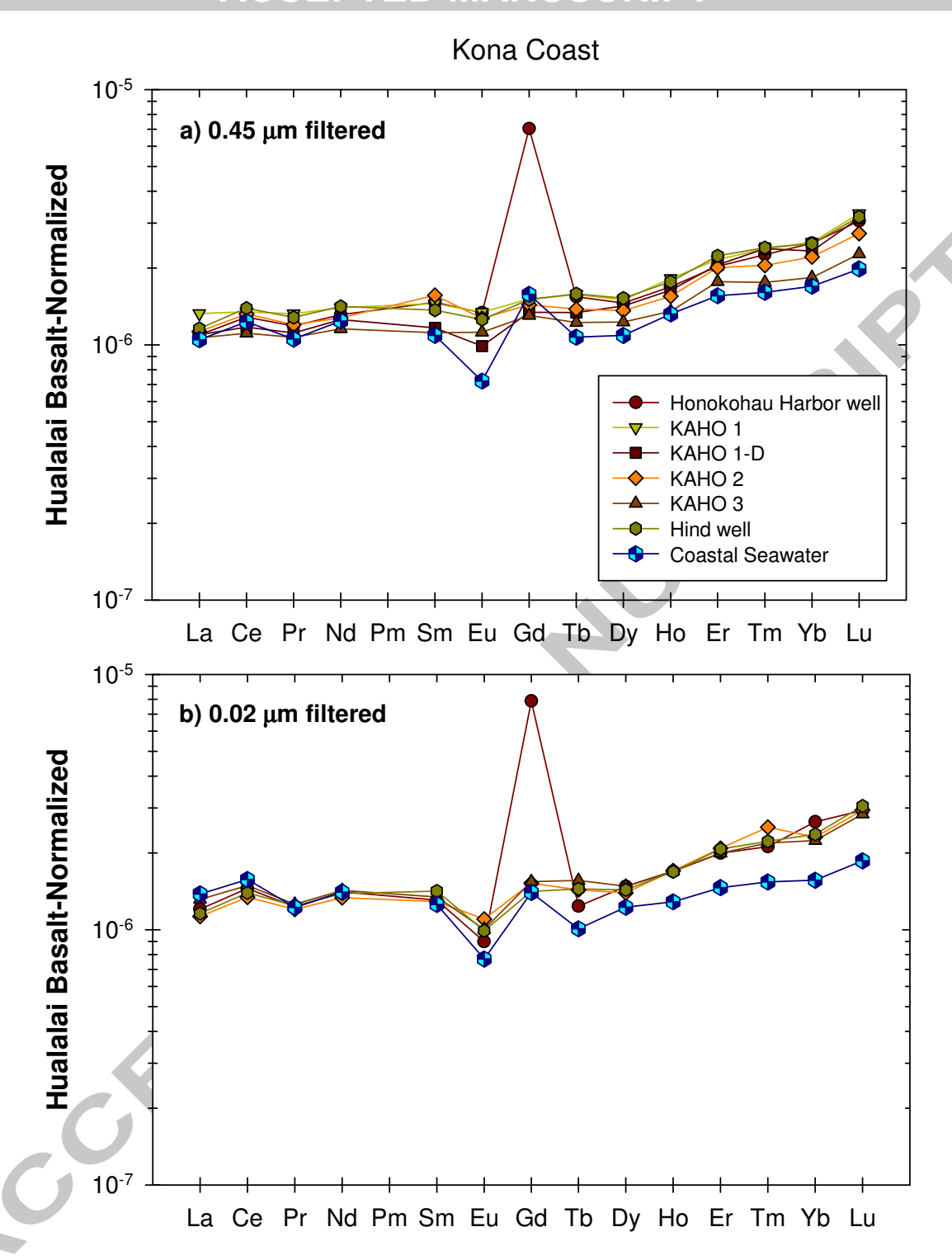


Figure 5

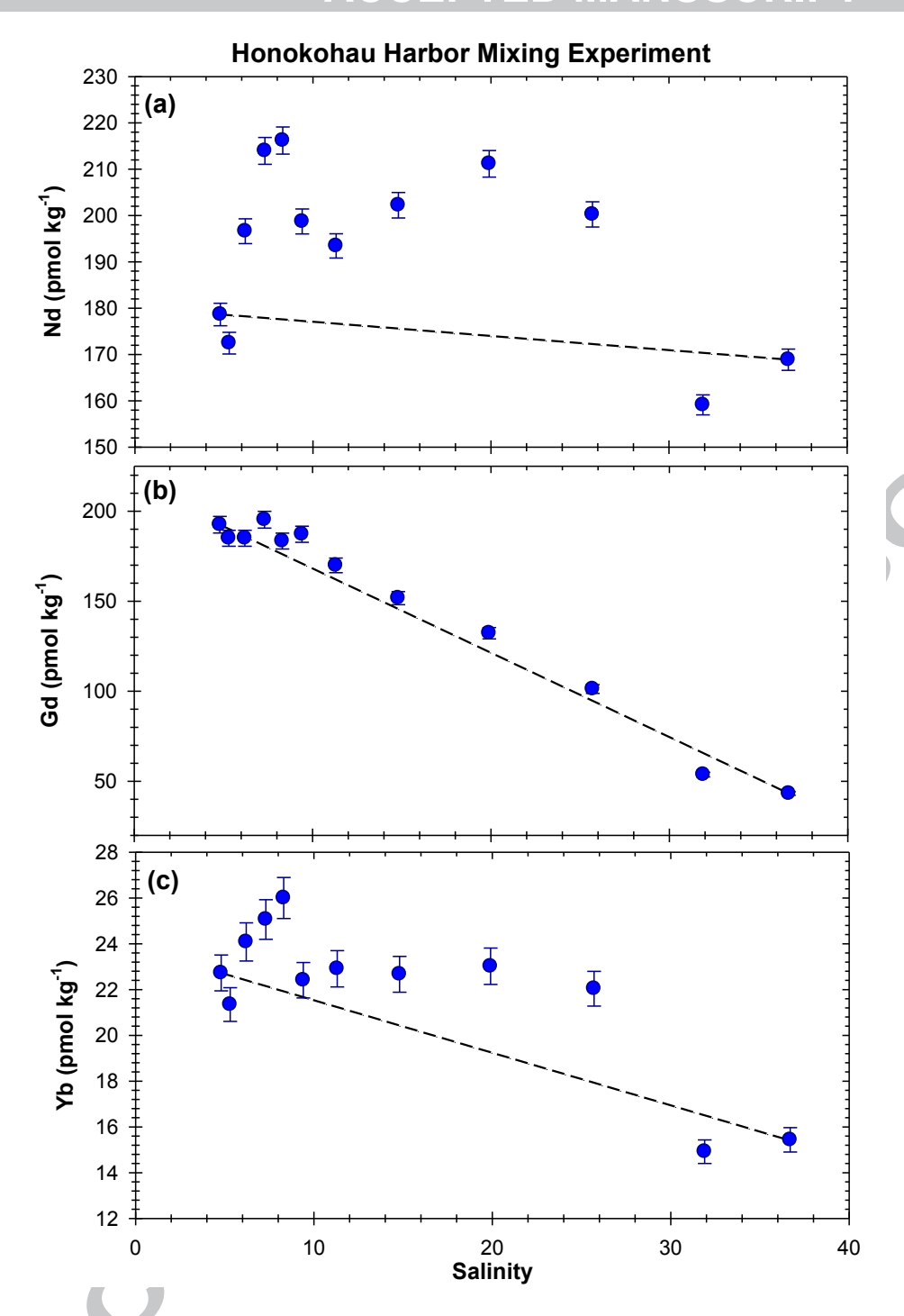


Figure 6

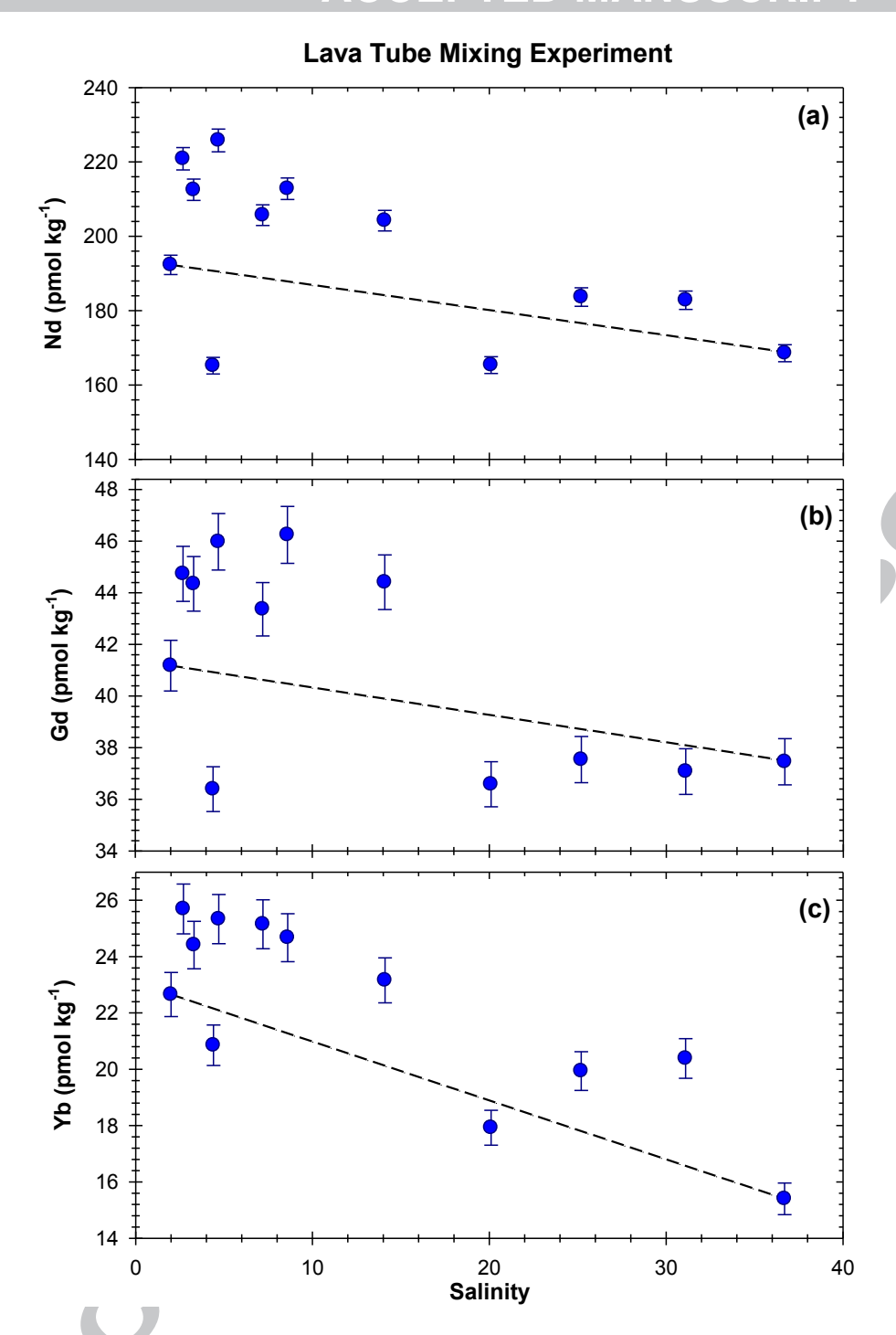


Figure 7

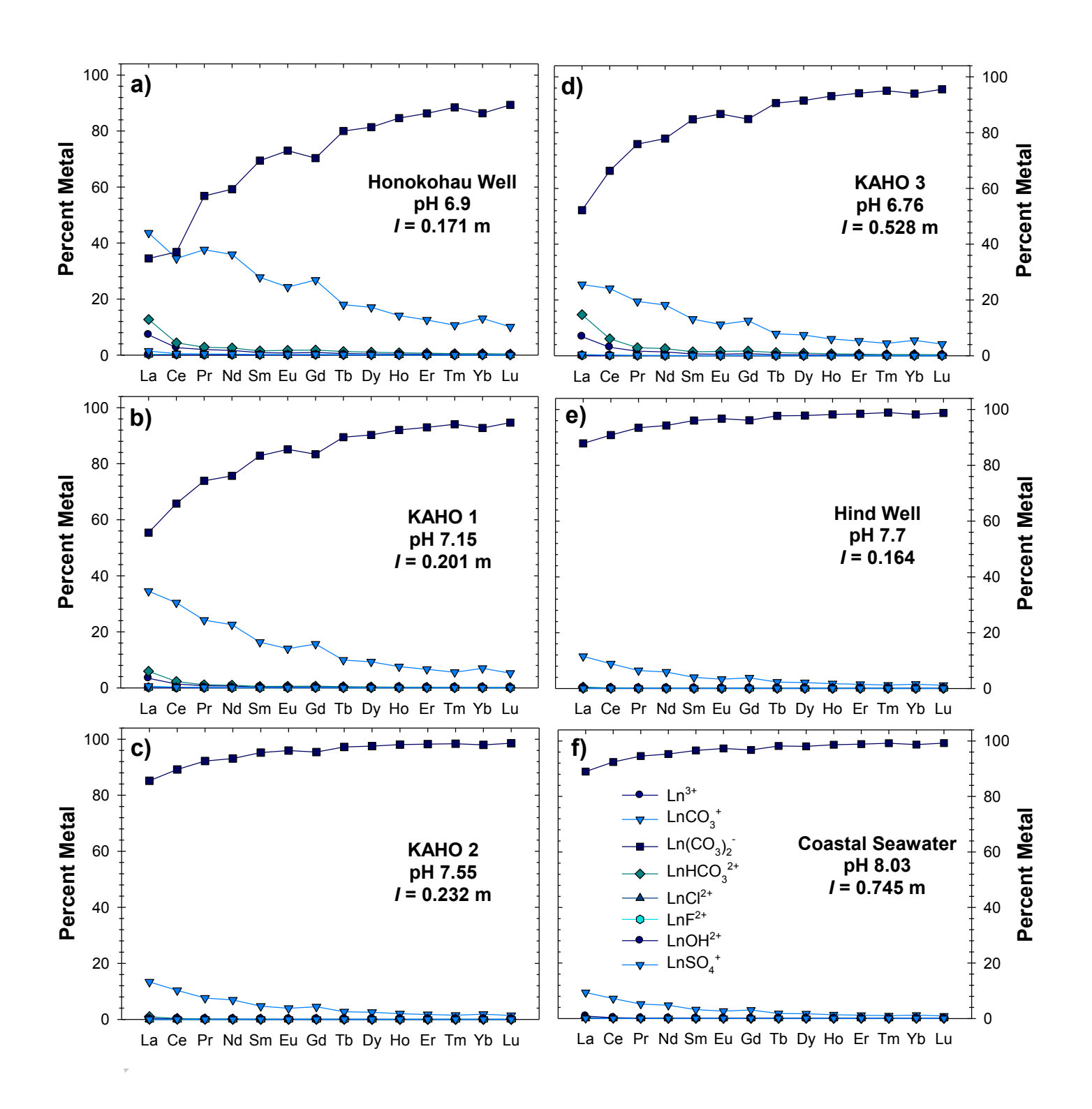


Figure 8

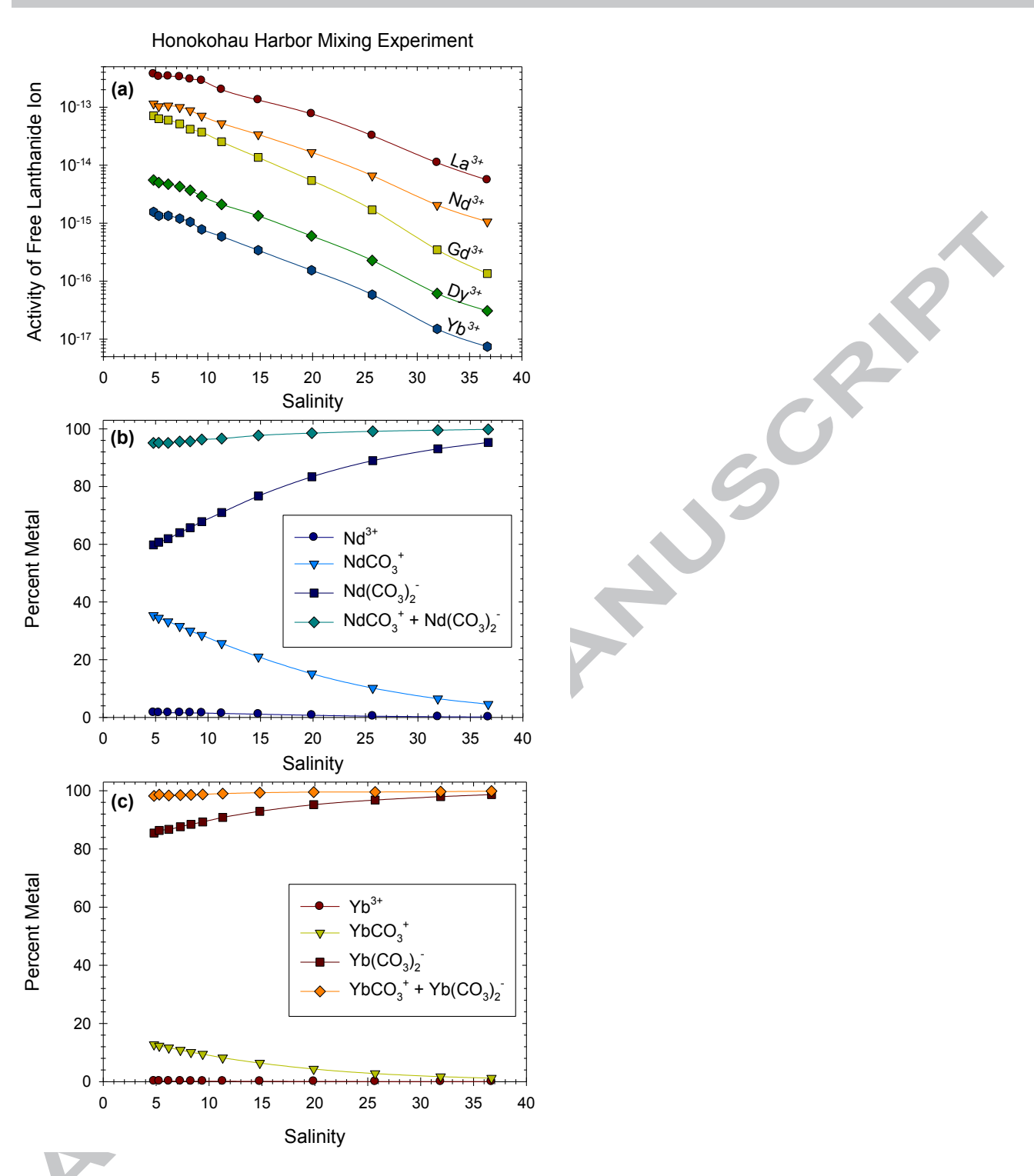


Figure 9

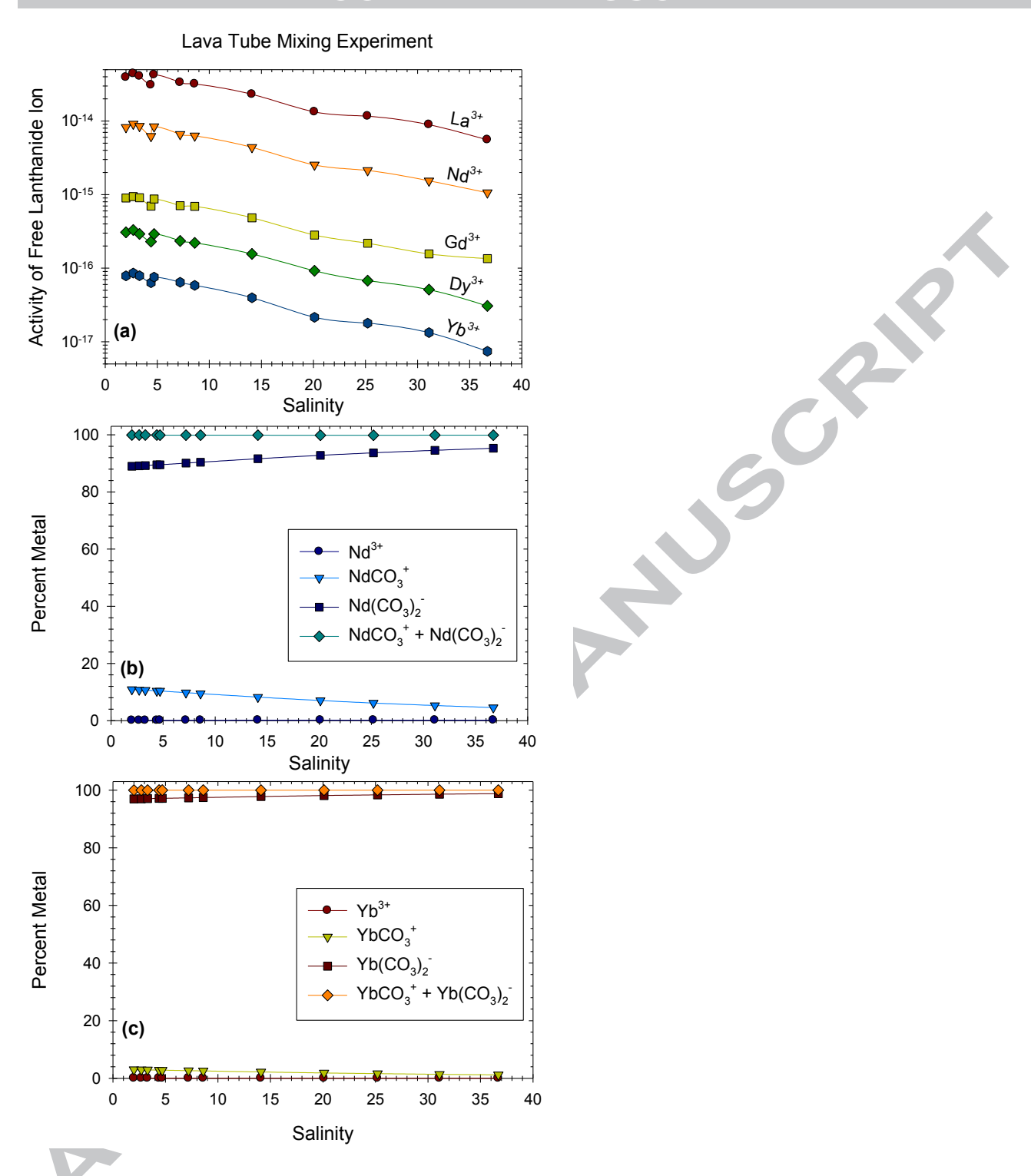


Figure 10

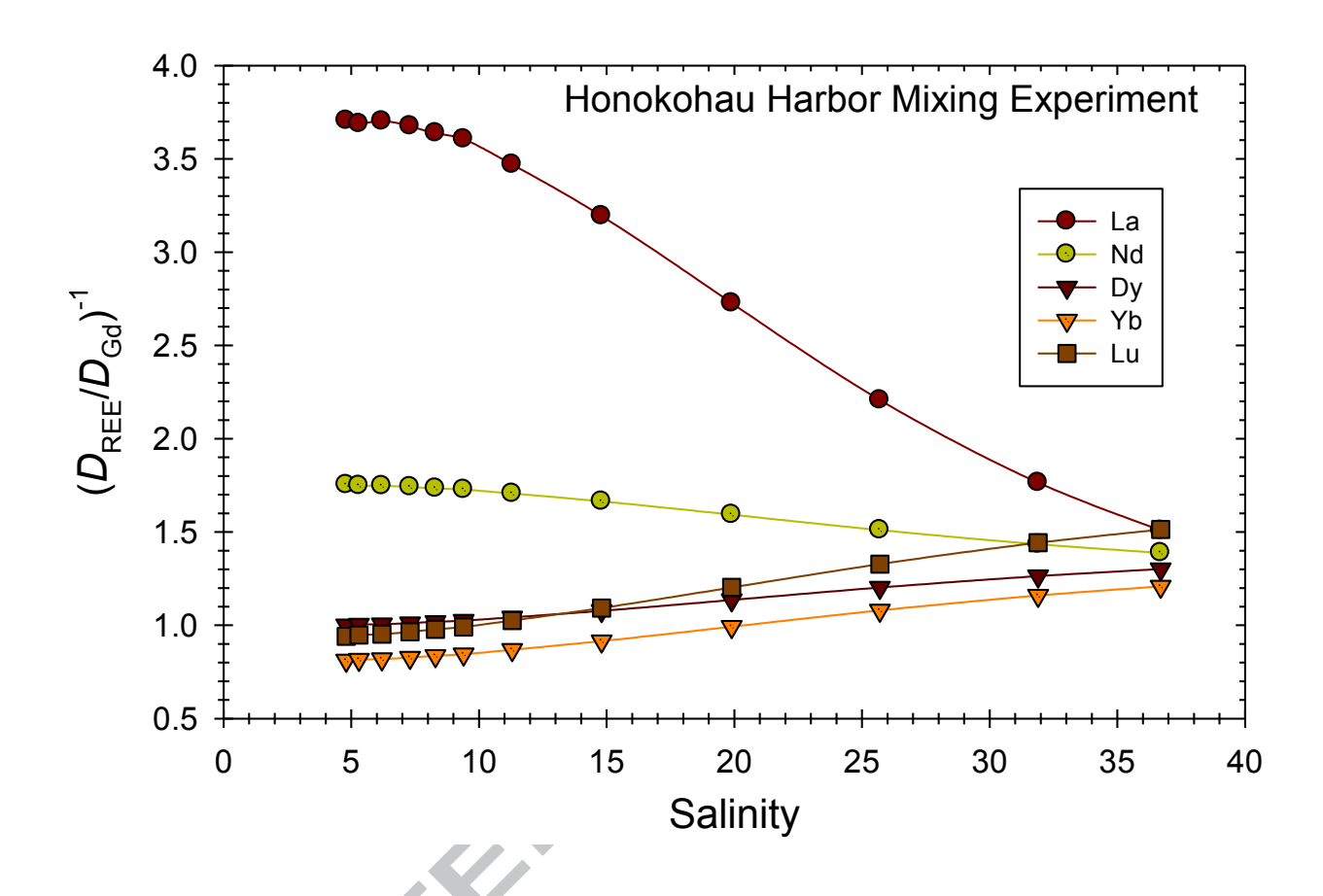


Figure 11

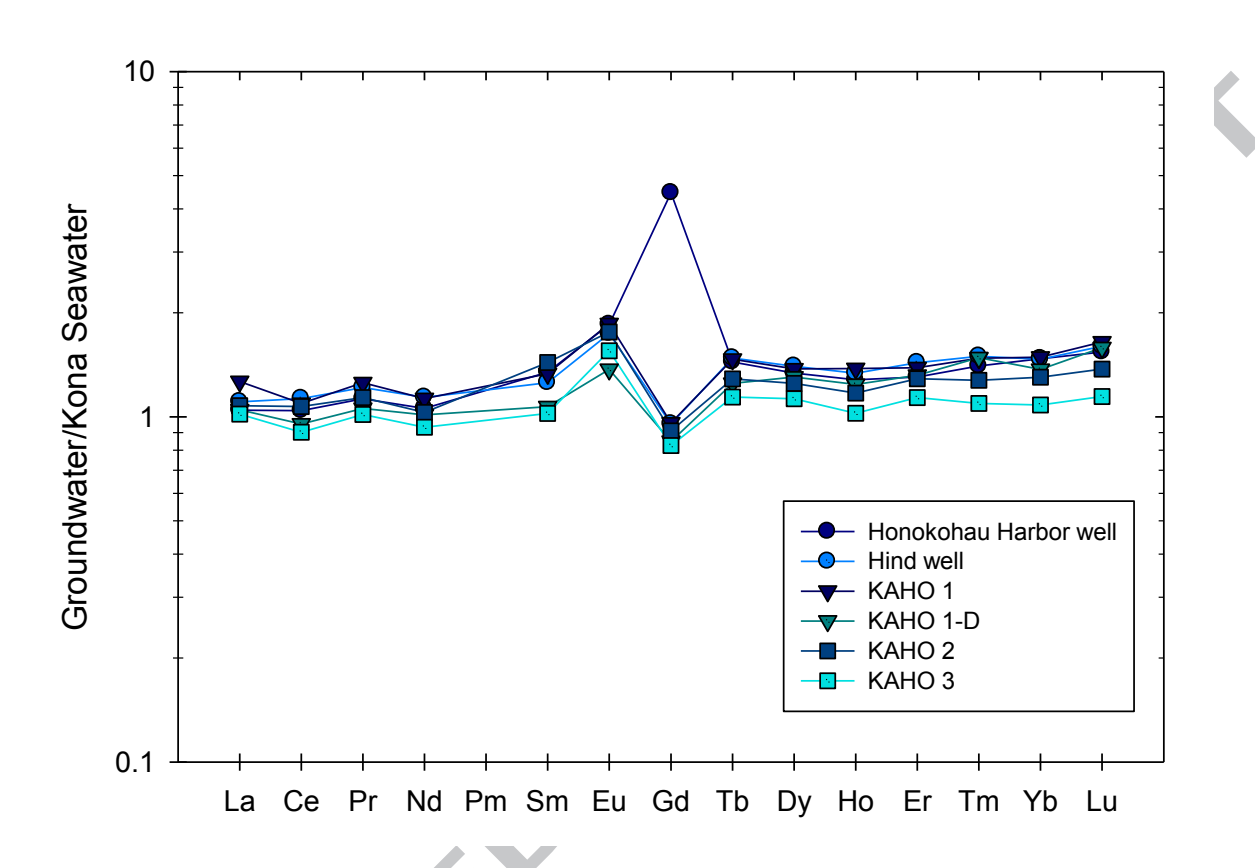


Figure 12

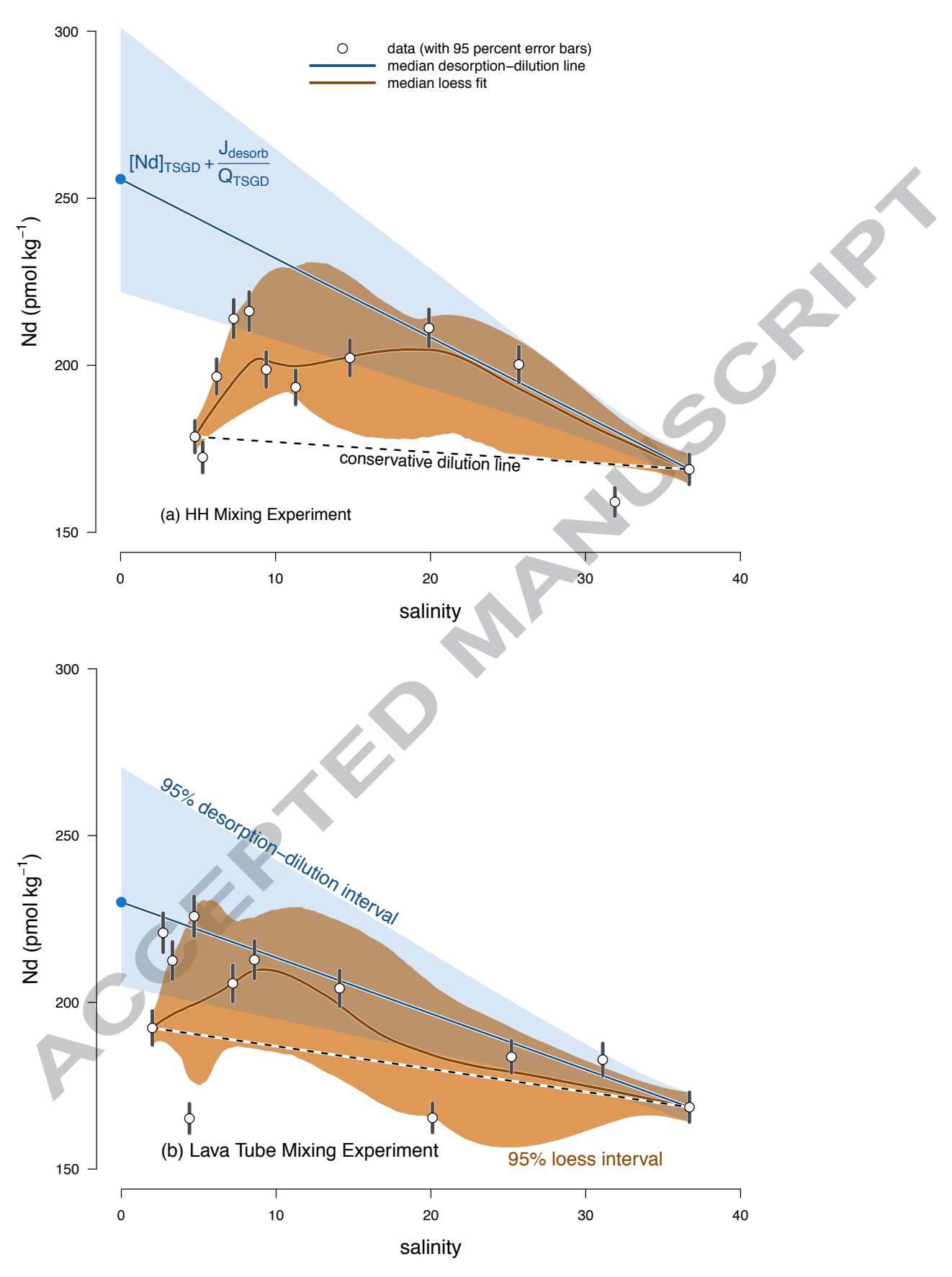


Figure 13

1654 Table 1. Location and sampling data for groundwater wells and seawater samples collected along the Kona Coast.

	Latitude	Longitude	Elevation	Hole Depth	Well Depth	Depth to	Notes
	(North)	(West)	(m)	(m)	(m)	Water	
						(m)	
Seawater	19°40'07.98"	156°01'58.80"	0	0	0	Surface	~ 0.62 km offshore
Honokohau Harbor Wel	19°40'06.60"	156°01'15.60"	-	-	_	12.1	Outside harbor road
KAHO 1 Well	19°40'42.06"	156°01'19.99"	11.1	15.8	13.1	6.96	entrance
KAHO 2 Well	19°41'09.04"	156°01'25.01"	16.3	21	18.4	16.1	USGS, 8-4061-01
KAHO 3 Well	19°41'14.06"	156°01'44.99"	7.02	10.4	9.48	11	USGS, 8-4161-02
Hind Well	19°51'14.40"	155°55'22.80"	_	_	_	~1.5	USGS, 8-4161-01
							In collapsed lava tube

Table 2. Chemistry of coastal groundwaters and seawater from the Kona Coast of Hawaii. Major solutes, nutrients, and Fe and Mn concentrations are for the dissolved fraction ($< 0.45 \, \mu m$)

fraction (< 0.45	μm).					
	Coastal	Honokohau				
	Seawater	HarborWell	KAHO 1	KAHO 2	KAHO 3	Hind Well
рН	8.03	6.9	7.15	7.55	6.76	7.7
Temp. °C	~27	23.1	20.1	20.9	21.1	22.3
Cond.a	53.4	9.08	10.7	8.81	18.7	3.93
Salinity ^b	36.7	4.8	5.7	4.5	12.5	2
Ionic Strength ^c	0.745	0.187	0.223	0.263	0.649	0.178
DO^d	_	83.4	173	197	154	252
DO^e	_	31.9	63	72.7	58.9	93.8
Eh (volts) ^f	0.744	0.804	0.794	0.771	0.817	0.763
SPM^{f}	7.79	2.02	2.13	1.74	2.04	8.0
mmol kg ⁻¹						
Ca	6.5	1.22	1.26	1.1	1.91	0.76
Mg	54.5	8.21	11.2	8.17	15.4	4.34
Na	633	153	179	230	548	88.8
K	10.6	1.8	2.05	1.65	3.04	0.86
Cl	572	74.8	89.6	70.2	195	31.6
Alk ^g	123	89.9	106	172	370	138
SO_4	34.6	4.26	4.96	3.86	10.2	1.88
F	0.37	0.12	0.15	0.14	0.19	0.28
Br	0.99	0.14	0.15	0.11	0.3	0.05
μmol kg ⁻¹						
$NO_3 + NO_2$	4.2	187	66.5	31.2	39.3	26.5
NH ₄	0.1	1.3	0.9	1.1	2.2	0.3
PO ₄	0.15	37.3	3.6	2.1	2.7	1.9
H ₄ SiO ₄	28.4	376	389	392	311	432
DOC	_	236	45	51.6	35.8	_
nmol kg ⁻¹						
Fe	11.6	11.3	ND	62.5	11.5	ND
Mn	1.2	0.6	7.9	11.6	2.1	6.4
auS cm-1						

¹⁶⁶⁰

1657

1658

¹⁶⁶¹ bComputed from Cl concentration using S (g kg⁻¹) = $1.80655 \times \text{Cl}$ (g kg⁻¹).

cmoles kg-1 1662

dμmol kg-1 1663

ePercent saturation 1664

^fSuspended particulate matter (mg L⁻¹) 1665

gAlkalinity estimated from charge balance and is reported as HCO₃- (Willis and Johannesson, 1666

1668 ^fComputed based on dissolve oxygen concentration.

1669 ND = not detected.



Table 3. Summary of published geochemical data for rivers and estuaries^a.

Table 3. Summary		Fe	Mn	DOC	Nd	Nd Removed ^b
River	рН	nmol kg ⁻¹	nmol kg ⁻¹	μmol kg ⁻¹	pmol kg ⁻¹	%
Mississippi						
Upper	7.7	_	7.46	_	_	_
Mouth	7.8	_	12 - 33	_	76.3	_
Connecticut	7.0	108	42	267	2475	56
St. Lawrence	8.0	1990	114	_	263	_
Mullica	4.6	60	62	_	2856	81
Delaware	7.5	9	9.4	217	180	70
Hudson	7.0	_	_	_	416	-
Great Whale	6.9	580	_	441	1158	66
Amazon						
Mean	6.89	_	923	425	837 ± 259	93 – 95
< 0.2 μm ^c	7.1	770	60	420	-	
Orinoco (< 0.2 μm)	6.51	2500	124	452	2000	7 -
Congo	6.19	3400	-	-	2465	-
Changjang	7.8	555	18	-	485	_
Fly	7.8	_	_	267	180	87
Sepik	7.3	110	-	283	250	81
Gironde	7.3	140	60	258	263	68
Luce	4.5	140	43	749	367	73
Tamar Springs	7.25	35	17.3	_	257	65
Tamar Neaps	7.25	43	34	_	229	40

^aData are compiled from a number of sources following the recent summary of Rousseau et al. (2015) that reported all the data published to date for Nd in surface water estuaries.

et al. (2015) that reported all the data published to date for Nd in surface water estudion to those cited by Rousseau et al. (2015) include: Sholkovitz and

1675 Copland (1981), Goldstein and Jacobsen (1988a), Elderfield et al. (1990), Fox (1990),

Sholkovitz (1992, 1993, 1995), Dupré et al. (1996), Kraepiel et al. (1997), Sholkovitz and

Szymczak (2000), Gaillardet et al. (2005), and Milliman and Farnsworth (2011).

bThe percent of dissolved river-borne Nd removed in the estuary as computed by

Rousseau et al. (2015).

^cFiltrate passed through 0.2 μm pore-size filters

1682

1672

1676

1677

1678

1679

1680 1681

1684Table 4. Rare earth element concentrations and relative standard deviation (in pmol kg-1685¹) for coastal groundwaters and seawater from the Kona Coast of Hawaii. The relative 1686standard deviation is based on five replicate analyses of each sample. KAHO 1-D is a 1687duplicate sample from the KAHO 1 well.

	Seawater	HH Well	KAHO 1	KAHO 1-D	KAHO 2	KAHO 3	Hind Well
	(0.45 µm)	(0.45 μm)	(0.45 μm)	(0.45 μm)	(0.45 μm)	(0.45 µm)	(0.45 μm)
La	127 ± 0.58	133 ± 1.01	161 ± 1.18	133 ± 0.98	137 ± 1.29	129 ± 0.65	140 ± 0.74
Ce	329 ± 2.25	342 ± 0.8	359 ± 1.72	313 ± 0.31	352 ± 1.79	297 ± 1.91	371 ± 3.93
Pr	35.1 ±	39.6 ±	44.1 ± 0.8	37.2 ±	39.9 ±	35.7 ±	42.7 ±
Nd	0.24	0.28	191 ± 2.4	0.15	0.07	0.07	1.02
Sm	169 ± 4.1	179 ± 1.53	42.7 ± 1.8	171 ± 1.97	174 ± 1.57	158 ± 2.44	192 ± 2.6
Eu	32.1 ±	43.2 ±	13.1 ±	34.3 ±	46.1 ±	32.8 ±	40.3 ±
Gd	1.15	0.35	0.16	0.56	1.91	0.69	1.35
Tb	7.02 ±	13 ± 0.27	41.5 ±	9.63 ±	12.4 ±	10.9 ±	12.2 ±
Dy	0.42	192 ± 2.77	1.26	0.05	0.17	0.19	0.29
Но	43.2 ±	6.45 ±	6.57 ±	36.7 ±	39.4 ± 1.3	35.7 ±	41.2 ±
Er	0.58	0.16	0.11	0.85	5.76 ±	0.92	1.09
Tm	4.47 ±	34.9 ± 0.5	35.9 ±	5.59 ±	0.12	5.1 ± 0.07	6.62 ± 0.1
Yb	0.06	7.6 ± 0.15	0.53	0.04	32.6 ±	29.4 ±	36.5 ±
Lu	26.1 ± 0.5	23.4 ±	8.19 ±	34 ± 1.68	0.64	0.42	0.63
	5.94 ±	0.28	0.18	7.37 ±	10.4 ±	6.08 ± 0.1	7.95 ±
Ce/Ce*	0.47	$3.37 \pm$	24.8 ±	0.12	0.06	$20.4 \pm$	0.06
Eu/Eu*	17.9 ±	0.11	1.06	23.6 ±	23.1 ±	0.61	25.7 ±
Gd/Gd*	0.85	22.7 ±	$3.55 \pm$	0.59	0.53	2.62 ±	0.34
	2.4 ± 0.21	0.76	0.11	3.56 ±	3.06 ±	0.03	3.59 ±
$(Yb/Nd)_{SN}$	15.4 ±	3.94 ±	23 ± 0.48	0.12	0.05	16.7 ± 0.6	0.16
	1.26	0.08	4.21 ±	21.2 ±	20.1 ±	2.92 ±	22.7 ±
	2.56 ±		0.05	0.59	0.47	0.05	0.42
	0.18	1.01		$4.05 \pm$	3.51 ±		4.09 ±
		1.47	0.98	0.03	0.03	1.0	0.04
	1.13	5.05	1.48			1.2	
	1.1		1.08	1.02	1.09	1.02	1.09
	1.6	1.74		1.33	1.4		1.44
			1.65	1.14	1.09	1.45	1.08
	1.25						
				1.7	1.59		1.62
	Seawater	HH Well	KAHO 1	KAHO 1-D	KAHO 2	КАНО 3	Hind Well
	$(0.02 \mu m)$	(0.02 µm)	$(0.02 \mu m)$	$(0.02 \mu m)$	$(0.02 \mu m)$	$(0.02 \mu m)$	$(0.02 \mu m)$
La	167 ± 0.62	146 ± 0.43			137 ± 1.5	159 ± 5.35	140 ± 1.25
Ce	419 ± 4.7	388 ± 1.28			358 ± 1.2	398 ± 4.06	372 ± 1.91
Pr	40.8 ±	41 ± 1.43			40.1 ±	42 ± 0.93	41.4 ±
Nd	0.83	192 ± 4.04			0.12	194 ± 6.7	0.77
Sm	191 ± 6.64	38.4 ±			182 ± 2.12	39.6 ±	189 ± 2.96
Eu	37 ± 2.56	1.85			37.9 ±	2.26	41.8 ± 1.3
Gd	7.48 ±	8.75 ±			1.57	9.77 ±	9.65 ± 0.3
Tb	0.48	0.21			10.7 ±	1.03	38.7 ±
Dy	38.3 ±	216 ± 4.14			0.28	42.2 ±	1.39
Ho	2.58	5.16 ±			41.7 ±	2.05	6.04 ±
Er	4.21 ±	0.12			0.68	6.52 ±	0.03
LI	0.17	35.4 ±			5.98 ±	1.24	34.3 ±
Tm		2.36			U.ZZ	35.5 ±	1.13
Tm Yb	29.3 ±	2.36 7.61 ±			0.22 33.4 ±	35.5 ± 2.19	1.13 7.58 ±
Tm		2.36 7.61 ± 0.11			0.22 33.4 ± 1.56	35.5 ± 2.19 7.63 ±	1.13 7.58 ± 0.22

Eu/Eu*	16.8 ± 0.5	3.16 ±	0.08	23 ± 1.14	0.73
Gd/Gd*	2.3 ± 0.28	0.24	24 ± 0.3	3.27 ±	3.32 ±
	14.2 ±	24.1 ±	3.24 ±	0.04	0.08
$(Yb/Nd)_{SN}$	1.07	0.79	0.22	20.3 ±	21.5 ±
	2.4 ± 0.27	$3.78 \pm$	21 ± 0.59	1.18	0.87
		0.32	3.79 ±	$3.65 \pm$	3.93 ±
	1.17		0.21	0.09	0.11
	1.09	1.15			
	1.4	1.16	1.11	1.12	1.17
		6.84	1.36	1.17	1.15
	1.41		1.2	1.13	1.1
		1.87			
			1.58	1.43	1.6

 $1688Ce/Ce^* = [Ce/(0.5La + 0.5Pr)]_{SN}$.

 $1689Eu/Eu^* = [Eu/(0.67Sm + 0.33Tb)]_{SN}$.

 $1690 \text{Gd/Gd}^* = [\text{Gd/(0.33Sm} + 0.67 \text{Tb})]_{SN}.$

1691SN = Post Archean Australian Shale (PAAS) normalized (Nance and Taylor, 1976; Taylor and 1692McLennan, 1985).

1693

169Eable 5. Computed SGD fluxes of REEs using the results of the Honokohau Harbor mixing 169Experiment and assuming that the terrestrial SGD at Honokohau Harbor is 8600 m³ day⁻¹ 169(Peterson et al., 2009).

	HH well	J ^{Ln} TSGD	[Ln] _{eff}	J desorb	$J^{ m Ln}_{ m TotSGD}$	J desorb
	(pmol kg ⁻¹)	(µmol day-1)a	(pmol kg ⁻¹)b,c	(µmol day ⁻¹) ^{b,d}	(µmol day-1)b,e	(% of TotSGD) ^b
La	133	1144	201 (170, 239)	585 (318, 912)	1729 (1462,	33.8 (21.8, 44.4)
Ce	342	2941	506 (433, 599)	1410 (783,	2055)	32.4 (21, 42.9)
Pr	19.6	167	52.8 (47.3, 59.9)	2210)	4352 (3724,	25 (16.3, 33.9)
Nd	179	1539	256 (222, 301)	114 (66.2, 175)	5151)	30.1 (19.4, 40.5)
Sm	43.2	372	56.3 (45.1, 76.9)	662 (370, 1049)	454 (407, 515)	23.3 (4.42, 43.8)
Eu	13	112	14.1 (13.4, 18.6)	113 (17.2, 290)	2202 (1909,	7.8 (2.99, 30.1)
Gd	192	1651	236 (226, 256)	9.46 (3.44, 48.2)	2589)	18.6 (15, 25)
Tb	6.45	55.5	9.65 (7.47, 15.6)	378 (292, 550)	484 (389, 661)	33.2 (13.7, 58.7)
Dy	34.9	300	50.7 (42.2, 59.8)	27.5 (8.77, 78.7)	121 (115, 160)	31.2 (17.3, 41.6)
Ho	7.6	65.4	10.3 (8.7, 12)	136 (62.8, 214)	2030 (1944,	26.2 (12.6, 36.7)
Er	23.4	201	30.8 (26.5, 36.5)	23.2 (9.46, 37.8)	2202)	24 (11.7, 35.9)
Tm	3.37	29	4.42 (3.68, 5.36)	63.3 (26.7, 113)	83 (64.2, 134)	23.8 (8.42, 37.1)
Yb	22.7	195	32.5 (27.3, 38.6)	9.03 (2.67, 17.1)	436 (363, 514)	30.2 (16.8, 41.2)
Lu	3.94	33.9	5.07 (4.28, 6.04)	84.3 (39.6, 137)	88.6 (74.8, 103)	22.3 (7.94, 34.8)
				9.72 (2.92, 7.94)	265 (228, 314)	
					38 (31.6, 46.1)	
					280 (235, 332)	
					43.6 (36.8, 51.9)	

1698 a[Ln]_{TSGD} × Q_{TSGD}, where [Ln]_{TSGD} is REE concentrations of Honokohau Harbor (i.e., HH) well (pmol kg⁻¹)

and $Q_{TSGD} = 8600 \text{ m}^3 \text{ day}^{-1}$, and TSGD indicates terrestrial submarine groundwater discharge (SGD).

1700 bMedian value, with lower and upper bounds in parentheses.

1701 cLeft-hand side of equation 10. Represents the *y*-intercept at salinity zero on Figs. 12, EA4 – EA17.

1702 ${}^{d}J^{Ln}_{TotSGD} - J^{Ln}_{TSGD}$, where TotSGD is the total SGD.

1703 $e[Ln]_{eff} \times Q_{TSGD}$, where $Q_{TSGD} = 8600 \text{ m}^3 \text{ day}^{-1}$.

1704

1705 1706

1707able 6. Computed SGD fluxes of REEs using the results of the Lava Tube mixing experiment and 1708suming that the terrestrial SGD at Kiholo Bay is 6300 m³ day⁻¹ (Peterson et al., 2009).

La	ol kg ⁻¹) (μm 140	_ , , ,	[Ln] _{eff} pmol kg ⁻¹) ^{b,c}	J _{desorb} (μmol day ⁻¹) ^{b,d}	J ^{Ln} _{TotSGD} (μmol day ⁻¹) ^{b,e}	desorb
		882 17			(pillor day	(% of TotSGD)b
	271	002 1	79 (161, 221)	246 (132, 510)	1128 (1014,	21.8 (13, 36.7)
Ce :	3/1	2337 46	67 (418, 565)	605 (296, 1222)	1392)	20.6 (11.2, 34.3)
Pr 4	12.7	269 49	9.9 (45.2, 59)	45.4 (15.8, 103)	2942 (2633,	14.4 (5.53, 27.6)
Nd	192 1	1210 23	30 (205, 270)	239 (81.9, 491)	3560)	16.5 (6.34, 28.9)
Sm	10.3	254 46	6 (41.2, 54.4)	35.9 (5.67, 88.8)	314 (285, 372)	12.4 (2.18, 25.9)
Eu 1	12.2	76.9 1	2.7 (12, 17)	3.15 (-1.3, 30.2) ^f	1449 (1292,	3.94 (-1.7, 28.2) ^f
Gd	11.2	260 48	.8 (42.4, 56.6)	47.9 (7.56, 96.4)	1701)	15.6 (2.82, 27.1)
Tb 6	5.62	41.7 7.1	16 (6.76, 8.39)	3.4 (0.88, 11.2)	290 (260, 343)	7.54 (2.07, 21.1)
Dy 3	36.5	230 43	.2 (39.2, 51.3)	42.2 (17, 93.2)	80 (75.6, 107)	15.5 (6.89, 28.8)
Ho 7	7.95	50.1 9.6	67 (8.63, 12.3)	10.8 (4.28, 27.4)	307 (267, 356)	17.8 (7.88, 35.5)
Er 2	25.7	162 29	.3 (26.8, 35.2)	22.7 (6.93, 59.9)	45.1 (42.6, 52.9)	12.3 (4.1, 27)
Tm 3	3.59	22.6 4	.53 (4, 5.71)	5.92 (2.58, 13.4)	272 (247, 323)	20.8 (10.3, 37.1)
Yb 2	22.7	143 28	.5 (25.5, 36.3)	36.5 (17.6, 85.7)	60.9 (54.4, 77.5)	20.4 (11, 37.5)
Lu 4	1.09	25.8 4.7	74 (4.28, 5.75)	4.1 (1.2, 10.5)	185 (169, 222)	13.7 (4.22, 28.9)
					28.5 (25.2, 36)	
					180 (161, 229)	
					29.9 (27, 36.2)	

1709 $_{a}$ [Ln]_{TSGD} × Q_{TSGD}, where [Ln]_{TSGD} is REE concentrations of Hind well (pmol kg⁻¹) and Q_{TSGD} = 6300 m³ 1710 day-1, and TSGD indicates terrestrial submarine groundwater discharge (SGD). 1711 ^bMedian value, with lower and upper bounds in parentheses. 1712 cLeft-hand side of equation 10. Represents the y-intercept at salinity zero on Figs. 12, EA4 – EA17. ACCEPALED MANUSCRIP 1713 ${}^{\mathrm{d}} J^{\mathrm{Ln}}_{\mathrm{TotSGD}}$ – $J^{\mathrm{Ln}}_{\mathrm{TSGD}}$, where TotSGD is the total SGD. 1714 $e[Ln]_{eff} \times Q_{TSGD}$, where $Q_{TSGD} = 6300 \text{ m}^3 \text{ day}^{-1}$. 1715 1716 1717 1718

Table A1. Rare earth element concentrations (pmol kg⁻¹) for the Honokohau Harbor (HH) well mixing experiment as a function of pH, salinity, ionic strength (*I*, mol kg⁻¹), and the Cl concentration (mmol kg⁻¹). Salinity (S) was computed from S (g kg⁻¹) = 1.80655 x Cl (g kg⁻¹)

0.45 μm	HH Well											Seawate
Salinity	4.8	5.3	6.2	7.3	8.3	9.4	11.3	14.8	19.9	25.7	31.9	36.7
рН	6.9	6.99	7.12	7.12	7.19	7.18	7.25	7.32	7.49	7.67	7.88	8.03
mol kg ⁻¹												
I	0.17	0.18	0.2	0.22	0.24	0.26	0.29	0.36	0.46	0.57	0.69	0.78
											K	
mmol kg ⁻¹	- 40	00	0.5	440	400	4.45	456	000	040	Coa	405	
Cl	74.8	82	97	113	130	147	176	230	310	401	497	572
11 1												
pmol kg ⁻¹	122	120	140	155	150	1.00	140	140	164	152	126	127
La	133	128	142	155	159	169	148	148	164	153	126	127
Ce	342	329	374	405	414	420	376	386	418	391	318	329
Pr	39.6	38.2	42.6	45.2	45.7	41.7	39.3	42.8	43.1	41.7	34.8	35.1
Nd	179	173	197	214	216	199	193	202	211	200	159	169
Sm	43.2	37.8	43.7	43.1	43.7	39.3	39.1	39.9	45.7	39.9	29.9	32.1
Eu	13	12.3	10.7	10.8	11.2	8.98	8.53	11.1	9.11	8.98	9	7.02
Gd	192	185	196	195	183	187	170	152	132	101	53.7	43.2
Tb -	6.45	6.13	6.79	6.36	7.5	6.92	5.34	6.17	7.8	5.68	4.95	4.47
Dy	34.9	34.2	36.2	38.3	38.8	35.5	34.4	37.3	37.3	35.2	24.9	26.1
Но	7.6	7.24	8.02	7.84	8.51	7.64	7.59	7.74	7.87	7.72	5.4	5.94
Er	23.4	21.4	24.9	24.3	26.1	23	22.6	23.5	23.4	23.5	16	17.9
Tm	3.37	3.13	3.33	3.46	3.61	3.16	3.09	3.19	3.26	3.3	2.19	2.4
Yb	22.7	21.3	24.1	25.1	26	22.4	22.9	22.7	23	22	14.9	15.4
Lu	3.94	3.64	3.92	3.83	4.14	3.62	3.59	3.65	3.74	3.46	2.36	2.56
Ce/Ce*	1.01	1.07	1.10	1.11	1.11	1.15	1.13	1.11	1.14	1.12	1.1	1.13
Eu/Eu*	1.47	1.55	1.19	1.24	1.2	1.05	1.1	1.35	0.93	1.12	1.42	1.1
Gd/Gd*	5.05	5.23	4.95	5.18	4.31	4.8	5.24	4.21	2.98	2.97	1.89	1.6
(17) (11)	4.54	4.5	4.60	1.61	4.65	4 55	4.60	4 5 4	4.40	4 54	4.00	4.05
(Yb/Nd) _s	1.74	1.7	1.68	1.61	1.65	1.55	1.62	1.54	1.49	1.51	1.29	1.25
N 02	1111 TA7 - W											C
0.02 μm	HH Well		()	7.2	0.2	0.4	11 2	140	10.0	25.7	21.0	Seawate
Salinity	4.8	5.3	6.2	7.3	8.3	9.4	11.3	14.8	19.9	25.7	31.9	36.7
pmol kg ⁻¹	146	142	176	102	151	150	150	151	1 / 1	152	127	1.7
La Co	146 388	143 277	176 425	182 486	151 207	156 200	156	151 402	141 260	153 276	137 226	167 410
Ce	388 41	377 40.4	435 46.1	486 51.0	397 41.2	399 42 E	403	402	369	376	326	419 40.8
Pr		40.4	46.1	51.9	41.2	42.5	41.8	42.5	38	38.4	33.1	40.8
Nd	192	194	212	228	200	204	196	199	179	171	146	191
Sm	38.4	41.7	44.7	47.8	41.5	43.8	40.9	41.5	37.3	34	30	37
Eu	8.75	8.72	9.05	17.1	8.86	10.2	9.02	9.28	8.71	7.1	6.03	7.48
Gd	216	201	210	186	207	193	170	163	50.1	91	58.1	38.3
Tb	5.16	5.22	7.34	9.7	5.77	6.13	7.05	5.95	5.91	3.76	3.44	4.21
Dy	35.4	36.1	38.1	44.1	36.6	39.1	37.2	36.9	31.1	28.7	24.2	29.3
Ho	7.61	8.08	8.43	9.27	8.24	8.65	7.93	8.15	6.71	6.12	5.07	5.78
Er	23	23.2	24.3	28.6	24.4	24.9	23.9	24.8	19	18.6	14.9	16.8
Tm	3.16	3.34	3.42	4.01	3.47	3.58	3.31	3.47	2.75	2.5	2.02	2.3
Yb	24.1	23.6	25.8	29	25.3	25.1	23.7	23.5	18.8	17.1	12.5	14.2
Lu	3.78	3.99	4.05	4.57	3.96	4.37	3.79	3.98	3.01	2.88	2.22	2.4
0 10 1	4.4=						4 4 =	4.4=	4 4 -	4.4-		
Ce/Ce*	1.15	1.14	1.11	1.15	1.15	1.12	1.15	1.15	1.16	1.13	1.11	1.17
Eu/Eu*	1.16	1.09	0.96	1.56	1.07	1.17	1.02	1.13	1.12	1.13	1.08	1.09

	Gd/Gd*	6.84	6.15	4.98	3.53	5.94	5.24	4.25	4.58	1.46	3.71	2.62	1.4
	(Yb/Nd) _S	1.87	1.81	1.67	1.89	1.88	1.83	1.8	1.75	1.56	1.49	1.26	1.41
1722 1723 1724 1725 1726 1727	Ce/Ce* = [I Eu/Eu* = [Gd/Gd* = [SN = Post A McLennan	Eu/(0.67) Gd/(0.33 Archean <i>A</i>	Sm + 0.33' Sm + 0.67	Tb)] _{SN} . Tb)] _{SN} .	PAAS) n	ormalize	ed (Nanc	e and Ta	ylor, 197	'6; Taylo	r and	2	
1728											2		
									G				
)				
						O							
					0								
			?	*									
•													

1729 Table A2. Rare earth element concentrations (pmol kg^{-1}) for the Lava Tube (i.e., Hind well) mixing experiment as a function of pH, salinity, ionic strength (*I*, mol kg^{-1}), and the Cl concentration (mmol kg^{-1}). Salinity (S) was computed from S (g kg^{-1}) = 1.806555 × Cl (g kg^{-1}).

kg ⁻¹). Salin 0.45 μm	Hind		•	(0	0)		,	0 0 7				Seawater
Salinity	Well 2	2.7	3.3	4.4	4.7	7.2	8.6	14.1	20.1	25.2	31.1	36.7
рН	7.7	7.78	7.78	7.73	7.72	7.78	7.8	7.84	7.89	7.92	7.96	8.03
7.7 1												$\hat{}$
mol kg ⁻¹ I	0.1	0.11	0.13	0.146	0.15	0.2	0.23	0.34	0.45	0.55	0.67	0.78
•	0.1	0.11	0.15	0.110	0.15	0.2	0.25	0.51	0.15	0.55	0.07	0.70
mmol kg ⁻¹												
Cl	31.6	42.6	51.6	68.6	72.6	113	135	220	313	392	484	572
pmol kg ⁻¹												
La	140	163	155	125	174	158	163	160	128	147	153	127
Ce	371	425	410	323	454	411	426	413	335	382	385	329
Pr	42.7	46.3	44.7	37	49.2	44.6	46.8	44.3	37.9	39.8	40.6	35.1
Nd	192	221	213	165	226	206	213	204	165	184	183	169
Sm	40.3	43.3	41.8	36.9	45.6	41	44.3	41.1	34.6	37.2	39	32.1
Eu	12.2	11	9.73	10.7	10.9	9.93	9.6	9.87	10.9	8.35	8.85	7.02
Gd	41.2	44.7	44.3	36.4	46	43.4	46.2	44.4	36.6	37.5	37.1	43.2
Tb	6.62	6.4	6.03	5.93	6.61	6.13	6.32	6.13	5.53	5.15	5.35	4.47
Dy	36.5	40.8	37.2	31.3	40.2	37.7	38.5	37.6	31.5	30.8	32.1	26.1
Но	7.95	9.1	8.26	6.43	8.67	8.52	8.63	7.8	6.49	6.88	7.37	5.94
Er	25.7	26.8	25.3	21.5	26.3	26.5	25.8	24	20.2	21.4	20.2	17.9
Tm	3.59	4.12	3.88	3.19	4.06	3.88	3.69	3.86	2.83	3.3	3.03	2.4
Yb	22.7	25.7	24.4	20.9	25.3	25.1	24.7	23.2	17.9	19.9	20.4	15.4
Lu	4.09	4.7	4.43	3.55	4.29	4.23	4.25	3.9	3.11	3.13	3.37	2.56
Ce/Ce*	1.09	1.12	1.13	1.09	1.12	1.12	1.12	1.12	1.1	1.15	1.12	1.13
Eu/Eu*	1.44	1.25	1.16	1.38	1.19	1.19	1.08	1.18	1.51	1.13	1.15	1.1
Gd/Gd*	1.08	1.18	1.23	1.06	1.17	1.2	1.22	1.23	1.4	1.21	1.14	1.6
,												
(Yb/Nd) _{SN}	1.62	1.59	1.57	1.73	1.54	1.68	1.59	1.55	1.49	1.49	1.53	1.25
0.02 μm	Hind	\langle / \rangle										Seawater
Salinity	Well 2	2.7	3.3	4.4	4.7	7.2	8.6	14.1	20.1	25.2	31.1	36.7
pmol kg ⁻¹												
La	140	140		154		139		145				167
Ce	372	366		390		368		369				419
Pr	41.4	40.9		44.2		40		40.2				40.8
Nd	189	186		197		183		180				191
Sm	41.8	36.9		40.1		37.8		37.2				37
Eu	9.65	9.54		10.5		9.94		9.6				7.48
Gd	38.7	38.7		41.3		38.6		38.6				38.3
Tb	6.04	5.89		6.06		5.87		6.11				36.3 4.21
Dy	34.3	32.8		36		33.5		32.1				29.3
Но	7.58	7.29		7.87		7.33		7.02				5.78
Er	23.8	23.1		24.9		23.2		22.7				16.8
Tm	3.32	3.14		3.33		3.13		3.05				2.3
Yb	21.5	21.1		22.6		20.7		21				14.2
Lu	3.93	3.8		4.06		4.05		3.72				2.4
Ce/Ce*	1.17	1.1		1.08		1.13		1.11				1.17

Eu/Eu* Gd/Gd*	1.15 1.1	1.24 1.14	1.28 1.16	1.28 1.13	1.22 1.1	1.09 1.4
(Yb/Nd) _{SN}		1.56	1.57	1.55	1.6	1.41
Ce/Ce* = [0] Eu/Eu* = [1] Gd/Gd* = [0] SN = Post A McLennan,	Eu/(0.67 Gd/(0.33 Archean <i>I</i>	Sm + 0.33T Sm + 0.67T	b)] _{SN} . b)] _{SN} .	ormalized (Na	ince and Taylor, 1976	5; Taylor and
r						CP-11
					6	O'
					10"	
				D		
				W		
				▼		
		?				
)					